Hadean geodynamics and the nature of early continental crust

2	Jun Korenaga
3	Department of Earth and Planetary Sciences, Yale University
4	P.O. Box 208109, New Haven, CT 06520-8109, USA
5	jun.korenaga@yale.edu
6	Tel: (203) 432-7381; Fax: (203) 432-3134

Submitted to Precambrian Research, July 2020; Revised, March 2021.

Abstract. Reconstructing Earth history during the Hadean defies the traditional rock-based approach in geology. Given the extremely limited locality of Hadean zircons, some indirect approach needs to be employed to gain a global perspective on the Hadean Earth. In this review, two 10 promising approaches are considered jointly. One is to better constrain the evolution of continental 11 crust, which helps to define the global tectonic environment because generating a massive amount 12 of felsic continental crust is difficult without plate tectonics. The other is to better understand the 13 solidification of a putative magma ocean and its consequences, as the end of magma ocean solidification marks the beginning of subsolidus mantle convection. On the basis of recent developments 15 in these two subjects, along with geodynamical consideration, a new perspective for early Earth 16 evolution is presented, which starts with rapid plate tectonics made possible by a chemically heterogeneous mantle and gradually shifts to a more modern-style plate tectonics with a homogeneous 18 mantle. The theoretical and observational stance of this new hypothesis is discussed in conjunction 19 with a critical review of existing proposals for early Earth dynamics, such as stagnant lid convection, sagduction, episodic and intermittent subduction, and heat pipe. One unique feature of the 21 new hypothesis is its potential to explain the evolution of nearly all components in the Earth sys-22 tem, including the atmosphere, the oceans, the crust, the mantle, and the core, in a geodynamically 23 sensible manner.

Keywords: Plate tectonics; Early atmosphere; Magma ocean; Continental growth

25

26 Contents

27	1	Intr	oduction	4	
28	2	Maj	Iajor existing hypotheses for early Earth evolution		
29		2.1	Stagnant lid convection	9	
30		2.2	Archean onset of plate tectonics	12	
31		2.3	Mafic early crust	17	
32		2.4	Sagduction	19	
33		2.5	Episodic and intermittent Archean subduction	22	
34		2.6	Heat pipe	25	
35	3	Evol	ution of continental crust through Earth history	29	
36		3.1	Some remarks on the history of crustal growth research	30	
37		3.2	New models of continental growth	32	
38		3.3	Composition of the early continental crust	37	
39		3.4	Hadean geodynamics inferred from crustal evolution	39	
40	4	Phys	sics and chemistry of magma ocean solidification	41	
41		4.1	1993: Annus mirabillis	41	
42		4.2	Thermodynamics of lower mantle melting	43	
43		4.3	Gravitational stability of a solidifying magma ocean	46	
44		4.4	How Hadean geodynamics may have started	48	
45	5	Synt	chesis: A new picture of early Earth evolution	50	
46	6	Sum	mary and outlook	57	

1 Introduction

The Hadean starts from the birth of a fully grown Earth at ~4.5 billion years ago (Ga) (e.g., Barboni et al. 2017; Thiemens et al. 2019) and ends at 4 Ga, which approximately coincides with the age of the oldest dated rock (Bowring and Williams 1999). As such, reconstructing the history of this eon using rock records, which is a traditional approach in geology, seems impossible. One can still try to infer its surface conditions and tectonic environment from the geochemistry of Hadean zircons (e.g., Wilde et al. 2001; Watson and Harrison 2005; Hopkins et al. 2008; Trail et al. 2011, 2018; Turner et al. 2020). However, in addition to uncertainties associated with such geochemical inferences, these efforts have so far relied on detrital zircon grains from a single locality (Jack Hills in Western Australia), which makes it difficult to generalize to global situations. This lack of an empirical backbone is particularly troublesome because the Hadean is the time when Earth is expected to have gone through the most drastic changes in Earth history, i.e., the formation of a magma ocean and its solidification, the appearance of oceans, and the transition from a massive CO₂-rich atmosphere to a more moderate one (e.g., Zahnle et al. 2007). These events during the Hadean are responsible for the making of a habitable planet and set the stage for its subsequent evolution. 62

To gain a global perspective on the Hadean Earth, we need to adopt some indirect approach, and there are at least two different routes. One approach is to focus on a certain kind of geochemical data that are sensitive to global processes in the early Earth. In particular, the geochemical data that can constrain the growth of continental crust are invaluable because generating a massive amount of felsic continental crust requires the prevalent operation of plate tectonics, thus defining the global tectonic environment. The other approach is to better understand the solidification of a magma ocean, which prescribes initial conditions for subsolidus mantle convection. If theoretical predictions based on the aftermath of magma ocean solidification are consistent with what geochemical observations suggest for the early Earth, then, it becomes possible to draw a coherent picture for the Hadean Earth with some confidence. We may also require such characterization

to have some connectivity to the Archean Earth, for which we now have a reasonably secured understanding (e.g., Herzberg et al. 2010; Korenaga 2018a).

The purpose of this review is, therefore, to provide a new synthesis on the likely evolution of the 75 Hadean Earth, on the basis of recent developments in the studies of continental growth and magma ocean solidification. As it may be too myopic to consider the Hadean in isolation, the implications 77 of the new synthesis for the early Archean are also discussed. Before presenting such a synthesis, however, it is important to examine various existing ideas put forward for the evolution of the early Earth. In recent years, a typical narrative of the early Earth starts with stagnant lid convection and mafic crust, followed by the onset of global plate tectonics and the appearance of felsic continental 81 crust sometime in the mid-Archean (e.g., O'Neill et al. 2007; Shirey and Richardson 2011; Dhuime et al. 2012; van Hunen and Moyen 2012; Debaille et al. 2013; Piper 2013; Moore and Webb 2013; 83 Tang et al. 2016; Cawood et al. 2018; Smit et al. 2019). At the same time, there is also a growing literature that provides different views, i.e., the onset of plate tectonics in the Hadean (e.g., Hopkins et al. 2008; Rosas and Korenaga 2018; Hyung and Jacobsen 2020) and the felsic early crust (e.g., Greber et al. 2017; Ptacek et al. 2020; Guo and Korenaga 2020; Keller and Harrison 2020), which 87 necessitates a critical look at the observational and theoretical foundations of the popular narrative. The structure of this paper is the following. I begin with a review of major existing conjectures, such as stagnant lid convection in the early Earth, the Archean onset of plate tectonics, and mafic early crust. Then, I provide a brief review on the evolution of continental crust and follow with 91 a summary of previous studies on magma ocean solidification. There have been a fair number of reviews written on these topics, so my attempt here focuses on the issues that are most relevant to global Hadean geodynamics. Finally, I describe an emerging view on the dynamics of the early Earth, covering from the Hadean to the early Archean. This view naturally contains a number of assumptions and extrapolations, but care has been taken that they are consistent with available observations as well as theoretical considerations. I close by discussing some possible future directions to advance our understanding of this critical era of Earth history.

In this article, the term 'plate tectonics' is used in a broad sense, referring to the mode of mantle convection that allows the continuous, wholesale recycling of the top boundary layer. From the perspective of planetary evolution on a global scale, what is most important about mantle convection is whether it is stagnant lid convection or plate tectonics. Whereas stagnant lid convection severely limits the recycling of surface materials into the deep interior, plate tectonics encourages material circulation from the interior to the surface and back to the interior, activating deep geochemical cycles. The details of how such 'plate tectonics' operates, e.g., how closely it resembles modern-style plate tectonics (e.g., Brown et al. 2020), are important when applying our understanding of modern systems to interpret ancient geological records, but the continuous recycling of the surface layer is what distinguishes plate tectonics from stagnant lid convection. Some intermediate modes of convection may be possible, such as intermittent plate tectonics and sagduction, and they do not fall into the category of 'plate tectonics' here. These intermediate modes have been proposed based mainly on numerical simulation, and their theoretical standings are discussed in §2.

Furthermore, the term 'continental crust' is used to refer to a surface geochemical reservoir that is more long-lived and more enriched in incompatible elements than the oceanic crust. The relative enrichment of incompatible elements with respect to the oceanic crust implies that the continental crust needs to involve more than a single-stage melting of the mantle. This definition is in accord with how the continental crust is treated in geochemical box modeling; the oceanic crust is recycled back to the mantle as part of subducting plates, so it is usually lumped together with the convecting mantle in geochemical box modeling. This definition of continental crust makes most sense in the presence of plate tectonics, but it can still be used in case of stagnant lid convection. In stagnant lid convection, the crustal layer would be long-lived because of no subduction, but being mostly the product of single-stage mantle melting, such crust would not be as enriched in incompatible elements as the present-day continental crust. In other words, a planet in the mode of stagnant lid convection is covered predominantly by oceanic crust equivalent, and this is indeed the case for Venus and Mars. If there is a mechanism to process oceanic crust further

and concentrate incompatible elements with stagnant lid convection, such evolved crust can be called 'continental crust' in this context. Note that we are concerned with the average composition of a long-lived surface reservoir. If part of continental growth owes to the accretion of oceanic plateaus, for example, some fraction of continental crust would not be particularly enriched in incompatible elements, but such regional variations would not negate the overall enrichment of those elements in continental crust. The adopted definition of continental crust avoids to specify physical characteristics or formation mechanisms, and this strategy may be useful when discussing the putative continental crust in the most nebulous time of Earth history.

With regard to continental growth, it is also important to distinguish among 'net crustal growth,'
'crustal generation,' 'crustal recycling,' and 'crustal reworking.' Crustal generation refers to the
addition of new crustal materials from the mantle to the continental crust, and crustal recycling
refers to the loss of crustal materials to the mantle (via subduction or delamination). Net crustal
growth is a net change in the mass of continental crust, i.e., the difference between crustal generation and crustal recycling. Crustal reworking encompasses various intracrustal processes, such as
partial melting, that can modify the age of the original crustal generation event.

2 Major existing hypotheses for early Earth evolution

When examining various ideas proposed for early Earth processes, it is important to distinguish between theoretical and observational inferences. The assessment of a theoretical inference can generally be conclusive; we can decompose it into several components, such as assumption, approximation, and interpretation, each of which can be discussed solely on a theoretical basis. On the other hand, the assessment of an observational inference, especially regarding the early Earth, is less straightforward, because the paucity of relevant geological records is further compounded by preservation bias. Preservation bias is a difficult issue to discuss because there is probably no solution to alleviate the bias. Consider, for example, the East Pilbara Terrane in Western Australia, which is often described as the oldest and best-preserved remnant of the Archean crust.

Based on its geological history, Van Kranendonk and his colleagues have argued that Earth experienced a major shift from plume-driven vertical tectonics to subduction-driven horizontal tectonics 151 at ~3.2 Ga (e.g., Van Kranendonk et al. 2004, 2007; Hickman 2012). The areal extent of this craton 152 is, however, approximately 200×200 km², covering only 0.02 % of the surface of the present-day 153 continental crust. Thus, we need to ask whether it is legitimate to infer a global tectonic regime 154 from such extremely local observations. The fact that the East Pilbara Terrane has survived for a 155 few billion years, despite the destructive nature of plate tectonics, can be interpreted in two contrasting ways. Cratons like the East Pilbara Terrane could have been ubiquitous in the early Earth, 157 and thanks to this, the characteristics of early crust are able to have survived to the present day 158 despite the billions of years of plate tectonic recycling. Alternatively, the survival of the craton could also mean that it is unusual in a certain sense. It may have been supported from below by 160 highly depleted (and thus mechanically strong) lithospheric mantle that is expected from the high-161 degree partial melting of mantle plumes (e.g., Jordan 1988; Doin et al. 1997). In this case, the 162 geological history of the East Pilbara Terrane may not be generalized to a global context. A third 163 possibility is that the craton is not representative of the early crust but is not special either; there 164 may have been a wide variety of Archean crust, and the preservation of this particular craton could 165 be a sheer random event. Field observations alone cannot distinguish between these possibilities. For example, the Itsaq Gneiss Complex in Greenland has been suggested to exhibit some traces of 167 subduction in the early Archean (e.g., Komiya et al. 1999; Nutman et al. 2002), but this locale is 168 of even smaller spatial extent ($\sim 3000 \text{ km}^2$). The scarcity of extant early Archean terranes prevents 169 to make statistically meaningful inferences for global tectonics. 170

Thus, theoretical considerations naturally play an important role in evaluating the significance of a certain field area in the context of global tectonics. If theory suggests, for example, that the early Earth must have started with stagnant lid convection, then the East Pilbara Terrane could be recognized as the precious geological evidence that tells us when and how a transition from stagnant lid to plate tectonics took place. If, on the other hand, theory suggests that plate tectonics

has been possible throughout Earth history, it would be unwarranted to extrapolate the geology of the East Pilbara Terrane to global tectonics. As mentioned above, the validity of theoretical inferences can be assessed in a definitive manner, so I start this section by examining the notion of stagnant lid convection in the early Earth.

2.1 Stagnant lid convection

If plate tectonics started sometime in the middle of Earth history, mantle convection has to have operated in a different regime before. One of the popular choices for such a pre-plate-tectonics regime is stagnant lid convection (e.g., Debaille et al. 2013; Piper 2013; Stern 2018; Cawood et al. 2018). This idea has a certain narrative appeal. The early Earth could have been a very different world morphed by an entirely different kind of mantle convection, and then the advent of plate tectonics brought dramatic changes to everything. It provides a powerful storyline that could stimulate people's imagination. The only problem is that one has to specify what caused this change in the mode of mantle convection in the middle of Earth history.

Most geologists who advocate stagnant lid convection for the early Earth refer to, as a theo-189 retical justification, the numerical modeling of O'Neill et al. (2007), which suggests that higher 190 internal heating in the past results in a hotter mantle, reducing convective stress and making it 191 difficult to drive plate tectonics. It is yet to be widely appreciated, however, that their numerical model suffers from several design issues, and that it cannot be used to discuss Earth evolution. 193 This fact has already been pointed out by Korenaga (2017b), but it is buried in a rather technical 194 tutorial aimed at geodynamicists, so its essence is summarized here. Some of the key numerical 195 results obtained by O'Neill et al. (2007) are reproduced in Figure 1a-d. They conducted a series 196 of numerical simulation by varying the amount of internal heating, and a higher amount of inter-197 nal heating is seen to lead to a hotter interior. Correspondingly, convective stress decreases with 198 increasing temperature (Figure 1i, solid circles), confirming the argument put forward by O'Neill et al. (2007). However, this effect of internal heating on convective stress is not relevant to Earth's

mantle convection. In the model of O'Neill et al. (2007), the bottom temperature is fixed to a constant value, so their model mantle is heated from within as well as from below; this is the 202 so-called mixed heating mode. One important attribute of mixed heating is the internal heating 203 ratio, which quantifies the contribution to surface heat flux from internal heating. In the case of 204 no internal heating (Figure 1a), the internal heating ratio is zero, meaning that all of surface heat 205 flux is supported from heat flux from below (i.e., core heat flux). The three examples shown in 206 Figure 1a-c span the range of internal heating ratio from 0 to \sim 1, i.e., pure basal heating to almost pure internal heating. Thus, even though the corresponding change in internal temperature is mod-208 est (Figure 1i; \sim 250 K), the influence of the bottom boundary varies substantially. In contrast, the 200 contribution of core heat flux to surface heat flux is limited on Earth (e.g., Lay et al. 2008), and the internal heating ratio would not vary much through Earth history (Figure 1j). To understand how 211 much of the stress change seen in the mixed-heating model is caused by the change in basal heat 212 flux, Korenaga (2017b) ran another set of numerical simulation, which is identical to those shown 213 in Figure 1a-c except that the bottom was insulated to suppress basal heat flux (Figure 1e-g). A 214 similar change in the interior temperature is seen (compare Figure 1d and Figure 1h), but a change 215 in the convective stress is almost negligible in these purely internally heated cases (Figure 1i, open 216 circles). This is also consistent with the stress scaling of Solomatov (2004). The conjecture of O'Neill et al. (2007), therefore, is not applicable to Earth. Additionally, the internal heating ratio 218 is likely to have been *lower* in the past, i.e., the contribution from basal heat flux was greater in-219 stead of smaller (Figure 1j), despite higher radiogenic heating in the past. This is partly because 220 "internal heating" in steady-state convection simulation (as those shown in Figure 1) includes not 221 only radiogenic heating but also secular cooling (e.g., Daly 1980) and partly because core heat flux 222 is likely to have been higher in the past (e.g., Nimmo 2015; O'Rourke et al. 2017). In general, 223 modeling mantle convection with internal heat production needs great care, and Korenaga (2017b) concluded his tutorial with a list of seven pitfalls to avoid: 1. using only radiogenic heating when 225 running a model for steady state, 2. using Turcotte & Schubert's model of internal heat production, 226

3. modifying more than one variable in a control experiment, 4. overlooking the viscosity contrast across lithosphere, 5. neglecting to measure the internal heating ratio, 6. running complicated models without understanding simpler ones, and 7. running simulations with an unrealistic evolution of the internal heating ratio. Falling into just one or two pitfalls usually constitutes a fatal error. The work of O'Neill et al. (2007) falls into all of them.

The inconsistency between the work of O'Neill et al. (2007) and the scaling of Solomatov 232 (2004) was noted by Korenaga (2013) (see its section 2.2), but an in-depth discussion of design issues in the former study was not available until 2017. In the meantime, the notion of stagnant 234 lid convection in the early Earth has become quite popular, though relevant arguments put forward 235 are of varying quality. For example, Debaille et al. (2013) argued that ¹⁴²Nd/¹⁴⁴Nd variations in late Archean rocks were consistent with the operation of stagnant lid convection in the early Earth, 237 but as Roth et al. (2014) pointed out, their observations do not require stagnant lid convection if 238 one considers the effect of continental growth on the evolution of isotopic heterogeneities in the 239 mantle. Indeed, the same Nd isotope data can also be explained by the combination of rapid crustal 240 growth and efficient crustal recycling (Rosas and Korenaga 2018), which is recently corroborated 241 by the history of argon degassing (Guo and Korenaga 2020). A more recent example may be seen 242 in the work of Caro et al. (2017), who studied the formation history of Eoarchean supracrustal rocks (3.6-3.8 Ga) from the Inukjuak domain in the Superior Province. They estimated that the 244 Eoarchean rocks were derived by a foundering of \sim 4.4 Ga mafic crust, and the time lag of 0.6-245 0.8 Gyr between the formation of the Hadean mafic crust and its foundering was used to argue 246 for subdued lithospheric recycling, thus preferring stable lithosphere as in stagnant lid convection. 247 However, this argument is strange in two accounts. First, the crustal residence time of 0.6-0.8 Gyr 248 by itself does not immediately indicate subdued recycling. With the present-day continental mass, 249 for example, it corresponds to the recycling rate of 2.5-3.3×10²² kg Gyr⁻¹, which is much higher than the present-day recycling rate. Second, the time lag between formation and recycling is not 251 equal to the crustal residence time unless the area under consideration represents a substantial

fraction of the then existing continental crust. This is clearly not the case for the study of Caro et al. (2017), whose survey area is only $\sim 2 \text{ km}^2$. This point may be better appreciated by looking at the formation age distribution of the continental crust (see §3.2); even with continuous recycling, it is possible to preserve rocks originally formed at >4 Ga to the present, if their mass is not too large.

Returning to the issue of what could possibly cause the transition from stagnant lid convection 258 to plate tectonics in the middle of Earth history, it is still premature to be conclusive about this, because what makes plate tectonics possible on Earth is still under active debate (e.g., Bercovici 260 et al. 2015; Korenaga 2020). As I argued in my recent review on this matter (Korenaga 2020), 261 however, it is difficult to find a more efficient weakening mechanism than the thermal cracking of oceanic lithosphere (Korenaga 2007), and in recent years, observational support for thermal 263 cracking is gradually accumulating as well (e.g., Korenaga 2017a; Chesley et al. 2019). The prime 264 requirement to activate this mechanism on terrestrial planets is the presence of surface water (Ko-265 renaga 2010a). As the oxygen isotope data of Hadean zircons suggest that Earth was covered by 266 oceans at least back to 4.4 Ga (Wilde et al. 2001; Mojzsis et al. 2001), there is no impediment for 267 the operation of plate tectonics in the Hadean. Conversely, with the current understanding of rock 268 mechanics, the notion of stagnant lid convection in the early Earth could conflict with the likely presence of surface water. 270

2.2 Archean onset of plate tectonics

In addition to the work of O'Neill et al. (2007), a few other studies helped to popularize the late onset of plate tectonics, and the continental growth model of Dhuime et al. (2012) is one of them.

However, the work of Dhuime et al. (2012) is affected by three major issues.

The first issue is that their way of estimating crustal growth does not yield an estimate on crustal growth. They basically followed the procedure proposed by Belousova et al. (2010), and how it works is illustrated in Figure 3, using four different synthetic examples. We first calculate two age

distributions from a detrital zircon database, one for U-Pb crystallization ages, and the other for depleted mantle model ages based on Hf isotopes. Then, we take the ratio of the depleted mantle 279 model age distribution over the sum of these two age distributions, and this ratio is assumed to 280 be the new crust generation rate. Finally, by taking the cumulative sum of this crust generation 281 rate, we obtain a new growth curve. To understand whether this approach actually works or not, 282 let us apply it to synthetic zircon age data, for which we know the true answer. The first row of 283 Figure 3 presents the simplest case, in which the continental crust grows linearly (Figure 3d), so the crust generation rate is constant through time (Figure 3a; gray histogram). Because the crystal-285 lization ages of old zircon grains tend to be reset by more recent crust generation events, the U-Pb 286 crystallization age distribution is skewed toward recent ages (Figure 3a; yellow line). Note that this resetting of crystallization ages does not refer to age-resetting by Pb loss, but to age-resetting 288 caused by dissolving zircon during intracrustal melting under appropriate temperatures and com-280 positions. The latter type of age-resetting is also assumed by Belousova et al. (2010); in their 290 model, the pairwise interaction of old and new zircon grains results in adopting the crystallization 291 age of the new grain and the average of their depleted mantle model ages for both grains (see also 292 Figure 1 of Korenaga (2018b)). Because of this mixing of old and new grains, the depleted mantle 293 model age distribution takes a maximum in the middle of Earth history (Figure 3a; magenta line), which reflects the average age of continental crust. The sum of these two age distributions has 295 greater population at younger ages (Figure 3b; orange line), an attribute inherited from the U-Pb 296 crystallization age distribution. If we divide the model age distribution by this aggregated one, the 297 resulting distribution, which is supposed to be the new crust generation rate, has greater population 298 at older ages (Figure 3c; blue line). This is at odds with the true distribution, which is constant 299 through time (Figure 3c; gray histogram). The reason for this discrepancy is simply that the ratio 300 of the model age distribution over the sum of the two age distributions always has greater values at older ages than at younger ages, no matter what the true distribution of crust generation rate 302 is, because the U-Pb crystallization ages, which occupy the half of the denominator, are always

biased toward younger ages, and the depleted mantle model ages, which occupy the other half, do not reverse this bias. This fact is perhaps best appreciated with the second example, in which the 305 true crust generation rate is biased toward the present (Figure 3e; gray histogram). The method 306 of Belousova et al. (2010) still yields a result that is biased toward older ages (Figure 3g; blue 307 line). As a result, the cumulative distribution is concave down (Figure 3h; blue line), though it 308 should be concave up in this example (Figure 3h; gray histogram). The method of Belousova et al. 309 (2010) can give an apparently successful solution only when the true distribution is similar to the artifact it produces, i.e., a distribution skewed toward older ages, as shown in the third example 311 (Figure 3i-1). The fourth example concerns a more complicated distribution with multiple peaks 312 in crust generation (Figure 3m; gray histogram). The method of Belousova et al. (2010) again provides a distribution skewed toward older ages (Figure 3o; blue line) and thus a concave-down 314 cumulative distribution (Figure 3p; blue line). These four examples should be sufficient to demon-315 strate the point made earlier; the method of Belousova et al. (2010) always produces a distribution 316 skewed toward older ages regardless of input data, simply because the U-Pb crystallization age 317 distribution, which can be reset by recent melting events, has always greater population at younger 318 ages than the depleted mantle model age distribution. As pointed out by Korenaga (2018b), the 319 method of Belousova et al. (2010) does not provide an estimate on the crust generation rate because there is no logical connection between their procedure and crustal growth. Their method can only 321 produce a smooth curve that may look like a growth curve, and it always produces a concave-down 322 curve even for synthetic input data made by an entirely different growth curve. Belousova et al. 323 (2010) themselves tested the performance of their method using two synthetic examples, which 324 are similar to the first and third examples shown here, but the outcome of the first example did not 325 prevent them to proceed. For comparison, the performance of the unmixing method of Korenaga 326 (2018b) is also shown in Figure 3 (red line).

Second, Dhuime et al. (2012) not only adopted the method of Belousova et al. (2010) but also added data screening using oxygen isotope data. Whereas oxygen isotope data could provide

important information on the nature of host rocks, their implementation of data screening is problematic. Because only a fraction of zircon age data have oxygen isotope data measured, they first
focused on this small fraction of the global zircon database (the number of data \sim 1400) to calculate the fraction of data to be rejected as a function of depleted mantle model age; for example, \sim 80 % and \sim 40 % of data would be rejected if the model age is 2 Ga and 3 Ga, respectively. Then,
they applied this age-based rejection criterion to the original global database (the number of data \sim 7000). In doing so, they discarded over 50 % of data irrespective of their potential oxygen isotope
information.

Third, detrital zircon ages cannot be used to estimate net crustal growth. By using crustal samples that have been preserved to the present, we can only hope to reconstruct the formation age distribution, not net crustal growth (§3.1). Nevertheless, Dhuime et al. (2012) presented their result as a new growth model, and because their 'growth model' shows a reduction in growth rate at \sim 3 Ga, they suggested that this reduction might be linked to the onset of plate tectonics. This suggestion is problematic in two aspects: (1) as demonstrated above, their model is an artifact and does not correspond to either net crustal growth or formation age distribution, and (2) net crustal growth and the onset of plate tectonics are not uniquely related. Net crustal growth reflects a balance between crustal generation and recycling (§3), so a change in net growth rate simply indicates a concurrent change in the rate of crustal generation or crustal recycling or both. It cannot be ascribed solely to a change in the recycling rate, as assumed by Dhuime et al. (2012).

Other arguments for the Archean onset of plate tectonics include those based on mineral inclusions in diamonds (Shirey and Richardson 2011; Smit et al. 2019) and the Nd isotope data
of magmatic zircons (Fisher and Vervoort 2018), and these studies deserve careful consideration.
Shirey and Richardson (2011) suggested the onset of plate tectonics at 3 Ga, based on the following
observation: the temporal distribution of eclogitic diamonds found in mantle xenoliths, which are
likely to have originated in subducted oceanic crust, are sharply truncated at ~3 Ga, whereas that
of peridotitic diamonds do not show such a behavior. Smit et al. (2019) followed up this hypoth-

esis by analyzing the sulfur isotope signature of sulfide inclusions in diamonds and showed that
mass-independently fractionated sulfur, which can be generated only before the Great Oxidation
Event at ~2.5 Ga (Farquhar et al. 2000; Gumsley et al. 2017), is observed for inclusions younger
than 2.9 Ga but not for those with an age of 3.5 Ga. These important observations, however, do
not necessarily contradict with the early onset of plate tectonics. Because those diamonds are all
sampled from continental lithosphere, they may reflect how the preservation potential of continental lithosphere, with regard to subducted oceanic crust, has changed through time, instead of
subduction process itself (Luo and Korenaga 2021).

Fisher and Vervoort (2018) analyzed the Hf isotope signature of magmatic zircons from Eoarchean 364 rocks in southern West Greenland, and because these zircons were found to be undepleted in terms of Hf isotopes before 3.8 Ga, they suggested that continental growth started only after 3.8 Ga. This 366 directly conflicts with the suprachondritic ¹⁴³Nd/¹⁴⁴Nd isotope signature reported from Eoarchean 367 rocks (e.g., Moorbath et al. 1997; Bennett et al. 2007). One explanation for this discrepancy is that the Nd isotope data of whole rock are subject to greater disturbances than the Hf isotope data of 369 zircon grains (e.g., Vervoort et al. 1996). Such relative fragility of whole-rock isotope data should 370 be at least partly responsible for the scattered nature of ¹⁴³Nd data in the early Archean (Figure 2a). 371 Another way to reconcile their Hf isotope observation with the Nd isotope records is to suppose that the Lu-Hf isotope system was decoupled from the Sm-Nd isotope system in the early Earth. 373 These two isotope systems are known to be usually well correlated (Vervoort et al. 1999), but it 374 is possible to decouple them by the unique partitioning behavior of lower mantle minerals, which 375 could take effect during the solidification of a magma ocean (Caro et al. 2005). Although Fisher 376 and Vervoort (2018) did not favor this possibility, by noting that "it does require a mantle melting 377 process that is no longer dominant on Earth," the solidification of a magma ocean is the process 378 that can only happen in the very early Earth. As the existence of a magma ocean is difficult to reject (§4.1), pursuing the possibility of Lu-Hf and Sm-Nd decoupling appears a worthy effort. It 380 could potentially provide important constraints on magma ocean solidification as well as the early

phase of subsolidus mantle convection.

2.3 Mafic early crust

383

The early continental crust is commonly thought to be more mafic than the present continental 384 crust (e.g., Taylor and McLennan 1985, 1995; Kemp and Hawkesworth 2003), although how much 385 more mafic it was differs among existing estimates. In this section, to make discussion concrete 386 and concise, I focus on the major element composition in terms of SiO₂, MgO, and K₂O. In their 387 classic work, Taylor and McLennan (1985) estimated, on the basis of the geochemistry of shales, the composition of present-day upper crust as 66 wt% SiO₂, 2.2 wt% MgO, 3.4 wt% K₂O, and 389 that of Archean upper crust as 60 wt% SiO₂, 4.7 wt% MgO, 1.8 wt% K₂O. Their estimate of 390 the Archean composition corresponds to a 2:1 mixture of basalt and TTG, i.e., a predominantly mafic continental crust. On the other hand, Condie (1993) suggested, on the basis of the geologic 392 mapping of the exposed continental crust, a much reduced secular evolution even after correcting 393 for the effect of erosion: 67 wt% SiO₂, 1.9 wt% MgO, 3.1 wt% K₂O for present, and 65 wt% SiO₂, 394 4.1 wt% MgO, 2.5 wt% K₂O for >3.5 Ga (Figure 4). Correspondingly, the proportion of mafic and ultramafic components varies from 9 % in the Phanerozoic to only 21 % in the early Archean 396 (Figure 4). 397

A recent analysis of the global compilation of terrigenous sediments (Ptacek et al. 2020) corroborates the secular compositional change of Taylor and McLennan (1985) with 66 wt% SiO₂, 2.4 wt% MgO, 3.2 wt% K₂O for present, and 61 wt% SiO₂, 6.1 wt% MgO, 1.8 wt% K₂O for 3.3 Ga. However, the lithologic decomposition of Ptacek et al. (2020) shows that the felsic component has to occupy >50 % persistently for the last 3.5 Gyr, because the compositions of end-member components (felsic, mafic, and komatiite) also change with time. In their decomposition, the mafic component occupies \sim 20 % at present and \sim 30 % at 3.5 Ga, with the komatiite component appearing at \sim 1.8 Ga and reaching \sim 10 % at 3.5 Ga. This is more comparable to the estimate of Condie (1993) than that of Taylor and McLennan (1985).

Another approach to estimating the major element composition of early continental crust is to 407 use trace element ratios as proxies, e.g., Ni/Co and Cr/Zn for MgO (Tang et al. 2016), Cr/U for 408 SiO₂ (Smit and Mezger 2017), and Cu/Ag for MgO and SiO₂ (Chen et al. 2019). These studies 409 tend to provide greater secular variations than mentioned above. For example, Tang et al. (2016) 410 estimated that MgO decreased from $\sim\!15$ wt% at 3.2 Ga to $\sim\!4$ wt% at 2.6 Ga, and Chen et al. 411 (2019) estimated that SiO₂ increased from 50-55 wt% at 3 Ga to 65 wt% at 2.4 Ga. As pointed out 412 by Keller and Harrison (2020), however, these suggested transitions in major element composition may simply reflect a redox change in surface environment brought by the Great Oxidation Event at 414 \sim 2.5 Ga, because the solubilities of these metallic elements are highly sensitive to their oxidation 415 states. As a null hypothesis, Keller and Harrison (2020) suggest that the SiO₂ content of continental crust could have been remain nearly constant at ∼59 wt% since 4 Ga, though MgO and K₂O still 417 exhibit secular change (6 wt% MgO and 1.5 wt% K₂O at 4 Ga and 4 wt% MgO and 2.5 wt% K₂O 418 at present) in their model. 419

Rollinson (2017) offers a different angle to the question of early crustal composition. He 420 argues that, if large volumes of felsic continental crust existed in the early Earth and were lost 421 to the mantle by subduction, they should manifest in the isotope signature of ocean island basalts 422 (OIB). Referring to the work of Stracke (2012), which shows that the contribution of recycled upper continental crust to OIB is subordinate to that of recycled oceanic crust, Rollinson (2017) questions 424 the presence of massive felsic crust in the early Earth. However, one cannot apply the geochemistry 425 of OIB to the problem of continental evolution in this way. In the geochemical literature, the 426 contribution of the continental crust to the sources for mid-ocean ridge basalts (MORB) and ocean 427 island basalts is usually discussed using the isotopic composition of the present-day continental 428 crust (e.g., Hofmann 1997). Because the present-day continental crust is isotopically quite distinct 429 and is also enriched in those isotopes, one only has to add a small amount of it to change the isotope composition of a source mantle. This does not preclude the possibility of recycling a 431 substantial amount of continental crust in the past. For example, what is shown in Figure 2a is the 432

143Nd/144Nd evolution of the depleted MORB source mantle according to the continental growth model of Rosas and Korenaga (2018), which is characterized by efficient crustal recycling in the early Earth (§3.2). In other words, the present-day isotopic composition of the convecting mantle (including both MORB and OIB sources) reflects the time-integrated effect of crustal generation and recycling, and one cannot deduce the long-term contribution of crustal recycling from the isotopic variance of present-day igneous products.

339 2.4 Sagduction

As a pre-plate-tectonics regime, some authors have proposed something less rigid than stagnant lid
convection. In the so-called 'sagduction' regime, the base of thick oceanic crust can delaminate and
sink. If such delaminated crust is originally hydrated, its partial melting can create felsic magma,
so sagduction can potentially contribute to continental growth in the absence of plate tectonics.
Quite a few numerical models have been published to support the possibility of this hypothetical
geodynamic process, but they all involve questionable model assumptions. The dissection of some
representative studies is conducted below.

Johnson et al. (2014) considered the gravitational stability of a 45-km-thick magnesium-rich 447 crust. Based on thermodynamic modeling, they showed that the lowermost part of the crust could 448 become denser than the underlying mantle, and their numerical simulation indicates that the dense layer can delaminate on a time scale of a few Myr. They used, however, the rheology of dry dia-450 base when calculating crustal viscosity, which is inconsistent with the fact that the densification of 451 the lowermost crust is caused by phase change, with increasing modal proportions of garnet and 452 pyroxenes, which are considerably stronger than diabase (Karato 2008). Mondal and Korenaga 453 (2018) showed that, if we instead use the rheology of eclogite for the densified layer, the time scale 454 of crustal delamination would become on the order of 1-10 Gyr, i.e., delamination is virtually impossible. More recently, Roman and Arndt (2020) pointed out that fractional crystallization during crustal accretion would leave olivine-rich cumulates in the lower crust with little aluminum, thus being unlikely to yield garnet to begin with. They also noted that crustal accretion with repeated extrusion and intrusion would result in too hot a thermal structure to retain hydrous minerals in the lower crust. Although thermal cracking can still hydrate the lower crust after crust emplacement, such hydration would be highly localized as deep thermal cracks can form only with an interval of a few tens of kilometers (Korenaga 2007, 2017a). Thus, a pervasive hydration of lowermost crust as assumed by Johnson et al. (2014) is difficult to achieve.

Sizova et al. (2015) considered a similar dynamic problem, but with a different initial condition. Their model starts with a 40-km-thick basaltic crust, with the top 20 km being hydrated, 465 and the crustal layer is underlain by a \sim 200-km-thick layer of melt-bearing peridotite. Their sim-466 ulation results exhibit highly dynamic features, starting with lithospheric mantle delamination, then lower crustal delamination and crustal overturn, followed by oceanic plate subduction, slab 468 breakoff, and even back arc spreading. Their model is, however, set up to become unrealistically 460 unstable. First of all, their initial thermal structure is superheated. They set 0 °C at the surface, 470 1200 °C at the Moho, 1590 °C at 80 km depth, and 2040 °C at the bottom boundary (500 km 471 depth). The asthenospheric mantle thus initially has a thermal gradient of ~ 1 K km⁻¹, which is 472 twice as high as the adiabatic gradient of the solid mantle (e.g., Turcotte and Schubert 1982). This 473 high heat content prescribed by the initial condition allows a prolonged period of extensive melting in their model. Second, their model consistently exhibits a >100-km-thick layer of melt-bearing 475 peridotite, because they assume that the melt porosity in peridotite can become as high as 5 % be-476 fore being extracted by melt migration. Dihedral angles in the olivine-basalt system are, however, lower than 60°, so melt can be interconnected and be extracted even with less than 0.5 % porosity 478 (e.g., von Bargen and Waff 1986; Daines and Richter 1988). Geochemical observations suggest 479 similarly low residual melt porosities: 0.1-0.5 % from the rare earth element chemistry of abyssal 480 peridotites (Johnson and Dick 1992), and ~0.1 % from the U-series activity ratios of MORB (McKenzie 2000). The presence of a thick melt-bearing peridotite layer in the model of Sizova 482 et al. (2015) is particularly problematic because they assume a reference density of 2900 kg m^{-3} for the melt-bearing phase, which is much more buoyant than solid peridotite with a reference density of 3300 kg m⁻³. This thick, unrealistically buoyant melt-bearing peridotite layer facilitates the delamination of the lower crust. Third, they assume that, when melt extraction happens in their model, the yield strength of a lithology in the column between the source of the melt and the surface is decreased by three orders of magnitude (for example, down to \sim 1 MPa at 50 km depth). This essentially voids the effects of rock friction and temperature-dependent viscosity and prepares the otherwise strong cold surface layer for intense deformation and delamination. The superheated nature of their model also helps to sustain the feedback of delamination and melting.

The sagduction model of Rozel et al. (2017) is more reasonably set up than that of Sizova 492 et al. (2015), although the strong nature of eclogite rheology (Jin et al. 2001) is still not taken into account. As such, their model prediction for felsic crust (or more precisely, TTG) production may 494 be regarded as the upper limit we can expect from sagduction. TTG is produced in their model 495 in two stages, first by initial eclogite dripping, which lasts 100-200 Myr, and later by resurfacing, 496 which takes place after a few hundred Myrs of stagnant lid convection, and most of felsic crust 497 production occurs in the initial dripping stage. They tested a number of different cases by varying 498 the brittle strength and the ratio of extrusive and intrusive magmatism, and they were able to show 490 that their model can produce up to 1.5×10^9 km³ of TTG, which translates to $\sim 0.4 \times 10^{22}$ kg with a density of 2900 kg m⁻³. Citing the work of Dhuime et al. (2012), Rozel et al. (2017) argued 501 that this was sufficient to explain early continental growth. As explained in §2.2, however, one 502 cannot read off new crust generation rate from a net growth curve (see also §3.2), and the model of Dhuime et al. (2012) is not a net growth model to begin with. For comparison, the crustal evolution 504 model of Guo and Korenaga (2020) suggests that $\sim 5 \times 10^{22}$ kg of felsic rocks had to be produced 505 in the Archean. More critically, TTG production in the model of Rozel et al. (2017) is quite shortlived, with the majority of production confined in the first 100-200 Myr, whereas TTG is observed throughout the Archean (e.g., Moyen and Laurent 2018). Similar comments apply to the work of 508 Piccolo et al. (2019), which is a more recent take on sagduction.

2.5 Episodic and intermittent Archean subduction

When assessing various numerical models of sagduction in the previous section, the importance of 511 using eclogite rheology was noted. Rheology dictates how quickly instabilities can grow, so it is always worth examining an adopted rheological setup. In this regard, existing numerical studies 513 tend to be oblivious to upper mantle rheology, which plays a decisive role in controlling the stability 514 of lithosphere. As indicated by the deep water cycle and the continental freeboard (Korenaga et al. 2017), the convecting mantle is likely to have been drier in the past, probably almost dry in the 516 early Archean. Because of this, the early mantle does not necessarily have a lower viscosity than 517 the present-day mantle. The effect of decreasing water content can compensate for the effect of 518 increasing temperature (e.g., Korenaga 2008a; Crowley et al. 2011). Nevertheless, it is common to see wet oliving rheology being used for the asthenospheric mantle in deep time. 520

Figure 5 compares the yield strength of the suboceanic mantle beneath a 100-Myr-old seafloor, 521 for the cases of the potential temperature of 1350 °C (present) and 1650 °C (Archean). Because the wet asthenospheric mantle at present starts to dehydrate at ~ 110 km depth by partial melting, 523 dry rheology is used for shallower depths (for a more realistic treatment of dehydration, see, for 524 example, Katz et al. (2003)). As can be seen here, the yield strength is determined by the weakest 525 deformation mechanism, which varies with depth. At present, the asthenosphere is dominated by wet diffusion creep, the lower half of lithosphere by dry dislocation creep, and the upper half 527 of lithosphere by brittle failure assisted by thermal-cracking. Without thermal cracking, the yield 528 strength of the coldest part of lithosphere would be controlled mostly by low-temperature plasticity and be as high as ~ 1 GPa, which is high enough to inhibit the operation of plate tectonics (e.g., 530 Moresi and Solomatov 1998; Richards et al. 2001; Stein et al. 2004). With the potential temperature 531 raised to 1650 °C, but with a dry asthenosphere, the yield strength of the suboceanic mantle does not change much (Figure 5b). This is partly because, when compared at the same seafloor age, the 533 shallow part of the lithosphere is similarly cold owing to cooling from above. The largest difference 534 is thus expected in the asthenosphere, but the effects of water and temperature are almost canceled

out there. It should be noted that upper mantle rheology is still not well understood, and the yield strength profiles in Figure 5 are subject to large uncertainty. Whereas many simulations studies use 537 the flow-law parameters compiled by Karato and Wu (1993) or Hirth and Kohlstedt (2003), most 538 of those flow-law parameters are not well constrained, as a series of reanalysis of experimental 530 studies have demonstrated (Jain et al. 2017, 2018, 2019). Figure 5 is based on just one of possible 540 flow-law parameter combinations sampled from the statistical representation of Jain et al. (2019). 541 Despite this uncertainty in flow law parameters, we should acknowledge the possibility that a hotter mantle is not guaranteed to develop weaker lithosphere, if we are to understand the evolution of the 543 Earth system as a whole, in which surface environment and mantle dynamics can interact through 544 deep water cycle.

With this understanding of lithospheric strength, I now turn to discuss the possibility of episodic 546 and intermittent subduction in the Archean (van Hunen and van den Berg 2008; van Hunen and 547 Moyen 2012; Moyen and van Hunen 2012). van Hunen and van den Berg (2008) built a numerical 548 model to study how the style of subduction might change with different mantle potential temper-549 atures, and their modeling results indicate that slab breakoff would take place more frequently in 550 a hotter mantle, preventing continuous subduction. In their model, Archean subduction events are 551 short-lived, lasting only 5-10 Myrs, and Moyen and van Hunen (2012) noted that such short-term episodicity was consistent with the intermittent arc signatures seen in the Abitibi greenstone belt. 553 As explained above, however, the Archean convecting mantle is not necessarily weaker than the 554 present-day mantle, even though the former is certainly hotter. Positive net water flux from the 555 surface to the mantle has long been suggested by the present-day budget of water fluxes (Ito et al. 556 1983; Jarrard 2003) and is also supported by theoretical modeling (e.g., van Keken et al. 2011; 557 Magni et al. 2014; Karlsen et al. 2019). Though large net water influx has commonly been thought 558 to contradict with the constancy of continental freeboard (or equivalently, the constancy of sea level) (e.g., Ito et al. 1983; Parai and Mukhopadhyay 2012), it is actually required to satisfy the 560 freeboard constraint if one considers the secular evolution of hypsometry (Korenaga 2008a; Korenaga et al. 2017). A drier mantle in the Archean is a corollary of this deep water cycle, and it must always be considered in conjunction with the secular cooling of the mantle.

The aforementioned arc signatures within the Abitibi greenstone belt have been questioned by 564 Bedard (2018), who argues that calc-alkaline volcanics in the belt are not arc-related but were 565 instead formed through intermittent melting at the base of a thick basaltic crust. As geological 566 inferences are largely empirical, it is not easy to secure a unique interpretation, especially when 567 invoking a process with no modern analogue. Early Archean plate tectonics could have very different petrological and geochemical consequences, even if its kinematics is similar to that of modern 560 plate tectonics. Because of higher radiogenic heating in the past, the continental crust would cer-570 tainly be hotter and thus weaker (e.g., Rey and Houseman 2006; Rey and Coltice 2008). Also, the continental mantle lithosphere would be more easily influenced by convective currents (see §5), so 572 continental tectonics in the deeper time is expected to be generally more dynamic, characterized by 573 more mobile crust. This should not be confused with the strength of oceanic lithosphere, which can 574 remain strong as already discussed above. Higher mantle potential temperature results in thicker 575 oceanic crust with higher MgO content and thicker and more deplete oceanic mantle lithosphere 576 (Davies 1992; Korenaga 2006). In addition, the age of subducting slab tends to be older in the past 577 because of more sluggish plate tectonics (e.g., Korenaga 2003; Bradley 2008; Herzberg et al. 2010; Condie et al. 2015; Pehrsson et al. 2016). The combination of greater chemical differentiation and 579 greater age would lead to a thicker subducting slab characterized by a larger radius of curvature, 580 which in turn affects the geometry of the wedge mantle ($\S 5$). The volume of the oceans was greater, 581 so there would be little stable dry landmass yet (Rosas and Korenaga 2021), limiting the amount 582 of terrigenous sediments. Because continents could have been more easily deformed, however, the 583 continental crust can subduct as slivers, which may undergo partial melting. There are a number of possibilities to explore by modeling, and such theoretical efforts would be crucial to interpret Archean igneous rock records with some confidence (e.g., Moyen and Laurent 2018). 586

In contrast to the episodic subduction hypothesis of van Hunen and Moyen (2012), which is

587

characterized by a relatively short interval (~10 Myr), some authors have advocated intermittent plate tectonics with long-term episodicity. The work of O'Neill et al. (2007) is one of them, and 580 as discussed in §2.1, their numerical modeling does not apply to Earth evolution. On the basis of 590 the structure of dynamical equilibria in terrestrial mantle convection, Sleep (2000) once speculated 591 that, if early plate tectonics could not release high radiogenic heat efficiently, a magma ocean 592 could reappear, and that a cycle of plate tectonics and a magma ocean may have repeated in the 593 early Earth. Moore and Lenardic (2015) made a similar claim. As pointed out by Korenaga (2016), however, these arguments based on dynamical equilibria are incorrect, because they do not take 595 into account the thermal inertia of Earth's mantle. Observational support for long-term episodicity, 596 including crustal age distribution, apparent polar wander velocities, and geochemical proxies for subduction flux (O'Neill et al. 2007; Silver and Behn 2008), is rather weak, as already reviewed by 598 Korenaga (2013). Korenaga (2013) noted, however, that the possibility of a widespread magmatic 590 shutdown between 2.45 and 2.2 Ga (Condie et al. 2009) warranted further consideration, because 600 it was based on a rare coincidence of multiple proxies, such as no arc-type greenstones or TTG 601 suites, major unconformities on most cratons, and a gap in deposition of banded iron formation. A 602 more recent global compilation shows that the 250-Myr gap in magmatic activity shrinks to only 603 \sim 50 Myr, from 2.26 Ga to 2.21 Ga (Spencer et al. 2018). Interestingly, their compilation also shows that this period is enclosed by a \sim 130-Myr gap in passive margin sedimentation. Given the 605 presence of stable dry landmasses back then (Korenaga et al. 2017), the cessation of plate tectonics 606 would not prevent passive margin sedimentation. Thus, this 50-Myr gap in magmatic activity, even if it is real, probably requires an explanation that does not invoke the absence of plate tectonics; it 608 may well be simply a preservation issue. 600

2.6 Heat pipe

The heat pipe model was originally proposed to explain why Jupiter's Moon Io could have both high heat flow and thick lithosphere (O'Reilly and Davies 1981). Moore and Webb (2013) pro-

posed that this model might also be applicable to the Hadean and early Archean Earth when radiogenic heat production was higher. Based on numerical simulation, they also suggested that declining heat production over time could lead to an abrupt transition to plate tectonics.

Their model is not described with sufficient details, so its assessment has to involve some de-616 tective work. For example, the snapshots of temperature field for their convection simulation (their 617 Figure 1) show very thick lithosphere, occupying the top 10-40 % of the model domain. It is 618 tempting to think that their model domain corresponds to the upper mantle; if so, the thickness of their model lithosphere varies from \sim 60 km to \sim 260 km, which is reasonable. However, they 620 state that dimensionless internal heating rate (H^*) , defined as $\alpha HD^2/k$, where α is thermal expan-621 sivity, H is volumetric heat production, D is the system depth, and k is thermal conductivity, is \sim 2 for the present-day Earth (their Figure 2). Using the present-day radiogenic heat production 623 of $4 \times 10^{-12}~W~kg^{-1}$ (or $1.3 \times 10^{-8}~W~m^{-3}$ with mantle density of 3300 kg m $^{-3}$) for the bulk 624 silicate Earth (Lyubetskaya and Korenaga 2007) and typical mantle values ($\alpha = 3 \times 10^{-5}~\text{K}^{-1}$ 625 and $k = 2 \text{ W K}^{-1} \text{ m}^{-1}$), one would get $H^* \sim 0.085$ if we assume D = 660 km, and $H^* \sim 1.64$ for D = 2900 km. Thus, their model domain actually corresponds to the whole mantle, and their 627 model lithosphere has a thickness of ~ 300 km to ~ 1200 km, which is too thick for stagnant lid 628 convection on Earth and would hardly allow mantle melting. The Rayleigh number used in their simulation is likely to be too low to simulate an Earth-like situation. They state that they varied the 630 internal-heating Rayleigh number from 10^6 to 3×10^8 , but they did not specify which viscosity was 631 used when calculating the Rayleigh number. When viscosity is spatially variable (as in the case of stagnant lid convection), one needs to specify which viscosity (e.g., surface viscosity, internal 633 viscosity, and bottom viscosity) is actually used for the Rayleigh number, and without this infor-634 mation, the quoted range of the Rayleigh number carries little meaning. In any case, it is a common 635 practice to use relatively low Rayleigh number for numerical simulation for various computational 636 reasons, but to apply such numerical results to terrestrial planets, we usually develop a scaling rela-637 tion so that low-Rayleigh-number results can be adequately extrapolated to high-Rayleigh-number 638

situations (e.g., Solomatov and Moresi 2000). Such an effort on scaling is absent in the work of
Moore and Webb (2013).

When they ran a model with a decaying heat production, they started with a dimensionless 641 internal heating rate of 30, which is 18 times higher than the present-day value. With the present-642 day abundance ratio of radiogenic isotopes (U:Th:K = 1:4: (1.27×10^4) , 238 U/U = 0.9927, 235 U/U 643 = 0.0072, all Th is 232 Th, and 40 K/K = 1.28×10^{-4}), radiogenic heat production is only ~ 5 times greater even at 4.5 Ga, and to expect a 30-hold increase in heat production, the age of Earth has to be extended to \sim 7 Ga. Their model exhibits the first plate-breaking event (i.e., onset of subduction) 646 at a dimensionless time of 0.125 (their Figure 4). Their method description states that the time scale 647 is nondimensionalized by the diffusion time scale, D^2/κ , where κ is thermal diffusivity. With κ of 10^{-6} m² s⁻¹ and D of 2900 km, the diffusion time scale is 267 Gyr, so the dimensionless time 640 of 0.125 for subduction initiation is equivalent to \sim 33 Gyr. Even if we start the history of Earth 650 at 7 Ga, this subduction initiation corresponds to an event in the far distant future, at 26 Gyr from 651 now. In comparison, it takes only \sim 5 Gyr from now for our Sun to turn into a red giant and engulf 652 Earth (Schröder and Smith 2008). One possible way to keep their study relevant to Earth history, 653 though not technically correct, is to make use of the fact that the dimensionless internal heating 654 rate is varied from 30 to 10 in their model during a dimensionless period of 0.15 (their Figure 4), which indicates a dimensionless half-life of ~ 0.095 . Because the effective half-life of the relevant 656 radiogenic isotopes is \sim 2.6 Gyr, it may be possible to interpret a dimensionless time of 0.15 as 657 ~4.1 Gyr. With the age of Earth of 4.5 Ga, the model of Moore and Webb (2013) would then imply incipient plate tectonics in the Devonian. Nevertheless, the heat pipe model of Moore and 659 Webb (2013) has been cited as an early Earth process by the proponents of the mid-Archean onset 660 of plate tectonics (e.g., Cawood et al. 2018) as well as the Neoproterozoic onset of plate tectonics (e.g., Stern 2018). It is difficult to further examine their model because some basic information 662 on the assumed mantle rheology is missing, including the degree of temperature dependence of 663 viscosity (the so-called Frank-Kamenetskii parameter) and the yield stress.

The heat-pipe model is essentially stagnant lid convection with magmatism, and such dynamics 665 had already been studied by others (e.g., Reese et al. 1999, 2007). In particular, Korenaga (2009) 666 developed a scaling of stagnant lid convection with mantle melting, and this scaling has been used to study the evolution of Mars (Fraeman and Korenaga 2010) as well as terrestrial planets at large 668 (O'Rourke and Korenaga 2012). In those models, mantle rheology, internal heating, and mantle 669 melting are treated in a self-consistent manner to solve the coupled crust-mantle-core evolution, 670 and one representative result for an Earth-sized planet is shown in Figure 6. As the initial mantle potential temperature in this example is relatively low (1700 K), it takes ~ 0.7 Gyr for the mantle 672 to warm up and start melting extensively; for a hotter initial condition, one can simply imagine 673 that extensive mantle melting starts from the beginning. The basaltic crust grows to a thickness of \sim 70 km over a period of \sim 0.5 Gyr, and because heat-producing elements are all highly incompat-675 ible elements, they are mostly partitioned into the crust, leaving the mantle severely depleted in 676 those elements. Because of this high internal heating in the crust, the crust experiences repeated 677 melting for ~ 3 Gyr (until the Moho temperature starts to decline; Figure 6b). The mantle is largely 678 insulated by this hot crust, so it cools down only slowly. In other words, the declining internal heat-679 ing has little to do with the thermal state of the mantle, and it does not bring a drastic change to 680 mantle temperature and thus to convective stress as well, contrary to the suggestion made by Moore and Webb (2013). More important, because of the high internal heating within the crust, the crust 682 retains a high geotherm for ~ 3 Gyr. A heat-pipe Earth, if modeled correctly, does not yield a 683 low geothermal gradient across the bulk of the lithosphere, failing to satisfy perhaps the most im-684 portant observation among the geological evidence considered by Moore and Webb (2013). This 685 is critical, because other cited observations, such as rapid volcanic resurfacing, contractional de-686 formation, and burial of hydrated crust, can also be explained by plate tectonics, especially when 687 relevant geological records are spatially limited (recall the issue of preservation bias discussed at the beginning of $\S 2$). 689

As mentioned in §2.1, if the condition for plate tectonics is determined by the presence of

690

surface water, it is difficult to expect the onset of plate tectonics in the middle of Earth history, because Earth is supposed to have been covered by oceans for most of its history. The persistent 692 operation of plate tectonics, not just one-time subduction initiation, must involve similarly persis-693 tent weakening of strong oceanic lithosphere. A likely secular change in the convective stress by 694 declining internal heat production would be too minute in the real mantle to affect the mechanical 695 stability of lithosphere (Figure 1i); numerical studies claiming differently (e.g., O'Neill et al. 2007; 696 Moore and Webb 2013) are compromised by oversight in their model setup. As reviewed by Korenaga (2020), grain-size reduction (e.g., Bercovici and Ricard 2014; Foley 2018) does not affect 698 the strongest part of lithosphere, underlining the critical role of thermal cracking in activating plate 690 tectonics. With surface water, thermal cracking can reduce the yield strength of lithosphere down to \sim 100 MPa, regardless of mantle potential temperature (Figure 5). If this weakening mechanism 701 is important for the current operation of plate tectonics, then, it would also allow plate tectonics in 702 the early Earth (e.g., Korenaga 2011). 703

704 3 Evolution of continental crust through Earth history

As reviewed in the previous section, the popular notion of mid-Archean onset of plate tectonics, with stagnant lid convection in the early Earth, is not built on careful theoretical studies nor robust 706 geological evidence. In particular, the lack of theoretical requirement for stagnant lid convection 707 in the early Earth (§2.1) undermines the generality of field-based suggestions for the mid-Archean onset of plate tectonics (e.g., Van Kranendonk et al. 2007), as the spatial extent of the relevant 709 field area is trivial (§2). The very paucity of geological data in deep time, therefore, highlights 710 the importance of the two approaches mentioned in §1, i.e., focusing on the geochemical data that 711 are sensitive to the growth of continental crust, which could inform us of the likely geodynamic regime in the Hadean, and understanding the consequences of magma ocean solidification, which 713 would constrain how subsolidus mantle convection started on Earth. The preservation issue is still 714 problematic for the first approach with geochemical data, as the number of relevant localities is limited, but by using geochemical modeling, we can at least attempt to consider them simultaneously in a global framework. As such, the role of modeling is paramount. Just as the interpretation
of geochemical data always involves a certain set of assumptions, the reliability of modeling results depends on modeling assumptions. Furthermore, as regard to continental growth, no single
kind of geochemical probe would provide a decisive answer, and it would be important to combine
different kinds of geochemical data by appreciating their relative strengths and weaknesses.

The persistent generation of felsic continental crust on a substantial scale requires the continuous subduction of water into the mantle (e.g., Campbell and Taylor 1983), for which plate tectonics 723 is essential. Other mechanisms have been proposed to generate felsic magma, such as the melting 724 of hydrated crust by reheating (e.g., Petford and Gallagher 2001; Annen et al. 2006) or delamination (e.g., Sizova et al. 2015; Rozel et al. 2017; Piccolo et al. 2019), but these mechanisms are 726 incapable of generating a sizable amount of felsic magma. Some numerical studies suggest that 727 the delamination mechanism can account for a large fraction of early continental crust (e.g., Rozel 728 et al. 2017), but as discussed in §2.4, a closer look at these studies reveals that the efficacy of de-729 lamination is likely to have been exaggerated. The history of continental growth, therefore, could 730 directly constrain when plate tectonics started on Earth, and such a constraint is invaluable for a 731 better understanding of Hadean geodynamics. In this section, I will first touch on some persistent confusions in the study of continental growth; this is important because knowing what went wrong 733 in the past helps to avoid repeating the same mistakes. I will then discuss recent growth models 734 and their implications for the composition of early continental crust as well as the possible regimes 735 of Hadean geodynamics.

3.1 Some remarks on the history of crustal growth research

Whereas continental growth has always been a controversial topic, discussion was mostly reasonable until the 1990s. In particular, there are quite a few seminal papers published in the 1980s (e.g., Armstrong 1981b; Nelson and DePaolo 1985; Patchett and Arndt 1986; Jacobsen 1988), and

there was little confusion about the difference between "net crustal growth" and "formation age distribution" back then. It is vital to understand this difference. The former refers to how the mass of the continental crust has changed through time, whereas the latter describes the present-day distribution of the formation ages of the extant continental crust. These two can coincide only if no crust has been lost to the mantle, and any difference between them reflects the time-integrated effect of crustal recycling by subduction or delamination (Figure 7a).

It may be too obvious a statement that net crustal growth and formation age distribution are two different things, but this distinction has been largely absent in the literature since the 1990s, 748 i.e., when zircon-based studies on crustal evolution started to become popular. Because each zir-749 con grain provides its own crystallization age, and because detrital zircons represent some broad region of upper continental crust, a considerable amount of geochronological and geochemical 751 information can be extracted from detrital zircons. Apparently, the advent of this fascinating ge-752 ological probe gave some people an impression that zircon can address net crustal growth as well 753 (e.g., Rino et al. 2004; Condie and Aster 2010), though it is only the formation age distribution of 754 the extant continental crust, not net crustal growth, that can be inferred from detrital zircons (see, 755 for example, Figure 12 of Hawkesworth et al. (2010)). Then, Belousova et al. (2010) proposed a 756 new method to estimate a crustal growth curve using both the U-Pb crystallization age distribution and the Hf model age distribution of detrital zircons. As demonstrated in §2.2, their method 758 can produce only an artifact, but this reality escaped the notice of most geologists (the work of 759 Payne et al. (2016) appears to be a rare exception). On the contrary, their method was promoted by Dhuime et al. (2012), with some modification to incorporate oxygen isotope data, and the model of 761 Dhuime et al. (2012) has been repeatedly advertised by a series of review papers written by these 762 authors (Cawood et al. 2013; Kemp and Hawkesworth 2014; Hawkesworth et al. 2016; Dhuime 763 et al. 2017; Hawkesworth et al. 2017; Cawood et al. 2018; Hawkesworth et al. 2019). They often try to corroborate the model of Dhuime et al. (2012) by citing other similar growth models (e.g., 765 Campbell 2003; Pujol et al. 2013), but there are a wide variety of different looking growth models

in the literature (see Korenaga (2018a) for the strengths and weaknesses of these models). The model of Dhuime et al. (2012) has been widely cited, and it has affected a large number of pa-768 pers that relied on their crustal growth model. One recent example is the work of Dhuime et al. 769 (2018), who attempted to estimate the rates of generation and destruction of continental crust by box modeling. Their approach suffers from the assumption that the model of Dhuime et al. (2012) 771 represents net crustal growth. They also do not distinguish between the formation age distribution 772 and the surface age distribution (Figure 7a), thereby neglecting the important difference between crustal recycling (loss of crustal materials to the mantle) and crustal reworking (intracrustal pro-774 cesses). Such a misunderstanding of fundamentals would prevent a sensible estimate on the rates 775 of generation and destruction of continental crust.

7 3.2 New models of continental growth

Continental growth models can be categorized into three groups: (1) crust-based, (2) mantle-based, 778 and (3) others (Korenaga 2018a). Crust-based models are based on the formation age (or its proxy) 779 distribution of the continental crust that has been preserved to the present, and they can serve as the lower bound on net crustal growth. Though it is not about net growth, it is still important to properly 781 estimate the formation age distribution, which can constrain the extent of crustal recycling, once net 782 crustal growth is independently obtained, and also the extent of crustal reworking when combined with the surface age distribution (Figure 7a). In this regard, zircon-based models directly use the U-784 Pb crystallization ages of zircons (e.g., Rino et al. 2004) are unsatisfactory because crystallization 785 ages can be reset by intracrustal melting processes, thereby being more relevant to the surface age 786 distribution. The (igneous) formation age of a crustal rock refers to the time when the rock was first 787 extracted from the mantle by partial melting. Ancient zircons could experience many episodes of 788 crustal reworking (e.g., Iizuka et al. 2010), so crystallization ages, which can be reset by remelting, 789 tend to be biased to younger ages. Belousova et al. (2010) tried to correct for this bias by utilizing the Hf model ages of zircons, but they did not succeed (see §2.2). Korenaga (2018b) proposed a new method to estimate the formation age from the pair of the U-Pb crystallization age and the Hf model age of zircon (Figure 3, red lines), and he estimated the formation age distribution based on the database of detrital zircon ages compiled by Roberts and Spencer (2015) (Figure 8b).

Mantle-based models aim to constrain net crustal growth by tracking the depletion history of 795 the mantle, on the basis of the complementary nature of the continental crust and the depleted 796 mantle. That is, if the mantle at a certain time in the past was similarly depleted in some incom-797 patible elements as the present-day mantle, it indicates that the mass of continental crust at that time should be similar to the present-day mass, assuming that the continental crust back then was 790 similarly enriched in these elements. The coupled ¹⁴⁶Sm-¹⁴²Nd and ¹⁴⁷Sm-¹⁴³Nd system is a par-800 ticularly convenient tracer because of the vastly different half-lives of these two parent-daughter pairs; 146 Sm decays to 142 Nd with a half-life of \sim 103 Myr, whereas 147 Sm decays to 143 Nd with 802 a half-life of ~ 106 Gyr. The former is sensitive to crustal growth in the early Earth, and the latter 803 constrains the long-term depletion history. This coupled isotope system has been used to discuss 804 continental growth (e.g., Jacobsen and Harper 1996; Caro et al. 2006), but in recent years, the 805 interpretation of ¹⁴²Nd data in terms of mantle mixing (with or without the effect of continent ex-806 traction) has become more popular (e.g., Bennett et al. 2007; Debaille et al. 2013; Rizo et al. 2013; 807 Roth et al. 2014; Saji et al. 2018). Although some authors argued for the operation of stagnant lid convection in the early Earth based on such a mixing-based interpretation (e.g., Debaille et al. 800 2013), such an interpretation has been suggested to suffer from nonuniqueness if one considers the 810 effect of continent extraction (Roth et al. 2014). More important, the mixing model of Roth et al. 811 (2014), which is a generalization of the box model of Caro et al. (2006), points to the possibility of 812 rapid crustal growth and recycling in the early Earth. This is because, in their box model, the sizes 813 of the crust and mantle reservoirs do not change with time (probably just for the sake of simplic-814 ity), which is equivalent to the instantaneous formation of the continental crust with the present-day mass at the beginning of Earth history, and because their estimate of the crustal residence time is 816 as short as 500 Myr, which translates to the crustal recycling rate of 4×10^{22} kg Gyr⁻¹. This recy-817

cling rate is several times higher than the present-day recycling rate based on sediment subduction (Scholl and von Huene 2007; Stern and Scholl 2010).

Intrigued by this possibility, Rosas and Korenaga (2018) revisited this coupled isotope sys-820 tem with a more flexible parameterization of continental evolution and found that the available 821 ¹⁴²Nd/¹⁴⁴Nd and ¹⁴³Nd/¹⁴⁴Nd data are indeed consistent with the scenario of rapid crustal growth 822 and recycling in the early Earth (Figure 8). The crustal generation rate and the crustal recycling rate 823 both have to be sufficiently high to explain the ¹⁴²Nd/¹⁴⁴Nd data in the Archean, and they should then decline with time to explain the long-term trend of ¹⁴³Nd/¹⁴⁴Nd data over Earth history. It is 825 noted that the model of Rosas and Korenaga (2018) successfully reproduces the aforementioned 826 estimates on the present-day recycling rate without being forced to do so. Such rapid crustal growth is similar to what Armstrong suggested a few decades ago (Armstrong 1981a, b) (Figure 8a). The 828 Armstrong model has long been regarded as an unlikely end-member (the status of his model de-820 scribed in his valedictory paper (Armstrong 1991) has remained mostly the same), and one of the 830 main reasons behind this unpopularity is the nearly total absence of Hadean crust in the geological 831 record. Such criticism, however, does not appreciate that net crustal growth is maintained by a 832 dynamic balance between crustal generation and recycling (Figure 7b). In the presence of crustal 833 recycling, no net growth does not mean that the once produced crust remains intact; quite the contrary, to maintain zero net growth, the continental crust has to be kept generated and thus reju-835 venated. To place this argument on a quantitative ground, Rosas and Korenaga (2018) calculated 836 the present-day formation age distribution corresponding to their estimate of crustal generation and 837 recycling rates, which happens to be in good agreement with the formation age distribution esti-838 mated from detrital zircons (Korenaga 2018b) (Figure 8b). This level of agreement is unexpected 839 because the Nd isotope modeling of Rosas and Korenaga (2018) is not designed to fit the formation age distribution.

It is important to understand, however, that Nd isotope data alone, even with both ¹⁴²Nd/¹⁴⁴Nd and ¹⁴³Nd/¹⁴⁴Nd, do not uniquely constrain crustal evolution. The parameterization of Rosas and

Korenaga (2018) is flexible enough to cover most of existing growth models, but it is still limited to monotonic temporal variations in crustal growth and recycling (see Hyung and Jacobsen (2020) 845 for an example of non-monotonic crustal evolution). It thus becomes essential to test whether any suggested scenario of crustal evolution conforms to other observational constraints. The formation 847 age distribution is one such constraint. For example, if we calculate the formation age distribu-848 tion corresponding to the non-monotonic growth model of Hyung and Jacobsen (2020) (i.e., their 849 "modified Jabobsen & Harper" model, in which instantaneous growth at 4.5 Ga is followed by 0.5 Gyr of no crustal generation and recycling), we would find that \sim 6 % of the present-day conti-851 nental crust should have a formation age of 4.5 Ga. As the total of exposed and buried Archean 852 crust occupies only ~8 % of the present-day continental crust (Goodwin 1996), their model indicates that the majority of the preserved Archean crust would have originally formed right at the 854 beginning of Earth history. Checking with the formation age distribution thus helps to eliminate 855 unrealistic scenarios. Another important constraint is the secular evolution of continental basalt 856 chemistry. The work of Keller and Schoene (2018) suggests that the source mantle has been simi-857 larly depleted over the past 3.8 Gyr, which is equivalent to the mass of the continental crust being 858 roughly at the present-day level over that period. The net growth model of Rosas and Korenaga 850 (2018) is consistent with this observation as well.

The importance of constraining crustal evolution from a variety of angles naturally leads us to the third kind of growth models. Models in this category also aim at net crustal growth, but using less direct inference than mantle-based models. As reviewed by Korenaga (2018a), most of such indirect inferences are problematic. The model of Reymer and Schubert (1984), for example, depends critically on their assumption on the thermal evolution of Earth, which has since been shown to be inconsistent with a number of observations, such as the thermal budget of Earth (Lyubetskaya and Korenaga 2007), the cooling history of the upper mantle (Herzberg et al. 2010), and the atmospheric budget of radiogenic xenon (Padhi et al. 2012). An exception is the model of Pujol et al. (2013), which is based on the degassing history of radiogenic argon. Argon degassing,

however, depends not only on the generation of continental crust and its recycling, but also on other processes such as crustal reworking and mid-ocean-ridge magmatism. To make use of the 871 available argon data, therefore, we need to be able to model the coupled atmospheric-crust-mantle 872 system in a holistic manner. To this end, Guo and Korenaga (2020) constructed a new geochemical 873 box model in which the thermal evolution of Earth, crustal evolution, and argon degassing were 874 combined self-consistently. We now have reasonably sufficient observations to deconvolve those 875 processes, such as the potential temperature evolution of the mantle during the Proterozoic and the Archean (Herzberg et al. 2010) for mid-ocean ridge magmatism and the distributions of surface 877 age and crustal formation age (Roberts and Spencer 2015; Korenaga 2018b) for crustal recycling 878 and reworking. The net growth model of Guo and Korenaga (2020) is also similar to the Armstrong model, characterized by rapid crustal growth and recycling in the early Earth (Figure 8). Argon 880 degassing has been modeled repeatedly in the literature (e.g., Schwartzman 1973; Hamano and 881 Ozima 1978; Sleep 1979; Allegre et al. 1987; Tajika and Matsui 1993; Pujol et al. 2013; Stuart et al. 882 2016), but the full effect of crustal evolution, including both crustal recycling and reworking, on 883 argon degassing was not considered before. To assess the extent of crustal recycling and reworking, 884 a proper estimate on the formation age distribution is essential (Figure 7), which was not available 885 until recently.

The growth models of Rosas and Korenaga (2018) and Guo and Korenaga (2020) are both 887 similar to the Armstrong model, but they differ considerably in details (Figure 8). In terms of 888 the middle 50 % of their successful solutions, the start of crustal growth is tightly constrained 889 to 4.5-4.4 Ga in the former, whereas it is shifted to \sim 4.1-4.3 Ga in the latter (Figure 8a). They 890 are both characterized by high crustal generation and recycling rates in the early Earth, but the 891 crustal generation rate in the model of Rosas and Korenaga (2018) is twice as high as that in the 892 model of Guo and Korenaga (2020) (Figure 8c), and the opposite is the case for the crustal recycling rate (Figure 8d). Both models are consistent with the present-day formation age distribution 894 (Figure 8b), the present-day crustal recycling rate (Scholl and von Huene 2007; Stern and Scholl

2010), and the secular evolution of continental basalt chemistry over the past 3.8 Gyr (Keller and Schoene 2018), but the above differences indicate substantially different tectonics for >3 Ga. This 897 discrepancy between the two models is not unexpected because how crust-mantle differentiation 898 is treated differs between them. For example, in the model of Rosas and Korenaga (2018), only a 890 fraction of the whole mantle participates in differentiation, with the rest of the mantle remaining 900 primitive, and this is what has long been done for the geochemical modeling of Nd isotopes. On 901 the other hand, the whole mantle is prone to degassing in the model of Guo and Korenaga (2020), which is an attribute inherited from the classic work of Hamano and Ozima (1978). To reconcile 903 the differences between these models, it will be important to evaluate each of modeling assump-904 tions, and to build a more versatile model that can treat multiple isotope systems simultaneously. In the model of Rosas and Korenaga (2018), the fraction of the depleted mantle is time-invariant, 906 but it may be more realistic to assume that it grows with time (e.g., McCulloch and Bennett 1994). 907 In the model of Guo and Korenaga (2020), the mode of degassing changes from sudden degassing 908 to continuous degassing, and this change is supposed to coincide with the Moon-forming giant 909 impact. However, relatively large bolides (>1500 km in diameter) probably continued to bombard 910 Earth even after the giant impact (Marchi et al. 2018). Furthermore, both models start with a homo-911 geneous primitive mantle, but it is difficult to justify such an initial condition if one considers how a magma ocean would solidify (§4). The consideration of these realistic complications may help to 913 assimilate different geochemical constraints into a unifying model of crust-mantle differentiation. 914 An attempt to interpret geochemical data in a manner consistent with relevant geophysical and 915 geological observations has begun only recently, and it will probably take at least a few revisions 916 before we arrive at a fully satisfactory model of crustal evolution. 917

3.3 Composition of the early continental crust

018

The composition of early continental crust has been as controversial as the net growth of continental crust. One prevailing view is that the early continental crust is much more mafic than the

present-day crust (e.g., Taylor and McLennan 1985). This view is based primarily on the observed difference in trace element chemistry between Archean and post-Archean sedimentary rocks. As 922 noted by Harrison (2009), however, fine-grained Archean sediments were mostly derived from 923 greenstone belts, and the difference between Archean and post-Archean sediment chemistry may 924 represent an environmental, rather than temporal, difference. Interestingly, it is known that the 925 exposed continental crust itself does not exhibit a notable secular change in chemical composition 926 (Condie 1993). As discussed in §2.3, more recent analyses on the global database of sedimentary rocks suggest that the continental upper crust in the Archean is not so mafic as commonly believed 928 (Greber and Dauphas 2019; Ptacek et al. 2020). 920

Previous studies on the composition of early continental crust, whether they are based on sed-930 iment chemistry or exposed continental crust, are necessarily restricted to the upper continental 931 crust. Here I would like to take a broader view and consider possible secular changes in the com-932 position of the entire continental crust. One popular notion is that the Archean continental crust was 933 less internally differentiated than the modern continental crust (e.g., Taylor and McLennan 1985; Kemp and Hawkesworth 2003), and internal differentiation can enrich the upper crustal composi-935 tion with incompatible elements while keeping the same bulk composition. The net growth models 936 discussed in the previous section provide some insights into this matter. This is because, in the model of Rosas and Korenaga (2018), the crustal enrichment factors for Nd and Sm, which can 938 be regarded as the effective partition coefficients for these elements, are treated as time-varying 930 parameters to be determined by inversion. The successful solutions of Rosas and Korenaga (2018) 940 show that these enrichment factors are nearly constant through time, indicating that the crustal 941 composition also does not change with time, at least in terms of Nd and Sm. Admittedly, this is 942 not a particularly strong constraint because Nd and Sm are only moderately incompatible elements 943 with their partition coefficients being on the order of 0.1. However, a similar conclusion can be drawn even from the argon degassing modeling of Guo and Korenaga (2020), which is sensitive to 945 the crustal concentration of potassium. Potassium is a highly incompatible element, with a parti-

tion coefficient of ~ 0.01 , and a high potassium content is an important indicator for felsic rocks. In the model of Guo and Korenaga (2020), the crustal concentration of potassium is assumed to be 948 constant through time, and yet, their net growth model shows that the mass of continental crust is 949 already at the present-day level by the mid-Archean (Figure 8a). This means that if the Archean 950 crust were less felsic, its mass had to be greater than present. Though such a possibility is oc-951 casionally entertained in the literature (e.g., Fyfe 1978; McCoy-West et al. 2019), it would lead 952 to a unrealistic surface environment. The present-day potassium concentration of the continental 953 crust is estimated to be ~ 1.5 wt% (Rudnick and Gao 2003), and if its concentration in the early 954 continental crust is, for example, only 0.5 wt%, then, the Earth's surface would be occupied almost 955 fully by the continental crust in the Archean, because the continental crust is unlikely to have been much thicker in the past (Galer and Mezger 1998). This is a self-contradictory situation; a plane-957 tary surface mostly covered by continents would not allow the operation of plate tectonics, which 958 is essential for the generation of continental crust and its recycling. Parenthetically, the existence 959 of continental mass even at the present-day level in the Proterozoic and the Archean is already 960 troublesome for the geologists who work on continental reconstruction (e.g., Evans 2013). The 961 present-day formation age distribution shows that the amount of the continental crust preserved to 962 present decreases to $\sim 60 \%$ of the present-day mass when evaluated at 2 Ga and to only $\sim 20 \%$ at 3 Ga (Figure 8b). 964

965 3.4 Hadean geodynamics inferred from crustal evolution

Whereas the details differ, the new growth models of Rosas and Korenaga (2018) and Guo and Korenaga (2020) both suggest rapid crustal growth and efficient crustal recycling in the Hadean, and the model of Guo and Korenaga (2020) suggests that it may have persisted until the midArchean (Figure 8). As discussed in §2.4 and §3.1, the operation of plate tectonics is likely to be required for such a combination of crustal generation and recycling. If it is just to create a massive amount of felsic crust at the beginning of Earth history, some peculiar situation associated with the

solidification of a magma ocean might be sufficient (e.g., Morse 1986; Harrison 2009). However, such a crust has to be destroyed quickly at the same time, and crust generation has to continue 973 through the rest of Earth history. The most parsimonious explanation for such crustal evolution 974 would be the continuous operation of plate tectonics since the solidification of a magma ocean. 975 The onset time of plate tectonics on Earth is another controversial subject (e.g., Condie and Kröner 976 2008; Van Kranendonk 2010; Korenaga 2013), because one of the defining attributes of plate 977 tectonics is the recycling of the surface layer. That is, the very operation of plate tectonics leads to the absence of its evidence. Also, as we go deeper in time, available rock records become more 979 sparse, making it more difficult to generalize from local geological observations. Preservation bias 980 can be severe; the fact that a certain region has survived the billion years of plate tectonic recycling may suggest that the region is not a normal sample (§2). In this regard, crustal evolution inferred 982 from the history of argon degassing is notable. Being a heavy noble gas, argon, once degassed from 983 the solid Earth, remains in the atmosphere, and the argon isotope ratio in the atmosphere can always 984 be considered to be homogeneous. Thus, the atmospheric argon stores the time-integrated history 985 of degassing on a global scale, and argon-based inferences suffer much less from preservation bias 986 than typical rock-based inferences. The crustal evolution model of Guo and Korenaga (2020), 987 therefore, lends a strong support for the onset of plate tectonics in the Hadean (e.g., Watson and Harrison 2005; Hopkins et al. 2008, 2010; Korenaga 2011; Turner et al. 2014, 2020). 989

Assuming that plate tectonics started in the Hadean, the estimated rates of crustal generation and recycling suggest that the tempo of plate tectonics must have been much faster in the early Earth. This is contrasting to the regime of sluggish plate tectonics that most likely prevailed in the Proterozoic and the late Archean (e.g., Korenaga 2006; Herzberg et al. 2010). The geodynamic rationale for more sluggish plate tectonics, when the mantle was hotter in the past, is that, because of the effect of partial melting on mantle viscosity and density, a hotter mantle results in a thicker lithosphere. Obviously, such a physical framework developed around modern plate tectonics does not explain rapid plate tectonics in the Hadean. It appears that we need a drastically different

kind of plate tectonics. One reasonable starting point to search for a new geodynamic regime is the solidification of a putative magma ocean, which marks the initiation of subsolidus mantle convection.

4 Physics and chemistry of magma ocean solidification

4.1 1993: Annus mirabillis

1001

1002

According to the current understanding of planetary formation (e.g., Chambers 2014), the late-1003 stage accretion of Earth-size planets is characterized by multiple giant impacts, and in case of 1004 Earth, the last of such giant impacts is considered to be responsible for the formation of the Earth-1005 Moon system. Numerical studies of the Moon-forming giant impact suggest that the kinetic energy 1006 imparted by the impactor on the proto-Earth would be sufficient to melt a substantial fraction of the 1007 mantle (e.g., Canup 2004; Asphaug 2014). Whereas various authors had discussed how a magma 1008 ocean would solidify (e.g., Hofmeister 1983; Ohtani 1985; Kato et al. 1988; Tonks and Melosh 1000 1990), it is not until 1993 that a firm theoretical ground was laid out by a series of groundbreaking 1010 papers (Abe 1993a, b; Solomatov and Stevenson 1993a, b, c). In particular, the theoretical exposi-1011 tion in the 1993 trilogy of Solomatov and Stevenson is so comprehensive that no major theoretical 1012 development is needed since then (Solomatov 2000, 2015). The scenarios of magma ocean solid-1013 ification depicted by these papers were, however, still largely qualitative. The reason is simple. 1014 Because the slope of the mantle liquidus is generally steeper than that of the mantle adiabat, a 1015 magma ocean would start to solidify from the bottom, e.g., from the core-mantle boundary in case 1016 of a whole-mantle magma ocean. Therefore, to model the solidification of a deep magma ocean 1017 expected from the Moon-forming giant impact, we need to have a good understanding of mantle 1018 melting under lower mantle conditions, which was not available in the early 1990s. In the modeling 1019 of Abe (1993b), for example, the mantle solidus and liquidus are assumed be offset by only 200 K 1020 at all depths, and the melt fraction is assumed to vary linearly from solidus to liquidus. Melting in

the lower mantle was treated more carefully by Solomatov and Stevenson (1993b), but owing to the lack of reliable experimental control, they had to explore a range of possibilities, leaving their discussion mostly provisional.

The melting of lower mantle materials is a long-standing challenge in high-pressure mineral 1025 physics (e.g., Boehler 2000; Boehler and Ross 2015). The lower mantle is composed of three min-1026 erals, Si-perovskite, ferropericlase, and Ca-perovskite, with the first two making up about 90 %, 1027 and even the melting behaviors of these constituent minerals have been controversial. A good ex-1028 ample is the melting curve of MgO, which is a Mg end-member of ferropericlase. It has taken more 1020 than two decades for experimental studies to converge, with an initial suggestion of relatively low 1030 melting temperatures (Zerr and Boehler 1994), followed by much higher temperatures (Zhang and 1031 Fei 2008), and then somewhere in-between (Du and Lee 2014; Kimura et al. 2017). Theoretical 1032 attempts on MgO melting took a similarly tortuous path (e.g., Strachan et al. 1999; Alfè 2005; de 1033 Koker and Stixrude 2009). The melting experiments of peridotite (i.e., polymineralic assemblage) 1034 over the entire lower mantle conditions have become possible only in the last decade (Figuet et al. 1035 2010; Andrault et al. 2011; Nomura et al. 2014), though with somewhat conflicting results, part of 1036 which may be ascribed to different starting materials used in those studies. High-pressure melting 1037 experiments are still technically demanding, and the level of expectations in experimental accuracy 1038 is different from that for melting experiments relevant for crust and upper mantle; for example, it is 1039 not uncommon to see nontrivial differences between reported initial and final system compositions 1040 in high-pressure studies (e.g., Nomura et al. 2011; Tateno et al. 2014). Francis Birch once noted 1041 that terms like "certain," "undoubtedly," and "positive proof" in the high-pressure mineral physics 1042 literature actually meant, respectively, "dubious," "perhaps," and "vague suggestion" (Birch 1952, 1043 p. 234), and it may be prudent to keep this in mind even today. 1044

The persistent uncertainty in the melting of lower mantle did not discourage the exploration of new ideas for magma ocean solidification. Motivated by the possibility that the mantle liquidus may become less steep than the adiabat at the lowermost mantle (Mosenfelder et al. 2007),

1045

1046

1047

for example, Labrosse et al. (2007) suggested that the terrestrial magma ocean may have started to solidify from the mid-mantle, leaving a basal magma ocean above the core-mantle boundary. 1040 Solidification from the mid-mantle is also suggested from later theoretical studies (Stixrude et al. 1050 2009; Boukaré et al. 2015), though such a scenario is inconsistent with the experimentally deter-1051 mined liquidus (Fiquet et al. 2010; Andrault et al. 2011). On a different thread, Elkins-Tanton 1052 (2008) suggested that the fractional crystallization of a magma ocean may have created a gravi-1053 tationally unstable structure, which then could have been overturned to a stable, compositionally 1054 stratified structure by the Rayleigh-Taylor instability. Plesa et al. (2014), however, pointed out that 1055 such a stratified structure would be too stable to allow subsequent convection. More recently, it 1056 is suggested that the Rayleigh-Taylor instability can take place before a magma ocean solidifies 1057 completely, which tends to homogenize the solidified mantle (Maurice et al. 2017; Ballmer et al. 1058 2017; Boukaré et al. 2018). 1059

If a magma ocean solidifies from the mid-mantle, the formation of a basal magma ocean would 1060 be inevitable, which has profound implications for the thermal and chemical evolution of Earth 1061 (e.g., Labrosse et al. 2007; Garnero et al. 2016). This possibility, however, depends critically on 1062 the details of mantle liquidus, on which there is no consensus (e.g., Stixrude et al. 2009; Fiquet 1063 et al. 2010). The gravitational stability of a solidifying magma ocean would shape the initial phase 1064 of mantle convection, but it has always been studied using a radically simplified thermodynamics 1065 of mantle melting (e.g., Elkins-Tanton 2008; Ballmer et al. 2017), which makes it difficult to 1066 quantitatively assess existing arguments. To break these impasses, some major improvement on 1067 our understanding of lower mantle melting is clearly needed. 1068

4.2 Thermodynamics of lower mantle melting

1060

To model the solidification of a magma ocean, knowing the phase diagram of a pyrolitic mantle is not enough, even if it covers the entire mantle depth. As soon as the mantle adiabat crosses the mantle liquidus and solidification starts, crystals can be fractionated, changing the local system

composition. Thus, to track the chemical evolution of magma ocean solidification, we have to be able to calculate a phase diagram for a wide range of possible mantle composition. Given the availability of a comprehensive thermodynamic database for mantle minerals (Stixrude and Lithgow-Bertelloni 2011), what we need is a self-consistent thermodynamic database for silicate liquids, which is necessary to conduct Gibbs energy minimization. For low pressures, there exist a few options such as used in MELTS (Ghiorso et al. 1983, 2002) and THERMOCALC (Holland and Powell 1998), but for high pressures relevant to lower mantle melting, there was nothing of the sort until very recently.

The closest one available was the work of Boukaré et al. (2015), who, on the basis of the theoretical work of de Koker and Stixrude (2009) on the MgO-SiO₂ system, built a self-consistent thermodynamic database for the MgO-FeO-SiO₂ system up to 140 GPa. Starting with this simple ternary system is reasonable because these three components represent more than 90 wt% of the mantle. Their approach is to supplement the theoretical prediction of de Koker and Stixrude (2009) with the thermodynamic data of FeO liquid and the non-ideal mixing parameters between FeO and SiO₂, which were obtained by fitting to relevant experimental data, such as the melting curve of FeO (Fischer and Campbell 2010), the density of liquid Fe₂SiO₄ (Thomas et al. 2012), and Mg/Fe partitioning between melt and silicates (e.g., Nomura et al. 2011; Tateno et al. 2014). Gibbs energy minimization using the resulting database, however, does not reproduce well the melting behavior of peridotite (Fiquet et al. 2010; Andrault et al. 2011) (see Figure 8 of Boukaré et al. (2015)). This discrepancy may be owing to the presence of other minor elements in the materials used in those experimental studies.

More recently, Miyazaki and Korenaga (2019a) also attempted to build a self-consistent thermodynamic database for the MgO-FeO-SiO₂ system, but with a different approach. They
developed a new nonlinear inverse method to estimate a set of relevant thermodynamic parameters
directly from a collection of experimental melting temperatures. They first benchmarked their inverse method with synthetic data, confirming that the new approach can recover the correct answers

within uncertainty. Then, they tested a different combinations of experimental data, to find out that 1099 it was impossible to obtain an acceptable solution if the experimental data of Andrault et al. (2011) 1100 were included; their liquidus temperatures appear to be simply too low. The inclusion of Andrault 1101 et al. (2011) data resulted in severe underprediction of not only the liquidus curve of peridotite 1102 (Figuret et al. 2010) but also the melting temperatures of MgSiO₃ (Zerr and Boehler 1993). That is, 1103 the difference between Figuet et al. (2010) and Andrault et al. (2011) is unlikely to be explained 1104 only by the difference in their starting materials. The experimental data of Andrault et al. (2011) 1105 were thus regarded as an outlier. Also, the inversion of Miyazaki and Korenaga (2019a) showed 1106 that mixing between FeO and MgO₂ was constrained only loosely by existing data, which indi-1107 cates that oxides with low concentrations would have minimal effects on melting, at least under 1108 lower-mantle pressures. Thus, we expect that the solidification of a magma ocean can be modeled 1109 reasonably accurately with the thermodynamics of the MgO-FeO-SiO₂ ternary system. 1110

Figure 9a shows the solidus and liquidus of a pyrolitic mantle based on the thermodynamic 1111 database of Miyazaki and Korenaga (2019a). Similar to the experimental results of Figuet et al. 1112 (2010), and contrary to the theoretical prediction of Stixrude et al. (2009), the slope of the liquidus 1113 is steeper than that of the mantle adiabat even at the core-mantle boundary. A magma ocean 1114 would thus start to solidify from its base. This underscores the still tentative nature of the concept 1115 of a basal magma ocean, which is sensitive to the subtle details of the mantle liquidus at high 1116 pressures. Another important feature of this phase diagram is that melt fraction varies nonlinearly 1117 between solidus and liquidus, and that the melt fraction of 0.4, which is commonly used to mark 1118 the rheological transition (below which a melt-solid mixture behaves as a solid) takes place only 1119 \sim 200 K below the liquidus. Though at variance with what has been suggested by Monteux et al. 1120 (2016) and Andrault et al. (2016), such high temperatures for the rheological transition prevent the 1121 rapid cooling of the mantle and the core during magma ocean solidification.

4.3 Gravitational stability of a solidifying magma ocean

1123

Understanding the thermodynamics of lower mantle melting is an important step, but it is just 1124 one of the few steps needed to model the solidification of a magma ocean with some confidence. 1125 Probably the most important remaining uncertainty is grain size evolution in a solidifying magma 1126 ocean. If crystals in a convecting magma ocean can grow as large as 1 cm, for example, they can 1127 be fractionated and accumulate at the bottom because they are usually denser than the coexisting 1128 melt. If grain size remains small, on the other hand, the whole magma ocean can solidify with 1120 equilibrium crystallization. However, in the case of equilibrium crystallization, the melt could 1130 become denser than the coexisting solids in the lowermost part of the mantle (note that a cumulate 1131 forms as soon as the melt fraction becomes lower than 0.4, containing a large amount of melt 1132 within), so if the grain size of the solids is large enough for melt to percolate quickly, chemical 1133 differentiation still takes place. 1134

Thus, two kinds of grain size are important: (1) grain size in a convecting magma ocean, 1135 and (2) grain size in a cumulate. As it is still difficult to theoretically predict those grain sizes 1136 (Solomatov 2015), Miyazaki and Korenaga (2019b) considered four end-member cases to explore 1137 the diversity of possible chemical differentiation. Shown in Figure 9b-d is the case with crystal 1138 accumulation but no matrix compaction, i.e., when grains can grow large enough to settle through 1139 a convecting magma ocean but are too small to allow efficient melt percolation. Several points 1140 are worth being noted. Because crystal fractionation modifies the local system composition, the 1141 rheological transition takes place at higher temperatures than expected from the phase diagram of the initial mantle composition (Figure 9b); the temperature of a solidifying magma follows closely 1143 the liquidus. Even with such high temperatures, the melt fraction of the cumulate is consistently 1144 around 0.4 (Figure 9d), because it is highly depleted. The Mg# (defined as molar Mg/(Mg+Fe) 1145 × 100) of the cumulate is as high as 95 (Figure 9c). Also, because the rheological transition 1146 takes place at the melt fraction of 0.4, perfect fractional crystallization, i.e., the formulation of a 1147 crystal cumulate with zero melt fraction, is unlikely to be materialized, though such end-member 1148

crystallization has been assumed by some previous studies (e.g., Elkins-Tanton 2008; Maurice et al. 2017; Boukaré et al. 2018). In Figure 9, only one case is shown, but the above points are 1150 mostly applicable to other cases as well, except for the case of homogeneous crystallization (i.e., 1151 no crystal accumulation nor matrix compaction), in which no chemical differentiation takes place. 1152 Having a self-consistent thermodynamic database allows one to calculate the densities of the 1153 melt and solid phases in an internally-consistent manner, and Miyazaki and Korenaga (2019b) 1154 also examined the stability of a solidifying magma ocean, by calculating the dispersion relation 1155 of the Rayleigh-Taylor instability. Without any formal analysis, it may be obvious that a solid-1156 ifying magma ocean is always gravitationally unstable because the slope of melting curves are 1157 steeper than that of adiabat (Figure 9a). The formation of a cumulate with the melt fraction of 0.4 1158 thus always results in a superadiabatic thermal structure, even in the case of homogeneous crys-1159 tallization. The dispersion relation of the Rayleigh-Taylor instability, however, provides important 1160 details such as the wavelength of the most unstable mode and its time scale. For the case of crystal 1161 accumulation, a highly-depleted, high Mg# cumulate is overlain by an iron-rich, low Mg# melt 1162 (Figure 9c), which becomes denser than the cumulate upon crystallization. The dispersion relation 1163 computed by Miyazaki and Korenaga (2019b) indicates a wavelength of a few hundred kilome-1164 ters and a time scale of less than 10 years, and the growth of the Rayleigh-Taylor instability with such a short wavelength is qualitatively similar to what previous studies suggested (Maurice et al. 1166 2017; Ballmer et al. 2017; Boukaré et al. 2018). In some sense, the destruction of a chemically 1167 differentiated structure by small-scale downwellings is a relief. In the global overturn model of 1168 Elkins-Tanton (2008), a resulting stably stratified structure has a potential density difference of 1169 >600 kg m⁻³ over the entire mantle depth. Such an intrinsic density difference is equivalent to a 1170 temperature difference of >7000 K (with a thermal expansivity of 2×10^{-5} K⁻¹ and a density of 1171 4300 kg m⁻³), which is impossible to generate during the course of Earth evolution. A potential temperature difference between the mantle and the surface would be less than ~ 1500 K after the 1173 solidification of a magma ocean (Figure 9a,b), and that between the mantle and the core would 1174

be less than ~ 1000 K (see Figure 11 of Miyazaki and Korenaga (2019b)). In other words, the present-day mantle would still have to be as strongly stratified as in the model of Elkins-Tanton (2008), and such a mantle cannot convect. With the small-scale Rayleigh-Taylor instabilities, on the other hand, it is possible to explain subsolidus mantle convection in the early Earth. In fact, a chemically heterogeneous mantle resulting from the small-scale instabilities leads to entirely new possibilities for Hadean geodynamics, as discussed next.

4.4 How Hadean geodynamics may have started

The small-scale downwellings of dense, iron-rich materials through the high Mg# matrix points to
the presence of a chemically heterogeneous mantle in the very early Earth (Figure 10). The bulk
composition of such a heterogeneous mantle would be the same as (or similar to) the composition
of a pyrolitic mantle, but because of lithologic differences, the chemically heterogeneous mantle
can exhibit a radically different dynamics.

First, the high Mg# matrix is depleted so that its melt production during adiabatic decompression is more reduced than the pyrolitic mantle, even though it is hot. This limited melting could make fast plate tectonics possible (Davies 2006). As discussed in §5, the mantle soon after magma ocean solidification was likely wet, and extensive melting expected from a homogeneous pyrolitic mantle would create thick crust as well as thick dehydrated lithospheric mantle (Figure 10a), both of which prevent rapid plate tectonics (e.g., Davies 1992; Korenaga 2006). However, the thickness of a dehydrated layer, which is rheologically strong, is limited with a chemically heterogeneous mantle, allowing rapid subduction. Given the rheology of lithosphere (§2.4), well-defined "plates" should still exist, but plate kinematics as well the nature of plate boundaries could be different from modern-style plate tectonics.

Second, the melting of the high Mg# matrix is likely to produce an ultramafic crust, and combined with the possibility of rapid plate tectonics, the abundant exposure of olivine and pyroxenes would make it possible to efficiently sequester atmospheric carbon by carbonate formation. The

rapid sequestration of atmospheric carbon is essential to convert the initially CO₂-rich, dense atmosphere to a habitable one (e.g., Zahnle et al. 2007), but how to do it in a physically plausible way has always been a challenge. For example, Sleep and Zahnle (2001) once suggested that, because of higher radiogenic heating in the past, the tempo of plate tectonics would have been faster in the past, thereby enabling a rapid carbon cycle. However, the suggested relation between internal heating and the rate of mantle convection is a common misconception (see section 3.1 of Korenaga (2017b)), and it is also at odds with the estimated cooling history of Earth's mantle (Herzberg et al. 2010). If the average subduction rate in the early Earth was lower than the modern rate, Sleep et al. (2014) conceded that the deep sequestration of the initial atmospheric carbon would have taken much of the Hadean. With the chemically heterogeneous mantle, on the other hand, it is possible to speculate on the advent of a habitable surface environment in the early Hadean.

Whereas the melting of the high Mg# matrix would be limited, the embedded iron-rich blobs would melt extensively upon upwelling. Because these blobs originate in the residual melt layer formed during magma ocean solidification (Figure 9d), they are likely to be enriched in incompatible elements including water. The melting of iron-rich blobs would produce an iron-rich crust, which contributes to reduce the chemical buoyancy of the oceanic lithosphere, thereby further facilitating rapid plate tectonics. Because these iron-rich blobs are intrinsically denser than the high Mg# mantle matrix, however, they would be normally sinking instead of upwelling unless their sizes are sufficiently reduced by convective stirring. The role of iron-rich blobs in Hadean geodynamics would thus depend on the competition of small-scale downwelling and mantle mixing.

Finally, chemical reaction between ultramafic crustal rocks and seawater is not limited to carbonate formation. Serpentinization could also take place, which releases hydrogen. Thus, even
though the early atmosphere was likely to be oxidizing (e.g., Abe et al. 2000; Zahnle et al. 2007),
we can expect that a locally reducing environment, which is generally considered important for
abiogenesis (e.g., Sleep et al. 2004; Schrenk et al. 2013; Menez et al. 2018), was widely available
on the seafloor. Another aspect relevant to the origin of life and its early evolution is the exis-

tence of the geomagnetic field. With rapid subduction, the mantle would have been cooled down efficiently, which would then helped to cool the hot core maintained during the solidification of a 1227 magma ocean (§4.2). The efficiency of core cooling is important to drive a geodynamo and gener-1228 ate a planetary magnetic field, particularly in the early Earth when the inner core was likely to have 1220 been absent (e.g., Buffett 2002). Though it might be possible to generate a magnetic field with a 1230 basal magma ocean (Ziegler and Stegman 2013), the formation of a basal magma ocean itself is 1231 not guaranteed (§4.2). The presence of the geomagnetic field in the Hadean is still controversial 1232 (e.g., Weiss et al. 2016; Tarduno et al. 2020), but it would contribute to the habitability of surface 1233 environment by shielding high-energy cosmic rays from the young Sun (Grießmeier et al. 2005). 1234

5 Synthesis: A new picture of early Earth evolution

1235

The regime of Hadean geodynamics, as mentioned in Introduction, may be inferred from how the 1236 continental crust has grown, which could constrain the onset time of plate tectonics, and from 1237 how a magma ocean solidified, which would have prescribed the initial state of subsolidus mantle 1238 convection. As reviewed in the preceding sections, latest crustal growth models suggest that the 1239 felsic continental crust started to emerge on a massive scale in the Hadean, and that the rates of crustal generation and recycling were much higher in the early Earth than at the present. Also, 1241 the latest modeling of magma ocean solidification, based on the self-consistent thermodynamics 1242 of lower mantle melting, points to the possibility of forming a chemically heterogeneous mantle, which could allow rapid plate tectonics, efficient carbon sequestration, felsic crust generation, and 1244 wide-spread serpentinization on the seafloor. These two angles are independent from each other; 1245 crustal growth models are built from geochemical observations, whereas a model of magma ocean 1246 solidification is a theoretical prediction based on high-pressure mineral physics, petrology, and fluid dynamics. It is thus encouraging that the notion of rapid plate tectonics in the early Earth, 1248 which is called for to explain continental growth, is also expected from the aftermath of magma 1240 ocean solidification.

A chemically heterogeneous mantle resulting from small-scale Rayleigh-Taylor instabilities can be recognized in some previous models of magma ocean solidification (Maurice et al. 2017; Ballmer et al. 2017; Boukaré et al. 2018), but the kind of chemical heterogeneities inferred from the model of Miyazaki and Korenaga (2019b) provides important specifics, i.e., hydrous ironrich blobs embedded in a high Mg# matrix (Figure 10). As speculated in §4.4, this particular lithologic heterogeneity has the potential to not only make rapid plate tectonics possible but also quickly convert the early Earth into a habitable world. Another interesting aspect is that this 'early Earth mode' of plate tectonics is expected to be eventually superseded by a more standard kind of plate tectonics, as chemical heterogeneities are homogenized by convecting mixing. Thus, starting Earth history with this type of a chemically heterogeneous mantle would allow us to naturally connect the vigorous Hadean Earth with the more steady Archean Earth. In this section, I attempt to draw a rough sketch for how this transition in mantle dynamics might have interacted with the other components of the Earth system such as the atmosphere, the oceans, the crust, and the core. Although this sketch is largely a speculation at the moment, care has been taken so that it is consistent with the current understanding of geodynamics. There are a number of details that need to be examined carefully, and it is my hope that this working hypothesis will encourage a fresh look at Hadean geodynamics and stimulate more synergistic research on the early Earth.

1251

1252

1253

1254

1255

1256

1257

1258

1259

1260

1261

1262

1263

1264

1265

1266

1267

The Moon-forming giant impact, which completed the major accretion phase of Earth, resulted 1268 in a deep magma ocean, the aftermath of which is likely to be characterized by a chemically hetero-1269 geneous mantle with a dense CO₂-rich atmosphere (Figure 11a). Owing to the difference between 1270 their solubilities in magma, CO₂ was mostly in the atmosphere, and water was mostly in the mantle 1271 at this stage, although the presence of shallow oceans is also expected (e.g., Abe and Matsui 1986; 1272 Zahnle et al. 1988; Abe 1993a). With surface water, thermal cracking can sufficiently weaken 1273 the otherwise stiff lithosphere, allowing the operation of plate tectonics (Korenaga 2007, 2020). Because the upwelling of the high Mg# matrix does not create thick buoyant crust and thick de-1275 hydrated lithosphere, the tempo of plate tectonics is controlled mostly by the viscosity of astheno-1276

sphere (Korenaga 2010b). Mantle viscosity is a strong function of temperature and water content (Karato and Wu 1993; Hirth and Kohlstedt 2003; Jain et al. 2019), and asthenospheric viscosity 1278 at the beginning of subsolidus mantle convection was probably much lower than the present-day 1279 value, because the initial mantle was not only hotter but also wetter than the present-day mantle; 1280 the matrix is highly depleted in terms of major element chemistry, but it is expected to have been 1281 initially wet. This is because of how a magma ocean solidifies. When a magma ocean is solid-1282 ifying, a melt porosity of \sim 40 % is maintained in the cumulate (Figure 9d), and this melt phase 1283 contains abundant water. Because melt percolation is not fast enough, the water originally stored 1284 in the melt phase remains mostly in the mantle when cooling by the Rayleigh-Taylor instabilities 1285 drives the porosity down to zero. 1286

The difference in water content between the initial and present-day mantle is difficult to quan-1287 tify with confidence, but it is important when estimating the tempo of plate tectonics, so one 1288 possible approach is given below. Roughly speaking, the present-day convecting mantle can be 1289 divided into two kinds of source mantle, one for MORB, and the other for OIB, with the former 1290 being generally more depleted in incompatible elements including water. The water content of the 1291 MORB source mantle is estimated to be 100-200 ppm (Michael 1988; Saal et al. 2002), and that 1292 of the OIB source mantle is around 300-900 ppm (Sobolev and Chaussidon 1996; Wallace 1998; 1293 Dixon et al. 2002; Aubaud et al. 2005). The fraction of the MORB source mantle is not well con-1294 strained, with existing estimates ranging from 30 % to 90 % (e.g., Allegre et al. 1983; Hofmann 1295 1997). With these uncertainties, the present-day mantle may contain ~ 0.5 -2 ocean worth of wa-1296 ter (or $\sim 200-700$ ppm H₂O). Soon after the solidification of a magma ocean, most of the present 1297 oceans are likely to have been contained in the mantle, so the initial mantle could have contained 1298 up to \sim 3 ocean worth of water or \sim 1000 ppm H₂O. 1299

The viscosity of the upper mantle, which is governed by that of olivine aggregates, is proportional to the water content to the power of 1 to 2 (Hirth and Kohlstedt 2003; Jain et al. 2019). So the factor of 2 to 4 difference of water content between the MORB source mantle and the OIB source

1301

1302

mantle means that the latter is 2 to 16 times weaker than the former. Because plate velocity is controlled mainly by the viscosity of the upper mantle, rather than the lower mantle (e.g., Korenaga 1304 2010b), the viscosity of the MORB source mantle, which probably occupies the most of the upper 1305 mantle, is most relevant for the tempo of modern plate tectonics. At the start of subsolidus mantle 1306 convection, however, there was no continental crust, so there was no depleted MORB source man-1307 tle, either. Thus, the viscosity of the upper mantle in the very early Earth, with up to 1000 ppm 1308 H_2O , could have been ~ 10 -100 times lower than that the present-day upper mantle. As plate ve-1309 locity is inversely proportional to viscosity to the two-thirds power (e.g., Turcotte and Schubert 1310 1982), this means that, with other factors being equal, plate tectonics in the very early Earth could 1311 be 5 to 20 times faster than the present-day counterpart. A hotter mantle in the Hadean makes it 1312 even faster, because of the temperature dependence of viscosity. 1313

With plate velocity 10 times faster than present, for example, the average age of subducting 1314 slab could be 10 times younger than the present-day value (\sim 50-60 Myr old (Parsons 1982)). Be-1315 cause the upwelling of the chemically heterogeneous mantle does not result in a thick layer of 1316 buoyant crust, the subduction of such young seafloor is free from the chemical buoyancy consid-1317 eration that applies to the case of a homogeneous mantle (Davies 1992, 2006). The melting of a 1318 composite mantle made of high Mg# matrix and iron-rich blobs is expected to produce a diverse 1319 range of melt composition, and the rapid subduction of a chemically heterogeneous crust, which 1320 is hydrated by its interaction with seawater, could result in an efficient construction of early con-1321 tinental crust (Figure 11b). Rapid plate tectonics would also help to degas most of water initially 1322 stored in the mantle. The production of an ultramafic crust would promote carbonate formation 1323 and serpentinization. Rapid plate tectonics with such an ultramafic seafloor quickly sequesters at-1324 mospheric carbon into the mantle and produces a number of locally reducing sites, which may be 1325 important for the origin of life. Even after the amount of atmospheric CO₂ is brought down to a steady-state level at which degassing and regassing are balanced, serpentinization at the seafloor 1327 continues to produce hydrogen, which reacts with CO₂ and becomes methane. Such methane pro-1328

duction would be sustained until the chemically heterogeneous mantle is mostly homogenized. As methane is a strong greenhouse gas, the chemically heterogeneous mantle may also contribute to 1330 resolving the faint young sun paradox in the early Earth (e.g., Kasting 1993). In addition to mix-1331 ing from the above by rapid subduction, the mantle is also stirred by mantle plumes. Because the 1332 core is cooled only slightly during the solidification of a magma ocean (§4.2), the efficient cooling 1333 of the mantle by rapid plate tectonics could induce high heat flux from the core. Mantle plumes 1334 are naturally characterized by higher potential temperatures than modern plumes, and the global 1335 plume flux should be greater in the early Earth, though whether such an increase in plume flux is 1336 achieved by more plumes or bigger plumes depends on the rheology of the core-mantle boundary 1337 region (Korenaga 2005). Core cooling during this stage is important not only for the generation of 1338 the geomagnetic field in the early Earth, but also for the formation of the inner core at a later time, 1339 for which the core needs to have been sufficiently cooled down (e.g., Stevenson et al. 1983; Buffett 1340 et al. 1996; Labrosse et al. 2001). 1341

The chemically heterogeneous mantle eventually ceases to exist because of convecting mixing. 1342 The timing of the transition to a chemically homogeneous mantle depends on the efficiency of 1343 mantle mixing, and it is expected to take a few tens to a few hundreds million years (e.g., Davies 1344 2006). Of course, convective mixing would not be able to completely homogenize the mantle; 1345 for example, some fraction of iron-rich blobs could escape mixing and accumulate at the core-1346 mantle boundary to form dense chemical piles (e.g., Garnero et al. 2016). However, most of the 1347 highly depleted matrix should have been mixed with iron-rich blobs to become a pyrolitic mantle, 1348 the upwelling of which would produce thick basaltic crust as the mantle temperature was still 1349 higher than present (Figure 11c). Positive chemical buoyancy associated with thick basaltic crust 1350 as well as depleted mantle lithosphere requires a growth of thick thermal boundary layer to make 1351 subduction possible; i.e., the tempo of plate tectonics has to slow down to allow such growth of boundary layer. The regime of sluggish plate tectonics thus began around this time. A thicker 1353 thermal boundary layer allows deeper thermal cracks and thus a more hydration of lithosphere, 1354

whereas more sluggish plate tectonics slows down degassing at mid-ocean ridges. A combination of more regassing and less degassing would materialize positive net water influx from the oceans to the mantle, and the once mostly dried-out mantle by rapid plate tectonics would start to be gradually hydrated again.

Sluggish plate tectonics is likely to have started in the late Hadean or the early Archean, and 1359 its subsequent evolution to the present is reasonably well understood (e.g., Korenaga 2013, 2018a) 1360 (Figure 12). I note that Aulbach and Arndt (2019) questioned the cooling history of Herzberg 1361 et al. (2010) (Figure 12a) on the basis of their interpretation of eclogite xenoliths, but as pointed 1362 out by Herzberg (2019), their interpretation assumes a highly unrealistic scenario of no fractional 1363 crystallization during the formation of oceanic crust. Also, it is worth remembering that the kind 1364 of thermal evolution indicated by Herzberg et al. (2010) is consistent with the present-day thermal 1365 budget of Earth (Korenaga 2008b; Jaupart et al. 2015), which is constrained by the observations of 1366 surface heat flow and the chemical compositions of the mantle and the crust. Deviating substan-1367 tially from the estimates of Herzberg et al. (2010) is thus equivalent to neglecting such established 1368 geophysical and geochemical constraints. At any rate, because sluggish plate tectonics probably 1369 started with a drier mantle than present, it could be different from modern-style plate tectonics in 1370 a few important ways. Because the convecting mantle was as dry as the continental mantle litho-1371 sphere, it can be deduced that continents could have been easily deformed, fragmented, and thus 1372 subducted. The reason is as follows. The continental crust itself is not particularly strong (e.g., 1373 Kohlstedt et al. 1995; Burgmann and Dresen 2008), so its mechanical integrity should originate in 1374 the strength of subcontinental lithosphere. Because the strength of continental mantle lithosphere 1375 and its longevity owe much to its being drier than the convecting mantle (e.g., Doin et al. 1997; 1376 Hirth et al. 2000; Katayama and Korenaga 2011; Chu and Korenaga 2012), the lack of an intrin-1377 sic viscosity difference between these two kinds of mantle in the past means that the continental mantle lithosphere could have easily been influenced by convective currents. Thus, as long as the 1379 convecting mantle remains relatively dry in the early phase of sluggish plate tectonics, it is dif-1380

ficult to expect stable, long-lasting continental blocks (Korenaga 2013). At the same time, a dry mantle is equivalent to voluminous oceans, which can suppress the emergence of dry landmasses 1382 (Korenaga et al. 2017) (Figure 12d), except for hotspot islands (Bada and Korenaga 2018; Rosas 1383 and Korenaga 2021). In addition, when plate tectonics was more sluggish than present, the age 1384 of subducting plates could have been over 300 Myr old (Korenaga 2008a); subducting plates can 1385 become quite thick. As it is generally more difficult to bend a thicker plate (e.g., Conrad and Hager 1386 1999; Rose and Korenaga 2011), the subduction of thick plates in the early Archean is likely to be 1387 characterized by large radii of curvature, with low dip angles at shallow depths (Figure 11c). Even 1388 with plate tectonics, therefore, the presence of the wedge mantle is not always guaranteed, and this 1380 may lead to a different style of arc magmatism back then. 1390

With positive net water influx maintained by plate tectonics, the convecting mantle becomes 1391 hydrated, and the continental mantle lithosphere becomes relatively stronger than the convective 1392 mantle, thus providing a stable foundation for the continental crust (Figure 11d). This relative 1393 strengthening of continents corresponds to what is generally referred to as the stabilization of cra-1394 tons, or cratonization, at around 3 to 2.5 Ga. Some geologists have advocated that cratonization is 1395 achieved by the gradual thickening of continental lithosphere (e.g., Cawood et al. 2018), but rela-1396 tive strengthening with gradual mantle hydration can also explain the geological records relevant to 1397 cratonization. The continuous subduction of water also leads to the emergence of dry landmasses 1398 (Korenaga et al. 2017) (Figure 12d). Because a cooler mantle produces thinner oceanic crust as 1390 well as thinner depleted mantle lithosphere, and because the wet and thus weak asthenosphere 1400 tends to prevent the growth of a thermal boundary layer, oceanic lithosphere becomes thinner. 1401 Thinner lithosphere is easier to bend and subduct, so plate tectonics gradually speeds up, although 1402 the rate of increase would be only $\sim 10 \% \ \mathrm{Gyr}^{-1}$ (Korenaga 2011). With thinner oceanic litho-1403 sphere, the radius of curvature can be smaller, making room for the wedge mantle and activating modern-style arc magmatism (Figure 11d). 1405

As mentioned earlier, the above scenario of Earth evolution is speculative, especially regarding

1406

the Hadean part. For one thing, the solidification of a magma ocean is assumed to result in the chemically heterogeneous mantle as depicted in Figure 10b. According to the current theoretical 1408 understanding, it is difficult to tell whether fractional crystallization is more likely than equilibrium 1409 crystallization (Solomatov 2015). Thus, if a magma ocean can solidify with equilibrium crystal-1410 lization, there would be no chemical differentiation, so subsolidus mantle convection would start 1411 with a homogeneous pyrolitic mantle (Figure 10a). However, even if crystals are not fractionated 1412 from convecting magma, a similar kind of chemical differentiation still occurs by matrix com-1413 paction following equilibrium crystallization (Miyazaki and Korenaga 2019b). It would therefore 1414 require certain special conditions to avoid the formation of the chemically heterogeneous mantle 1415 at the end of magma ocean solidification. Also, the formation of small-scale heterogeneities is 1416 supported not only theoretically by numerical simulation (e.g., Maurice et al. 2017; Boukaré et al. 1417 2018) and the Rayleigh-Taylor stability analysis (Miyazaki and Korenaga 2019b), but also empiri-1418 cally by the very fact that large-scale circulations have long been taking place in Earth's mantle. If 1419 a chemically differentiated mantle were instead overturned into a stably stratified mantle, as pro-1420 posed by Elkins-Tanton (2008), it would not allow any convection for the rest of Earth history. The 1421 potential density difference of 600 kg m $^{-3}$ (or \sim 500 kg m $^{-3}$ based on the fractional crystallization 1422 modeling of Miyazaki and Korenaga (2019b)), if applied to a stable stratification in the mantle, is 1423 simply so large that a planet remains geologically dead after magma ocean solidification. 1424

6 Summary and outlook

1425

On the basis of recent developments in the studies of continental growth and magma ocean solidification, along with geodynamical consideration, I have proposed one plausible scenario for early
Earth evolution. In this scenario, a chemically heterogeneous mantle resulting from the gravitational instability of a solidifying magma ocean allows rapid plate tectonics, which in turn leads
to the early emergence of a habitable surface environment by efficiently sequestering atmospheric
carbon. This may also explain the high crust generation rate in the early Earth suggested by recent

continental growth models. One attractive feature of this hypothesis is that this early Earth situation can naturally cease to exist by convective mixing and gradually transition to a more familiar 1433 style of plate tectonics with a chemically homogeneous mantle. This new synthesis is admittedly 1434 speculative, and it may require major revisions as many details need to be fleshed out in future. 1435 However, compared to other existing proposals for early Earth dynamics such as stagnant lid con-1436 vection, sagduction, and heat pipe, this scenario has a more solid theoretical footing, warranting 1437 further investigation. It provides a conceptual framework that can potentially explain nearly all as-1438 pects of Earth evolution in a coherent manner, including atmospheric evolution, deep water cycle, 1430 continental growth, mantle convection, and core cooling. 1440

Of course, testing this new hypothesis with a range of observations will be of vital importance, 1441 and this review article is written with the hope of stimulating geologists and geochemists in that di-1442 rection. At the same time, there are a number of major theoretical tasks to be done, to facilitate such 1443 observational testing by providing more concrete and specific model predictions. For example, the 1444 thermodynamic modeling of magma ocean solidification is still too crude, and the existing models 1445 do not adequately handle the final stage of solidification under upper mantle conditions (Boukaré 1446 et al. 2015; Miyazaki and Korenaga 2019a), mostly because they are tuned to lower mantle con-1447 ditions. Also, the Rayleigh-Taylor instability of a solidifying magma ocean is characterized by a very short time scale (Miyazaki and Korenaga 2019b), so it will remain a technical challenge 1449 to model both solidification and instability in a self-consistent fashion. The petrological and geo-1450 chemical consequences of mantle convection starting with a chemically heterogeneous mantle are 1451 virtually unexplored. It will be interesting to see how the new hypothesis affects our conventional 1452 wisdom on the geochemical evolution of the mantle, which is largely guided by geochemical box 1453 modeling with an initially homogeneous mantle. A new kind of geochemical modeling, which can 1454 take into account the chemical and isotopic heterogeneities of both mantle and crustal reservoirs, will be essential to generate model predictions that can be tested by some observational means. 1456 The Hadean is also the time characterized by large bolide impacts (e.g., Marchi et al. 2014, 2018), 1457

and their likely contributions to surface environment, in the presence of rapid plate tectonics and massive continents, remains to be understood.

This review on the global aspects of Hadean geodynamics does not place an emphasis on 1460 Hadean zircons, because of the limited locality of so far published geochemical data. However, as 1461 compiled by Harrison (2020), there are at least fourteen other localities across five continents, such 1462 as Barberton in South Africa, Acasta in Canada, Akilia Island in Greenland, and Buring County 1463 in Tibet. Although no locality outside the Jack Hills has yielded more than a few hundred Hadean zircons, there is a potential to substantially increase the discovery rate with an orchestrated use 1465 of numerous LA-ICPMS instruments around the globe (Harrison 2020). Such an expansion of 1466 Hadean zircon database, in addition to constraints on Hadean protoliths inferred from Archean rocks (e.g., Caro et al. 2017; O'Neil and Carlson 2017), will be essential to improve our under-1468 standing of the Hadean Earth by continual feedback between theories and observations. 1469

Competing interests

The author declares that he has no competing interest.

Funding

- This work was supported in part by U.S. National Science Foundation EAR-1753916 and the U.S.
- National Aeronautics and Space Administration under Cooperative Agreement No. 80NSSC19M0069
- issued through the Science Mission Directorate.

76 Availability of Data and Materials

This work is essentially a review of the existing relevant literature, and there is no additional data.

478 Acknowledgments

The author thanks Victoria Pease for her invitation to write this review, and Tony Kemp, Oliver
Nebel, and an anonymous reviewer for constructive suggestions, which helps to improve the clarity
and accuracy of the manuscript.

References

- Abe, Y., 1993a. Physical state of the very early Earth. Lithos 30, 223–235.
- Abe, Y., 1993b. Thermal evolution and chemical differentiation of the terrestrial magma ocean. In: Takahashi, E., Jeanloz, R., Rudie, R. (Eds.), Evolution of the Earth and Planets. AGU, Washington, D. C., pp. 41–54.
- Abe, Y., Matsui, T., 1986. Early evolution of the Earth: Accretion, atmosphere formation, and thermal history. J. Geophys. Res. 91, E291–E302.
- Abe, Y., Ohtani, E., Okuchi, T., Righter, K., Drake, M., 2000. Water in the early earth. In: Righter, K., Canup, R. M. (Eds.), The Origin of Earth and Moon. University of Arizona, Tucson, pp. 413–433.
- Alfè, D., 2005. Melting curve of MgO from first-principles simulations. Phys. Rev. Lett. 94, 235701.
- Allegre, C. J., Hart, S. R., Minster, J.-F., 1983. Chemical structure and evolution of the mantle and continents
 determined by inversion of Nd and Sr isotopic data, I. theoretical methods. Earth Planet. Sci. Lett. 66,
 177–190.
- Allegre, C. J., Staudacher, T., Sarda, P., 1987. Rare gas systematics: formation of the atmosphere, evolution and structure of the Earth's mantle. Earth Planet. Sci. Lett. 81, 127–150.
- Andrault, D., Bolfan-Casanova, N., Lo Nigro, G., Bouhifd, M. A., Garbarino, G., Mezouar, M., 2011.

 Solidus and liquidus profiles of chondritic mantle: Implication for melting of the Earth across its history.

 Earth Planet. Sci. Lett. 304, 251–259.

- Andrault, D., Monteux, J., Le Bars, M., Samuel, H., 2016. The deep Earth may not be cooling down. Earth
 Planet. Sci. Lett. 443, 195–203.
- Annen, C., Blundy, J. D., Sparks, R. S. J., 2006. The genesis of intermediate and silicic magmas in deep crustal hot zones. J. Petrol. 47, 505–539.
- Armstrong, R. L., 1981a. Comment on "crustal growth and mantle evolution: inferences from models of element transport and Nd and Sr isotopes". Geochim. Cosmochim. Acta 45, 1251.
- Armstrong, R. L., 1981b. Radiogenic isotopes: the case for crustal recycling on a near-steady-state nocontinental-growth Earth. Phil. Trans. R. Soc. Lond. A 301, 443–472.
- Armstrong, R. L., 1991. The persistent myth of crustal growth. Australian J. Earth Sci. 38, 613–630.
- Asphaug, E., 2014. Impact origin of the Moon? Annu. Rev. Earth Planet. Sci. 42, 551–578.
- Aubaud, C., Pineau, F., Hékinian, R., Javoy, M., 2005. Degassing of CO₂ and H₂O in submarine lavas from
 the Society hotspot. Earth Planet. Sci. Lett. 235, 511–527.
- Aulbach, S., Arndt, N. T., 2019. Eclogites as paleodynamic archives: Evidence for warm (not hot) and depleted (but heterogeneous) Archaean ambient mantle. Earth Planet. Sci. Lett. 505, 162–172.
- Baadsgaard, H., Nutman, A. P., Bridgwater, D., 1986. Geochronology and isotopic variation of the early

 Archaean Amitsoq gneisses of the Isukasia area, southern West Greenland. Geochim. Cosmochim.

 Acta 50, 2173–2183.
- Bada, J. L., Korenaga, J., 2018. Exposed areas above sea level on Earth >3.5 gyr ago: Implications for prebiotic and primitive biotic chemistry. Life 8, 55, doi:10.3390/life8040055.
- Ballmer, M. D., Lourenço, D. L., Hirose, K., Caracas, R., Nomura, R., 2017. Reconciling magma-ocean crystallization models with the present-day structure of the Earth's mantle. Geochem. Geophys. Geosys. 18, 2785–2806, doi:10.1002/2017GC006917.
- Barboni, M., Boehnke, P., Keller, B., Kohl, I. E., Schoene, B., Young, E. D., McKeegan, K. D., 2017. Early formation of the Moon 4.51 billion years ago. Sci. Adv. 3, e1602365.

- Bedard, J. H., 2018. Stagnant lids and mantle overturns: Implications for Archaean tectonics, magmagenesis, crustal growth, mantle evolution, and the start of plate tectonics. Geosci. Frontiers 9, 19–49.
- Belousova, E. A., Kostitsyn, Y. A., Griffin, W. L., Begg, G. C., O'Reilly, S. Y., Pearson, N. J., 2010. The growth of the continental crust: Constraints from zircon Hf-isotope data. Lithos 119, 457–466.
- Bennett, V. C., Brandon, A. D., Nutman, A. P., 2007. Coupled ¹⁴²Nd-¹⁴³Nd isotopic evidence for Hadean mantle dynamics. Science 318, 1907–1910.
- Bercovici, D., Ricard, Y., 2014. Plate tectonics, damage and inheritance. Nature 508, 513–516.
- Bercovici, D., Tackley, P. J., Ricard, Y., 2015. The generation of plate tectonics from mantle dynamics. In:

 Treatise on Geophysics, 2nd ed. Vol. 7. Elsevier, pp. 271–318.
- Birch, F., 1952. Elasticity and constitution of the Earth's interior. J. Geophys. Res. 57, 227–286.
- Boehler, R., 2000. High-pressure experiments and the phase diagram of lower mantle and core materials.

 Rev. Geophys. 38, 221–245.
- Boehler, R., Ross, M., 2015. Properties of rocks and minerals, high-pressure melting. In: Treatise on Geophysics, 2nd ed. Vol. 2. Elsevier, Ch. 22, pp. 573–582.
- Boukaré, C.-E., Parmentier, E. M., Parman, S. W., 2018. Timing of mantle overturn during magma ocean solidification. Earth Planet. Sci. Lett. 491, 216–225.
- Boukaré, C.-E., Ricard, Y., Fiquet, G., 2015. Thermodynamics of the MgO-FeO-SiO₂ system up to 140 GPa:
- Application to the crystallization of Earth's magma ocean. J. Geophys. Res. Solid Earth 120, 6085–
- 1542 6101, doi:10.1002/2015JB011929.
- Bowring, S. A., Williams, I. S., 1999. Priscoan (4.00-4.03 Ga) orthogneisses from northwestern Canada.

 Contrib. Mineral. Petrol. 135, 3–16.
- Bradley, D. C., 2008. Passive margins through earth history. Earth-Sci. Rev. 91, 1–26.
- Brown, M., Johnson, T., Gardiner, N. J., 2020. Plate tectonics and the Archean Earth. Annu. Rev. Earth
 Planet. Sci. 48, 291–320.

- Buffett, B. A., 2002. Estimates of heat flow in the deep mantle based on the power requirements for the geodynamo. Geophys. Res. Lett. 29(12), doi:10.1029/2001GL014649.
- Buffett, B. A., Huppert, H. E., Lister, J. R., Woods, A. W., 1996. On the thermal evolution of the earth's core. J. Geophys. Res. 101, 7989–8006.
- Burgmann, R., Dresen, G., 2008. Rheology of the lower crust and upper mantle: Evidence from rock mechanics, geodesy, and field observations. Ann. Rev. Earth Planet. Sci. 36, 531–567.
- Campbell, I. H., 2003. Constraints on continental growth models from Nb/U ratios in the 3.5 Ga Barberton and other Archaean basalt-komatiite suites. Am. J. Sci. 303, 319–351.
- Campbell, I. H., Taylor, S. R., 1983. No water, no granites no oceans, no continents. Geophys. Res. Lett. 10, 1061–1064.
- 1558 Canup, R. M., 2004. Simulations of a late lunar-forming impact. Icarus 168, 433–456.
- Caro, G., Bourdon, B., Birck, J.-L., Moorbath, S., 2006. High-precision ¹⁴²Nd/¹⁴⁴Nd measurements in terrestrial rocks: Constraints on the early differentiation of the Earth's mantle. Geochim. Cosmochim.

 Acta 70, 164–191.
- Caro, G., Bourdon, B., Wood, B. J., Corgne, A., 2005. Trace-element fractionation in Hadean mantle generated by melt segregation from a magma ocean. Nature 436, 246–249.
- Caro, G., Morino, P., Mojzsis, S. J., Cates, N. L., Bleeker, W., 2017. Sluggish Hadean geodynamics: Evidence from coupled ^{146,147}Sm-^{142,143}Nd systematics in Eoarchean supracrustal rocks of the Inukjuak domain (québec). Earth Planet. Sci. Lett. 457, 23–37.
- Cawood, P. A., Hawkesworth, C. J., Dhuime, B., 2013. The continental record and the generation of continental crust. GSA Bulletin 125, 14–32.
- Cawood, P. A., Hawkesworth, C. J., Pisarevsky, S. A., Dhuime, B., Capitanio, F. A., Nebel, O., 2018. Geological archive of the onset of plate tectonics. Phil. Trans. R. Soc. A 376, 20170405, http://dx.doi.org/10.1098/rsta.2017.0405.

- Chambers, J. E., 2014. Planet formation. In: Treatise on Geochemistry, 2nd ed. Vol. 2. Elsevier, Ch. 4, pp. 55–72.
- 1574 Chen, K., Rudnick, R. L., Wang, Z., Tang, M., Gaschnig, R. M., Zou, Z., He, T., Hu, Z., Liu, Y., 2019. How
 1575 mafic was the Archean upper continental crust? insight from Cu and Ag in ancient glacial diamictites.
 1576 Geochim. Cosmochim. Acta 278, 16–29.
- Chesley, C., Key, K., Constable, S., Behrens, J., MacGregor, L., 2019. Crustal cracks and frozen flow in oceanic lithosphere inferred from electrial anisotropy. Geochem. Geophys. Geosys. 20, 5979–5999.
- Chu, X., Korenaga, J., 2012. Olivine rheology, shear stress, and grain growth in the lithospheric mantle:

 Geological constraints from the Kaapvaal craton. Earth Planet. Sci. Lett. 333-334, 52–62.
- Condie, K., Pisarevsky, S., Korenaga, J., Gardoll, S., 2015. Is the rate of supercontinent assembly changing with time? Precambrian Res. 259, 278–289.
- Condie, K. C., 1993. Chemical composition and evolution of the upper continental crust: Contrasting results from surface samples and shales. Chem. Geol. 104, 1–37.
- Condie, K. C., Aster, R. C., 2010. Episodic zircon age spectra of orogenic granitoids: The supercontinent connection and continental growth. Precambrian Res. 180, 227–236.
- Condie, K. C., Kröner, A., 2008. When did plate tectonics begin? Evidence from the geologic record. In:

 Condie, K. C., Pease, V. (Eds.), When Did Plate Tectonics Begin on Planet Earth? Geol. Soc. Am., pp.

 281–294.
- Condie, K. C., O'Neill, C., Aster, R. C., 2009. Evidence and implications for a widespread magmatic shutdown for 250 My on Earth. Earth Planet. Sci. Lett. 282, 294–298.
- Conrad, C. P., Hager, B. H., 1999. Effects of plate bending and fault strength at subduction zones on plate dynamics. J. Geophys. Res. 104, 17551–17571.
- Crowley, J. W., Gerault, M., O'Connell, R. J., 2011. On the relative influence of heat and water transport on planetary dynamics. Earth Planet. Sci. Lett. 310, 380–388.

- Daines, M. J., Richter, F. M., 1988. An experimental method for directly determining the interconnectivity of melt in a partially molten system. Geophys. Res. Lett. 15, 1459–1462.
- Daly, S. F., 1980. Convection with decaying heat sources: Constant viscosity. Geophys. J. R. Astron. Soc. 61, 519–547.
- Davies, G. F., 1992. On the emergence of plate tectonics. Geology 20, 963–966.
- Davies, G. F., 2006. Gravitational depletion of the early Earth's upper mantle and the viability of early plate tectonics. Earth Planet. Sci. Lett. 243, 376–382.
- de Koker, N., Stixrude, L., 2009. Self-consistent thermodynamic description of silicate liquids, with application to shock melting of MgO periclase and MgSiO₃ perovskite. Geophys. J. Int. 178, 162–179.
- Debaille, V., O'Neill, C., Brandon, A. D., Haenecour, P., Yin, Q.-Z., Mattielli, N., Treiman, A. H., 2013.

 Stagnant-lid tectonics in early Earth revealed by ¹⁴²Nd variations in late Archean rocks. Earth Planet.

 Sci. Lett. 373, 83–92.
- Dhuime, B., Hawkesworth, C. J., Cawood, P. A., Storey, C. D., 2012. A change in the geodynamics of continental growth 3 billion years ago. Science 335, 1334–1336.
- Dhuime, B., Hawkesworth, C. J., Delavault, H., Cawood, P. A., 2017. Continental growth seen through the sedimentary record. Sed. Geol. 357, 16–32.
- Dhuime, B., Hawkesworth, C. J., Delavault, H., Cawood, P. A., 2018. Rates of generation and destruction of the continental crust: implications for continental growth. Phil. Trans. R. Soc. A 376, 20170403, http://dx.doi.org/10.1098/rsta.2017.0403.
- Dixon, J. E., Leist, L., Langmuir, C., Schilling, J.-G., 2002. Recycled dehydrated lithosphere observed in plume-influenced mid-ocean-ridge basalt. Nature 420, 385–389.
- Doin, M.-P., Fleitout, L., Christensen, U., 1997. Mantle convection and stability of depleted and undepleted continental lithosphere. J. Geophys. Res. 102, 2772–2787.

- Du, Z., Lee, K. K. M., 2014. High-pressure melting of MgO from (Mg,Fe)O solid solutions. Geophys. Res. Lett. 41, 8061–8066, doi:10.1002/2014GL061954.
- Elkins-Tanton, L. T., 2008. Linked magma ocean solidification and atmospheric growth for Earth and Mars.

 Earth Planet. Sci. Lett. 271, 181–191.
- Evans, D. A. D., 2013. Reconstructing pre-Pangean supercontinents. Geol. Soc. Am. Bull. 125, 1735–1751.
- Farquhar, J., Bao, H., Thiemens, M., 2000. Atmospheric influence of Earth's earliest sulfur cycle. Science 289, 756–758.
- Fiquet, G., Auzende, A. L., Siebert, J., Corgne, A., Bureau, H., Ozawa, H., Garbarino, G., 2010. Melting of peridotite to 140 gigapascals. Science 329, 1516–1518.
- Fischer, R. A., Campbell, A. J., 2010. High-pressure melting of wüstite. Am. Mineral. 95, 1473–1477.
- Fisher, C. M., Vervoort, J. D., 2018. Using the magmatic record to constrain the growth of continental crust

 the Eoarchean zircon Hf record of Greenland. Earth Planet. Sci. Lett. 488, 79–91.
- Foley, B. J., 2018. The dependence of planetary tectonics on mantle thermal state: applications to early
 Earth evolution. Phil. Trans. R. Soc. A 376, 20170409, http://dx.doi.org/10.1098/rsta.2017.0409.
- Fraeman, A. A., Korenaga, J., 2010. The influence of mantle melting on the evolution of Mars. Icarus 210, 43–57.
- Fyfe, W. S., 1978. The evolution of the Earth's crust: Modern plate tectonics to ancient hot spot tectonics?

 Chem. Geol. 23, 89–114.
- Galer, S. J. G., Mezger, K., 1998. Metamorphism, denudation and sea level in the Archean and cooling of the Earth. Precambrian Res. 92, 389–412.
- Garnero, E. J., McNamara, A. K., Shim, S.-H., 2016. Continent-sized anomalous zones with low seismic velocity at the base of Earth's mantle. Nature Geosci. 9, 481–488.

- Ghiorso, M., Hirschmann, M., Reiners, P., Kress, V., 2002. pMELTS: A revision of MELTS for improved calculation of phase relations and major element partitioning related to partial melting of the mantle to 1642 3 GPa. Geochem. Geophys. Geosys. 3, 2001GC000217. 1643
- Ghiorso, M. S., Carmichael, I. S. E., Rivers, M. L., Sack, R. O., 1983. The Gibbs free energy of mixing 1644 of natural silicate liquids: an expanded regular solution approximation for the calculation of magmatic 1645 intensive variables. Contrib. Mineral. Petrol. 84, 107–145. 1646
- Goodwin, A. M., 1996. Principles of Precambrian Geology. Academic Press, London.
- Greber, N. D., Dauphas, N., 2019. The chemistry of fine-grained terrigenous sediments reveals a chemically 1648 evolved Paleoarchean emerged crust. Geochim. Cosmochim. Acta 255, 247–264. 1649
- Greber, N. D., Dauphas, N., Bekker, A., Ptacek, M. P., Bindeman, I. N., Hofmann, A., 2017. Titanium 1650 isotopic evidence for felsic crust and plate tectonics 3.5 billion years ago. Science 357, 1271–1274. 1651
- Grießmeier, J.-M., Stadelmann, A., Motschmann, U., Belisheva, N. K., Lammer, H., Biernat, H. K., 2005. 1652 Cosmic ray impact on extrasolar Earth-like planets in close-in habitable zones. Astrobiology 5, 587-1653 603.
- Gumsley, A. P., Chamberlain, K. R., Bleeker, W., Soderlund, U., de Kock, M. O., Larsson, E. R., Bekker, 1655 A., 2017. Timing and tempo of the Great Oxidation Event. Proc. Nat. Acad. Sci. USA 114, 1811–1816. 1656
- Guo, M., Korenaga, J., 2020. Argon constraints on the early growth of felsic continental crust. Sci. Adv. 6, 1657 eaaz6234. 1658
- Hamano, Y., Ozima, M., 1978. Earth-atmosphere evolution model based on Ar isotopic data. In: 1659 E. C. Alexander, J., Ozima, M. (Eds.), Terrestrial Rare Gases. Japan Scientific Societies Press, pp. 1660 155–171. 1661
- Harrison, T. M., 2009. The Hadean crust: Evidence from >4 Ga zircons. Annu. Rev. Earth Planet. Sci. 37, 1662 479-505. 1663
- Harrison, T. M., 2020. Hadean Earth. Cham, Switzerland. Springer. 1664

1654

- Hawkesworth, C., Cawood, P. A., Dhuime, B., 2019. Rates of generation and growth of the continental crust.

 Geosci. Frontiers 10, 165–173.
- Hawkesworth, C. J., Cawood, P. A., Dhuime, B., 2016. Tectonics and crustal evolution. GSA Today 9, 4–11.
- Hawkesworth, C. J., Cawood, P. A., Dhuime, B., Kemp, A. I. S., 2017. Earth's continental lithosphere through time. Annu. Rev. Earth. Sci. 45, 169–198.
- Hawkesworth, C. J., Dhuime, B., Pietranik, A. B., Cawood, P. A., Kemp, A. I. S., Storey, C. D., 2010. The generation and evolution of the continental crust. J. Geol. Soc. London 167, 229–248.
- Herzberg, C., 2019. Origin of high-Mg bimineralic eclogite xenoliths in kimberlite: A comment on a paper by Aulbach and Arndt (2019). Earth Planet. Sci. Lett. 510, 231–233.
- Herzberg, C., Condie, K., Korenaga, J., 2010. Thermal evolution of the Earth and its petrological expression.

 Earth Planet. Sci. Lett. 292, 79–88.
- Herzberg, C., Rudnick, R., 2012. Formation of cratonic lithosphere: An integrated thermal and petrological model. Lithos 149, 4–15, doi:10.1016/j.lithos.2012.01.010.
- Hickman, A. H., 2012. Review of the Pilbara Craton and Fortescue Basin, Western Australia: Crustal evolution providing environments for early life. Island Arc 21, 1–31.
- Hirth, G., Evans, R. L., Chave, A. D., 2000. Comparison of continental and oceanic mantle electrical conductivity: Is the Archean lithosphere dry? Geochem. Geophys. Geosys. 1, 2000GC000048.
- Hirth, G., Kohlstedt, D., 2003. Rheology of the upper mantle and the mantle wedge: A view from the experimentalists. In: Eiler, J. (Ed.), Inside the Subduction Factory. American Geophysical Union, Washington,
 DC, pp. 83–105.
- Hirth, G., Kohlstedt, D. L., 1996. Water in the oceanic mantle: Implications for rheology, melt extraction, and the evolution of the lithosphere. Earth Planet. Sci. Lett. 144, 93–108.
- Hofmann, A. W., 1997. Mantle geochemistry: The message from oceanic volcanism. Nature 385, 219–229.

- Hofmeister, A. M., 1983. Effect of a Hadean terrestrial magma ocean on crust and mantle evolution. J. Geophys. Res. 88, 4963–4983.
- Holland, T. J. B., Powell, R., 1998. An internally consistent thermodynamic data set for phases of petrological interest. J. metamorphic Geol. 16, 309–343.
- Hopkins, M., Harrison, T. M., Manning, C. E., 2008. Low heat flow inferred from >4 Gyr zircons suggest

 Hadean plate boundary interactions. Nature 456, 493–496.
- Hopkins, M. D., Harrison, T. M., Manning, C. E., 2010. Constraints on Hadean geodynamics from mineral inclusions in >4 Ga zircons. Earth Planet. Sci. Lett. 298, 367–376.
- Hyung, E., Jacobsen, S. B., 2020. The ¹⁴²nd/¹⁴⁴nd variations in mantle-derived rocks provide constraints on the stirring rate of the mantle from the Hadean to the present. Proc. Nat. Acad. Sci. USA 117, doi:10.1073/pnas.2006950117.
- 1699 Iizuka, T., Komiya, T., Rino, S., Maruyama, S., Hirata, T., 2010. Detrital zircon evidence for Hf isotopic evolution of granitoid crust and continental growth. Geochim. Cosmochim. Acta 74, 2540–2472.
- Ito, E., Harris, D. M., Anderson, A. T., 1983. Alteration of oceanic crust and geologic cycling of chlorine and water. Geochim. Cosmochim. Acta 47, 1613–1624.
- Jackson, M. G., Carlson, R. W., 2012. Homogeneous superchondritic ¹⁴²Nd/¹⁴⁴Nd in the midocean ridge basalt and ocean island basalt mantle. Geochem. Geophys. Geosys. 13, Q06011, doi:10.1029/2012GC004114.
- Jacobsen, S. B., 1988. Isotopic constraints on crustal growth and recyling. Earth Planet. Sci. Lett. 90, 315–329.
- Jacobsen, S. B., Harper, C. L., 1996. Accretion and early differentiation history of the Earth based on extinct radionuclides. In: Earth Processes: Reading the Isotopic Code. AGU, pp. 47–74.
- Jain, C., Korenaga, J., Karato, S., 2017. On the yield strength of oceanic lithosphere. Geophys. Res. Lett. 44, 9716–9722, https://doi.org/10.1002/2017GL075043.

- Jain, C., Korenaga, J., Karato, S., 2018. On the grain-size sensitivity of olivine rheology. J. Geophys. Res.

 Solid Earth 123, 674–688, https://doi.org/10.1002/2017JB014847.
- Jain, C., Korenaga, J., Karato, S., 2019. Global analysis of experimental data on the rheology of olivine aggregates. J. Geophys. Res. Solid Earth 124, 310–334, https://doi.org/10.1029/2018JB016558.
- Jarrard, R. D., 2003. Subduction fluxes of water, carbon dioxide, chlorine, and potassium. Geochem. Geophys. Geosys. 4, 8905, doi:10.1029/2002GC000392.
- Jaupart, C., Labrosse, S., Lucazeau, F., Mareschal, J.-C., 2015. Temperatures, heat, and energy in the mantle of the Earth. In: Treatise on Geophysics, 2nd ed. No. 7. Elsevier, pp. 223–270.
- Jin, Z.-M., Zhang, J., Green, H. W., Jin, S., 2001. Eclogite rheology: Implications for subducted lithosphere.

 Geology 29, 667–670.
- Johnson, K. T. M., Dick, H. J. B., 1992. Open system melting and temporal and spatial variation of peridotite and basalt at the Atlantis II Fracture Zone. J. Geophys. Res. 97, 9219–9241.
- Johnson, T. E., Brown, M., Kaus, B. J. P., VanTongeren, J. A., 2014. Delamination and recycling of Archaean crust caused by gravitational instabilities. Nature Geosci. 47-52.
- Jordan, T. H., 1988. Structure and formation of the continental tectosphere. In: J. Petrol. Spec. Vol. pp. 11–37.
- Karato, S., 2008. Deformation of Earth Materials: Introduction to the Rheology of the Solid Earth. Cambridge, New York.
- Karato, S., Wu, P., 1993. Rheology of the upper mantle: A synthesis. Science 260, 771–778.
- Karlsen, K. S., Conrad, C. P., Magni, V., 2019. Deep water cycling and sea level change since the breakup of Pangea. Geochem. Geophys. Geosys. 20, 2919–2935, https://doi.org/10.1029/2019GC008232.
- Kasting, J. F., 1993. Earth's early atmosphere. Science 259, 920–926.

- Katayama, I., Korenaga, J., 2011. Is the African cratonic lithosphere wet or dry? In: Beccaluva, L., Bian-
- chini, G., Wilson, M. (Eds.), Volcanism and Evolution of the African Lithosphere. Vol. 478 of Geol.
- Soc. Am. Special Paper. Geol. Soc. Am., pp. 246–256.
- Kato, T., Ringwood, A. E., Irifune, T., 1988. Experimental determination of element partitioning between
- silicate perovskites, garnets, and liquids: Constraints on the early differentiation of the mantle. Earth
- 1739 Planet. Sci. Lett. 89, 123–145.
- Katz, R. F., Spiegelman, M., Langmuir, C. H., 2003. A new parameterization of hydrous mantle melting.
- Geochem. Geophys. Geosys. 4, 1073, doi:10.1029/2002GC000433.
- Keller, B., Schoene, B., 2018. Plate tectonics and continental basaltic geochemistry throughout earth history.
- Earth Planet. Sci. Lett. 481, 290–304.
- Keller, C. B., Harrison, T. M., 2020. Constraining crustal silica on ancient Earth. Proc. Nat. Acad. Sci. USA
- in revision, https://doi.org/10.31223/osf.io/75evw.
- Kemp, A. I. S., Hawkesworth, C. J., 2003. Granitic perspectives on the generation and secular evolution of
- the continental crust. In: Treatise on Geochemistry. Vol. 3. Elsevier, pp. 349–410.
- Kemp, A. I. S., Hawkesworth, C. J., 2014. Growth and differentiation of the continental crust from isotope
- studies of accessory minerals. In: Treatise on Geochemistry, 2nd ed. Vol. 4. Elsevier, pp. 379–421.
- Kimura, T., Ohfuji, H., Nishi, M., Irifune, T., 2017. Melting temperatures of MgO under high pressure by
- micro-texture analysis. Nature Comm. 8, 15735, doi:10.1038/ncomms15735.
- Kohlstedt, D. L., Evans, B., Mackwell, S. J., 1995. Strength of the lithosphere: Constraints imposed by
- laboratory experiments. J. Geophys. Res. 100, 17658–17602.
- Komiya, T., Maruyama, S., Masuda, T., Nohda, S., Hayashi, M., Okamotmo, K., 1999. Plate tectonics at
- 3.8-3.7 Ga: Field evidence from the Isua accretionary complex, southern west Greenland. J. Geol. 107,
- 1756 515–554.
- Korenaga, J., 2003. Energetics of mantle convection and the fate of fossil heat. Geophys. Res. Lett. 30, 1437,
- doi:10.1029/2003GL016982.

- Korenaga, J., 2005. Firm mantle plumes and the nature of the core-mantle boundary region. Earth Planet.
- 1760 Sci. Lett. 232, 29–37.
- Korenaga, J., 2006. Archean geodynamics and the thermal evolution of Earth. In: Benn, K., Mareschal, J.-C.,
- 1762 Condie, K. (Eds.), Archean Geodynamics and Environments. American Geophysical Union, Washing-
- ton, D.C., pp. 7–32.
- Korenaga, J., 2007. Thermal cracking and the deep hydration of oceanic lithosphere: A key to the generation
- of plate tectonics? J. Geophys. Res. 112, B05408, doi:10.1029/2006JB004502.
- Korenaga, J., 2008a. Plate tectonics, flood basalts, and the evolution of Earth's oceans. Terra Nova 20,
- 1767 419–439.
- Korenaga, J., 2008b. Urey ratio and the structure and evolution of Earth's mantle. Rev. Geophys. 46,
- 1769 RG2007, doi:10.1029/2007RG000241.
- Korenaga, J., 2009. Scaling of stagnant-lid convection with Arrhenius rheology and the effects of mantle
- melting. Geophys. J. Int. 179, 154–170.
- Korenaga, J., 2010a. On the likelihood of plate tectonics on super-Earths: Does size matter? ApJ 725,
- 1773 L43-L46.
- Korenaga, J., 2010b. Scaling of plate-tectonic convection with pseudoplastic rheology. J. Geophys. Res.
- 115, B11405, doi:10.1029/2010JB007670.
- Korenaga, J., 2011. Thermal evolution with a hydrating mantle and the initiation of plate tectonics in the
- early Earth. J. Geophys. Res. 116, B12403, doi:10.1029/2011JB008410.
- Korenaga, J., 2013. Initiation and evolution of plate tectonics on Earth: Theories and observations. Annu.
- 1779 Rev. Earth Planet. Sci. 41, 117–151.
- Korenaga, J., 2016. Can mantle convection be self-regulated? Sci. Adv. 2, e1601168.
- Korenaga, J., 2017a. On the extent of mantle hydration by plate bending. Earth Planet. Sci. Lett. 457, 1–9.

- Korenaga, J., 2017b. Pitfalls in modeling mantle convection with internal heating. J. Geophys. Res. Solid
 Earth 122, 4064–4085, doi:10.1002/2016JB013850.
- Korenaga, J., 2018a. Crustal evolution and mantle dynamics through Earth history. Phil. Trans. R. Soc. A 376, 20170408, http://dx.doi.org/10.1098/rsta.2017.0408.
- Korenaga, J., 2018b. Estimating the formation age distribution of continental crust by unmixing zircon age data. Earth Planet. Sci. Lett. 482, 388–395.
- Korenaga, J., 2020. Plate tectonics and surface environment: Role of the oceanic upper mantle. Earth-Sci.

 Rev. 205, 103185, https://doi.org/10.1016/j.earscirev.2020.103185.
- Korenaga, J., Planavsky, N. J., Evans, D. A. D., 2017. Global water cycle and the coevolution of Earth's interior and surface environment. Phil. Trans. R. Soc. A 375, 20150393, doi:10.1098/rsta.2015.0393.
- Labrosse, S., Hernlund, J. W., Coltice, N., 2007. A crystallizing dense magma ocean at the base of the Earth's mantle. Nature 450, 866–869.
- Labrosse, S., Poirier, J.-P., Mouel, J.-L. L., 2001. The age of the inner core. Earth Planet. Sci. Lett. 190, 111–123.
- Lay, T., Hernlund, J., Buffett, B. A., 2008. Core-mantle boundary heat flow. Nature Geosci. 1, 25–32.
- Luo, Y., Korenaga, J., 2021. Efficiency of eclogite removal from continental lithosphere and its implications for cratonic diamonds. Geology 49, https://doi.org/10.1130/G48204.1.
- Lyubetskaya, T., Korenaga, J., 2007. Chemical composition of Earth's primitive mantle and its variance, 2, implications for global geodynamics. J. Geophys. Res. 112, B03212, doi:10.1029/2005JB004224.
- Magni, V., Bouihol, P., van Hunen, J., 2014. Deep water recycling through time. Geochem. Geophys.

 Geosys. 15, 4203–4216, doi:10.1002/2014GC005525.
- Marchi, S., Bottke, W. F., Elkins-Tanton, L. T., Bierhaus, M., Wuennermann, K., Morbidelli, A., Kring,
 D. A., 2014. Widespread mixing and burial of Earth's Hadean crust by asteroid impacts. Nature 511,
 578–582.

- Marchi, S., Canup, R. M., Walker, R. J., 2018. Heterogeneous delivery of silicate and metal to the Earth by large planetesimals. Nature Geosci. 11, 77–81.
- Maurice, M., Tosi, N., Samuel, H., Plesa, A.-C., Hüttig, C., Breuer, D., 2017. Onset of solid-state mantle convection and mixing during magma ocean solidification. J. Geophys. Res. Planets 122, 577–598, doi:10.1002/2016JB005250.
- McCoy-West, A. J., Chowdhury, P., Burton, K. W., Sossi, P., Nowell, G. M., Fitton, J. G., Kerr, A. C.,
 Cawood, P. A., Williams, H. M., 2019. Extensive crustal extraction in Earth's early history inferred
 from molybdenum isotopes. Nature Geosci. 12, 946–951.
- McCulloch, M. T., Bennett, V. C., 1994. Progressive growth of the Earth's continental crust and depleted mantle: Geochemical constraints. Geochim. Cosmochim. Acta 58, 4717–4738.
- McKenzie, D., 2000. Constraints on melt generation and transport from U-series activity ratios. Chem. Geol. 162, 81–94.
- Mei, S., Suzuki, A. M., Kohlstedt, D. L., Dixon, N. A., Durham, W. B., 2010. Experimental constraints on the strength of the lithospheric mantle. J. Geophys. Res. 115, B08204, doi:10.1029/2009JB006873.
- Menez, B., Pisapia, C., Andreani, M., Jamme, F., Vanbellingen, Q. P., Brunelle, A., Richard, L., Dumas,
 P., Refregiers, M., 2018. Abiotic synthesis of amino acids in the recesses of the oceanic lithosphere.

 Nature.
- Michael, P. J., 1988. The concentration, behavior and storage of h₂0 in the suboceanic upper mantle: Implications for mantle metasomatism. Geochim. Cosmochim. Acta 52, 555–566.
- Miyazaki, Y., Korenaga, J., 2019a. On the timescale of magma ocean solidification and its chemical consequences: 1. thermodynamic database for liquid at high pressures. J. Geophys. Res. Solid Earth 124, 3382–3398, https://doi.org/10.1029/2018JB016932.
- Miyazaki, Y., Korenaga, J., 2019b. On the timescale of magma ocean solidification and its chemical consequences: 2. compositional differentiation under crystal accumulation and matrix compaction. J. Geophys. Res. Solid Earth 124, 3399–3419, https://doi.org/10.1029/2018JB016928.

- Mojzsis, S. J., Harrison, T. M., Pidgeon, R. T., 2001. Oxygen-isotope evidence from ancient zircons for liquid water at the Earth's surface 4,300 Myr ago. Nature 409, 178–181.
- Mondal, P., Korenaga, J., 2018. A propagator matrix method for the Rayleigh-Taylor instability of multiple layers: a case study on crustal delamination in the early Earth. Geophys. J. Int. 212, 1890–1901.
- Monteux, J., Andrault, D., Samuel, H., 2016. On the cooling of a deep terrestrial magma ocean. Earth Planet.

 Sci. Lett. 448, 140–149.
- Moorbath, S., Whitehouse, M. J., Kamber, B. S., 1997. Extreme Nd-isotope heterogeneity in the early

 Archaean fact or fiction? case histories from northern Canada and West Greenland. Chem. Geol. 135,

 213–231.
- Moore, W. B., Lenardic, A., 2015. The efficiency of plate tectonics and nonequilibrium dynamical evolution of planetary mantles. Geophys. Res. Lett. 42, 9255–9260, doi:10.1002/2015GL065621.
- ¹⁸⁴² Moore, W. B., Webb, A. A. G., 2013. Heat-pipe Earth. Nature 501, 501–505.
- Moresi, L., Solomatov, V., 1998. Mantle convection with a brittle lithosphere: thoughts on the global tectonic styles of the Earth and Venus. Geophys. J. Int. 133, 669–682.
- Morino, P., Caro, G., Reisberg, L., Schmacher, A., 2017. Chemical stratification in the post-magma ocean

 Earth inferred from coupled ^{146,147}Sm-^{142,143}Nd systematics in ultramafic rocks of the Saglek block

 (3.25-3.9 Ga; northern Labrador, Canada). Earth Planet. Sci. Lett. 463, 136–150.
- Morse, S. A., 1986. Origin of earliest planetary crust: role of compositional convection. Earth Planet. Sci.

 Lett. 81, 118–126.
- Mosenfelder, J. L., Asimow, P. D., Ahrens, T. J., 2007. Thermodynamic properties of Mg₂SiO₄ liquid at ultra-high pressures from shock measurements to 200 GPa on forsterite and wadsleyite. J. Geophys. Res. 112, B06208, doi:10.1029/2006JB004364.
- Moyen, J.-F., Laurent, O., 2018. Archaen teconic systems: A view from igneous rocks. Lithos 302-303, 99–125.

- Moyen, J.-F., van Hunen, J., 2012. Short-term episodicity of Archaean plate tectonics. Geology 40, 451–454.
- Murphy, D. T., Brandon, A. D., Debaille, V., Burgess, R., Ballentine, C., 2010. In search of a hidden long-
- term isolated sub-chondritic ¹⁴²Nd/¹⁴⁴Nd reservoir in the deep mantle: Implications for the Nd isotope
- systematics of the Earth. Geochim. Cosmochim. Acta 74, 738–750.
- Nelson, B. K., DePaolo, D. J., 1985. Rapid production of continental crust 1.7 to 1.9 b.y. ago: Nd isotopic
- evidence from the basament of the North American mid-continent. Geol. Soc. Am. Bull. 96, 746–754.
- Nimmo, F., 2015. Energetics of the core. In: Treatise on Geophysics, 2nd ed. Vol. 8. Elsevier, pp. 27–55.
- Nomura, R., Hirose, K., Uesugi, K., Ohishi, Y., Tsuchiyama, A., Miyake, A., Ueno, Y., 2014. Low core-
- mantle boundary temperature inferred from the solidus of pyrolite. Science 343, 522–525.
- Nomura, R., Ozawa, H., Tateno, S., Hirose, K., Hernlund, J., Muto, S., Ishii, H., Hiraoka, N., 2011. Spin
- crossover and iron-rich silicate melt in the Earth's deep mantle. Nature 473, 199–202.
- Nutman, A. P., Friend, C. R. L., Bennett, V. C., 2002. Evidence for 3650-3600 Ma assembly of the northern
- end of the Itsaq Gneiss Complex, Greenland: Implication for early Archean tectonics. Tectonics 21,
- 1005, 10.1029/2000TC001203.
- Ohtani, E., 1985. The primordial terrestrial magma ocean and its implication for stratification of the mantle.
- 1870 Phys. Earth Planet. Inter. 38, 70–80.
- O'Neil, J., Carlson, R. W., 2017. Building Archean cratons from Hadean mafic crust. Science 355, 1199-
- 1872 1202.
- O'Neill, C., Lenardic, A., Moresi, L., Torsvik, T. H., Lee, C.-T., 2007. Episodic Precambrian subduction.
- Earth Planet. Sci. Lett. 262, 552–562.
- O'Reilly, T. C., Davies, G. F., 1981. Magma transport of heat on Io: A mechanism allowing a thick litho-
- sphere. Geophys. Res. Lett. 8, 313–316.
- O'Rourke, J. G., Korenaga, J., 2012. Terrestrial planet evolution in the stagnant-lid regime: Size effects and
- the formation of self-destabilizing crust. Icarus 221, 1043–1060.

- O'Rourke, J. G., Korenaga, J., Stevenson, D. J., 2017. Thermal evolution of Earth with magnesium precipitation in the core. Earth Planet. Sci. Lett. 458, 263–272. 1880
- Padhi, C. M., Korenaga, J., Ozima, M., 2012. Thermal evolution of Earth with xenon degassing: A self-1881 consistent approach. Earth Planet. Sci. Lett. 341-344, 1–9. 1882
- Parai, R., Mukhopadhyay, S., 2012. How large is the subducted water flux? new constraints on mantle 1883 regassing rates. Earth Planet. Sci. Lett. 317-318, 396-406. 1884
- Parsons, B., 1982. Causes and consequences of the relation between area and age of the ocean floor. J. 1885 Geophys. Res. 87, 289-302. 1886
- Patchett, P. J., Arndt, N. T., 1986. Nd isotopes and tectonics of 1.9-1.7 Ga crustal genesis. Earth Planet. Sci. 1887 Lett. 78, 329-338. 1888
- Payne, J. L., McInerney, D. J., Barovich, K. M., Kirkland, C. L., Pearson, N. J., Hand, M., 2016. Strengths 1889 and limitations of zircon Lu-Hf and O isotopes in modeling crustal growth. Lithos 248-251, 175–192. 1890
- Pehrsson, S. J., Eglington, B. M., Evans, D. A. D., Huston, D., Reddy, S. M., 2016. Metallogeny and its 1891 link to orogenic style during the Nuna supercontinent cycle. In: Z.-X., L., Evans, D. A. D., Murphy, 1892 J. B. (Eds.), Supercontinent Cycles Through Earth History. Geological Society of London, pp. 83–94, 1893 doi:10.1144/SP424.5.
- Petford, N., Gallagher, K., 2001. Partial melting of mafic (amphibolitic) lower crust by periodic influx of 1895 basaltic magma. Earth Planet. Sci. Lett. 193, 483-499. 1896

1894

- Piccolo, A., Palin, R. M., Kaus, B. J. P., White, R. W., 2019. Generation of Earth's early con-1897 tinents from a relatively cool Archean mantle. Geochem. Geophys. Geosys. 20, 1679-1697, 1898 https://doi.org/10.1029/2018GC008079. 1899
- Piper, J. D. A., 2013. A planetary perspective on Earth evolution: Lid tectonics before plate tectonics. 1900 Tectonophysics 589, 44–56. 1901
- Plesa, A.-C., Tosi, N., Breuer, D., 2014. Can a fractionally crystallized magma ocean explain the thermo-1902 chemical evolution of Mars? Earth Planet. Sci. Lett. 403, 225–235. 1903

- Ptacek, M. P., Dauphas, N., Greber, N. D., 2020. Chemical evolution of the continental crust from a datadriven inversion of terrigenous sediment compositions. Earth Planet. Sci. Lett. 539, 116090.
- Puchtel, I. S., Touboul, M., Blichert-Toft, J., Walker, R. J., Bra, A. D., Nicklas, R. W., Kulikov, V. K., Samsonov, A. V., 2016. Lithophile and siderophile element systematics of Earth's mantle at the ArcheanProterozoic boundary: Evidence from 2.4 Ga komatiites. Geochim. Cosmochim. Acta 180, 227–255.
- Pujol, M., Marty, B., Burgess, R., Turner, G., Philippot, P., 2013. Argon isotopic composition of Archaean atmosphere probes early Earth geodynamics. Nature 498, 87–90.
- Reese, C. C., Solomatov, V. S., Moresi, L.-N., 1999. Non-newtonian stagnant lid convection and magmatic resurfacing on venus. Icarus 139, 67–80.
- Reese, C. C., Solomatov, V. S., Orth, C. P., 2007. Mechanisms for cessation of magmatic resurfacing on Venus. J. Geophys. Res. 112, B04S04, doi:10.1029/2006JE002782.
- Rey, P. F., Coltice, N., 2008. Neoarchean lithospheric strengthening and the coupling of Earth's geochemical reservoirs. Geology 36, 635–638.
- Rey, P. F., Houseman, G., 2006. Lithospheric scale gravitational flow: the impact of body forces on orogenic processes from Archean to Phanerozoic. In: Buiter, S. J. H., Schreurs, G. (Eds.), Analogue and Numerical Modelling of the Crustal-Scale Processes. Vol. 253. Geological Society of London, pp. 153–167.
- Reymer, A., Schubert, G., 1984. Phanerozoic addition rates to the continental crust and crustal growth.

 Tectonics 3, 63–77.
- Richards, M. A., Yang, W.-S., Baumgardner, J. R., Bunge, H.-P., 2001. Role of a low-viscosity zone in stabilizing plate tectonics: Implications for comparative terrestrial planetology. Geochem. Geophys. Geosys. 2, 2000GC000115.
- Rino, S., Komiya, T., Windley, B. F., Katayama, I., Motoki, A., Hirata, T., 2004. Major episodic increases of continental crustal growth determined from zircon ages of river sands; implications for mantle overturns in the Early Precambrian. Phys. Earth Planet. Inter. 146, 369–394.

- Rizo, H., Boyer, M., Blichert-Toft, J., O'Neil, J., Rosing, N. T., Paquette, J.-L., 2012. The elusive Hadean enriched reservoir revealed by ¹⁴²Nd deficits in Isua Archaean rocks. Nature 491, 96–100.
- Rizo, H., Boyet, M., Blichert-Toft, J., Rosing, M. T., 2013. Early mantle dynamics inferred from ¹⁴²Nd variations in Archean rocks from southwest Greenland. Earth Planet. Sci. Lett. 377-378, 324–335.
- Roberts, N. M. W., Spencer, C. J., 2015. The zircon archive of continent formation through time. In: Roberts,
 N. M. W., Van Kranendonk, M., Parman, S., Shirey, S., Clift, P. D. (Eds.), Continent Formation Through
 Time. Vol. 389 of Special Publications. Geological Society of London, pp. 197–225.
- Rollinson, H., 2017. There were no large volumes of felsic continental crust in the early Earth. Geosphere 13, doi:10.1130/GES01437.1.
- Roman, A., Arndt, N., 2020. Differentiated Archean oceanic crust: Its thermal structure, mechanical stability and a test of the sagduction hypothesis. Geochim. Cosmochim. Acta 278, 65–77.
- Rosas, J. C., Korenaga, J., 2018. Rapid crustal growth and efficient crustal recycling in the early Earth:

 Implications for Hadean and Archean geodynamics. Earth Planet. Sci. Lett. 494, 42–49.
- Rosas, J. C., Korenaga, J., 2021. Archean seafloor shallowed with age due to radiogenic heating in the mantle. Nature Geosci. 14, 51–56, https://doi.org/10.1038/s41561–020–00673–1.
- Rose, I. R., Korenaga, J., 2011. Mantle rheology and the scaling of bending dissipation in plate tectonics. J. Geophys. Res. 116, B06404, doi:10.1029/2010JB008004.
- Roth, A. S. G., Bourdon, B., Mojzsis, S. J., Rudge, J. F., Guitreau, M., Blichert-Toft, J., 2014. Combined

 1946

 1947,146Sm-143,142Nd constraints on the longevity and residence time of early terrestrial crust. Geochem.

 1947

 Geophys. Geosys. 15, 2329–2345.
- Rozel, A. B., Golabek, G. J., Jain, C., Tackley, P. J., Gerya, T., 2017. Continental crust formation on early
 Earth controlled by intrusive magmatism. Nature 545, 332–335.
- Rudnick, R. L., Gao, S., 2003. Composition of the continental crust. In: Holland, H. D., Turekian, K. K. (Eds.), Treatise on Geochemistry. Vol. 3. Elsevier, pp. 1–64.

- Saal, A. E., Hauri, E. H., Langmuir, C. H., Perfit, M. R., 2002. Vapour undersaturation in primitive midocean-ridge basalt and the volatile content of Earth's upper mantle. Nature 419, 451–455.
- Saji, N. S., Larsen, K., Wielandt, D., Schiller, M., Costa, M. M., Whitehouse, M. J., Rosing, M. T., Bizzarro,
- M., 2018. Hadean geodynamics inferred from time-varying ¹⁴²Nd/¹⁴⁴Nd in the early Earth rock record.
- 1956 Geochem. Persp. Lett. 7, 43–48.
- Scholl, D. W., von Huene, R., 2007. Crustal recycling at modern subduction zones applied to the past—
- issues of growth and preservation of continental basement, mantle geochemistry and supercontinent
- reconstruction. Geol. Soc. Am. Spec. Paper 200, 9–32.
- Schrenk, M. O., Brazelton, W. J., Lang, S. Q., 2013. Serpentinization, carbon, and deep life. Rev. Mineral.
- 1961 Geochem. 75, 575–606.
- Schröder, K.-P., Smith, R. C., 2008. Distant future of the Sun and Earth revisited. Mon. Not. R. astr. Soc.
- 1963 386, 155–163.
- Schwartzman, D. W., 1973. Ar degassing and the origin of the sialic crust. Geochim. Cosmochim. Acta 37,
- 1965 2479–2495.
- Servali, A., Korenaga, J., 2018. Oceanic origin of continental mantle lithosphere. Geology 46, 1047–1059.
- Shirey, S. B., Richardson, S. H., 2011. Start of the Wilson cycle at 3 Ga shown by diamonds from subconti-
- nental mantle. Science 333, 434–436.
- Silver, P. G., Behn, M. D., 2008. Intermittent plate tectonics? Science 319, 85–88.
- Sizova, E., Gerya, T., Stuwe, K., Brown, M., 2015. Generation of felsic crust in the Archean: A geodynamic
- modeling perspective. Precambrian Res. 271, 198–224.
- Sleep, N. H., 1979. Thermal history and degassing of the Earth: Some simple calculations. J. Geol. 87,
- 1973 671–686.
- 1974 Sleep, N. H., 2000. Evolution of the mode of convection within terrestrial planets. J. Geophys. Res. 105,
- 1975 17563–17578.

- Sleep, N. H., Meibom, A., Fridriksson, T., Coleman, R. G., Bird, D. K., 2004. H₂-rich fluids from serpentinization: Geochemical and biotic implications. Proc. Nat. Acad. Sci. USA 101, 12818–12823.
- Sleep, N. H., Zahnle, K., 2001. Carbon dioxide cycling and implications for climate on ancient Earth. J. Geophys. Res. 106, 1373–1399.
- Sleep, N. H., Zahnle, K. J., Lupu, R. E., 2014. Terrestrial aftermath of the Moon-forming impact. Phil.

 Trans. R. Soc. A 372, 20130172, doi:10.1098/rsta.2013.0172.
- Smit, K. V., Shirey, S. B., Hauri, E. H., Stern, R. A., 2019. Sulfur isotopes in diamonds reveal differences in continent construction. Science 364, 383–385.
- Smit, M. A., Mezger, K., 2017. Earth's early O₂ cycle suppressed by primitive continents. Nature Geosci.
- Sobolev, A. V., Chaussidon, M., 1996. H₂O concentrations in primary melts from supra-subduction zones and mid-ocean ridges: Implications for H₂O storage and recycling in the mantle. Earth Planet. Sci. Lett. 137, 45–55.
- Solomatov, V., 2015. Magma oceans and primordial mantle differentiation. In: Treatise on Geophysics, 2nd ed. Vol. 9. Elsevier, pp. 81–104.
- Solomatov, V. S., 2000. Fluid dynamics of a terrestrial magma ocean. In: The Origin of Earth and Moon.
 University of Arizona, pp. 323–338.
- Solomatov, V. S., 2004. Initiation of subduction by small-scale convection. J. Geophys. Res. 109, B01412, doi:10.1029/2003JB002628.
- Solomatov, V. S., Moresi, L.-N., 2000. Scaling of time-dependent stagnant lid convection: Application to small-scale convection on earth and other terrestrial planets. J. Geophys. Res. 105, 21795–21817.
- Solomatov, V. S., Stevenson, D. J., 1993a. Kinetics of crystal growth in a terrestrial magma ocean. J. Geophys. Res. 98, 5407–5418.
- Solomatov, V. S., Stevenson, D. J., 1993b. Nonfractional crystallization of a terrestrial magma ocean. J. Geophys. Res. 98, 5391–5406.

- Solomatov, V. S., Stevenson, D. J., 1993c. Suspension in convective layers and style of differentiation of a terrestrial magma ocean. J. Geophys. Res. 98, 5375–5390.
- Spencer, C. J., Murphy, J. B., Kirkland, C. L., Liu, Y., Mitchell, R. N., 2018. A Palaeoproterozoic tectonomagmatic lull as a potential trigger for the supercontinental cycle. Nature Geosci. 11, 97–101.
- Stein, C., Schmalzl, J., Hansen, U., 2004. The effect of rheological parameters on plate behavior in a selfconsistent model of mantle convection. Phys. Earth Planet. Inter. 142, 225–255.
- 2006 Stern, R. J., 2018. The evolution of plate tectonics. Phil. Trans. R. Soc. A 376, 20170406, http://dx.doi.org/10.1098/rsta.2017.0406.
- Stern, R. J., Scholl, D. W., 2010. Yin and yang of continental crust creation and destruction by plate tectonic processes. Int. Geol. Rev. 52, 1–31.
- Stevenson, D. J., Spohn, T., Schubert, G., 1983. Magnetism and thermal evolution of the terrestrial planets.

 Icarus 54, 466–489.
- Stixrude, L., de Koker, N., Sun, N., Mookherjee, M., Karki, B. B., 2009. Thermodynamics of silicate liquids in the deep Earth. Earth Planet. Sci. Lett. 278, 225–232.
- Stixrude, L., Lithgow-Bertelloni, C., 2011. Thermodynamics of mantle minerals, II, phase equilibria. Geophys. J. Int. 184, 1180–1213.
- Strachan, A., Çağin, T., Goddard, W. A., 1999. Phase diagram of MgO from density-functional theory and molecular-dynamics simulations. Phys. Rev. B 60, 15084–15093.
- Stracke, A., 2012. Earth's heterogeneous mantle: A product of convection-driven interaction between crust and mantle. Chem. Geol. 330-331, 274–299.
- Stuart, F. M., Mark, D. F., Grandanger, P., McConville, P., 2016. Earth-atmosphere evolution based on new determination of Devonian atmospheric Ar isotopic composition. Earth Planet. Sci. Lett. 446, 21–26.
- Tajika, E., Matsui, T., 1993. Evolution of seafloor spreading rate based on ⁴⁰Ar degassing history. Geophys.

 Res. Lett. 20, 851–854.

- Tang, M., Chen, K., Rudnick, R. L., 2016. Archean upper crust transition from mafit to felsic marks the onset of plate tectonics. Science 351, 372–375.
- Tarduno, J. A., Cottrell, R. D., Bono, R. K., Oda, H., Davis, W. J., Fayek, M., van 't Erve, O., Nimmo, F.,
- Huang, W., Thern, E. R., Fearn, S., Mitra, G., Smirnov, A. V., Blackman, E. G., 2020. Paleomagnetism
- indicates that primary magnenetite in zircon records a strong Hadean geodynamo. Proc. Nat. Acad. Sci.
- 2029 USA 117, 2309–2318.
- Tateno, S., Hirose, K., Ohishi, Y., 2014. Melting experiments on peridotite to lowermost mantle conditions.
- J. Geophys. Res. Solid Earth 119, 4684–4694, doi:10.1002/2013JB010616.
- Taylor, S. R., McLennan, S. M., 1985. The Continental Crust: its Composition and Evolution. Blackwell,
- Boston.
- Taylor, S. R., McLennan, S. M., 1995. The geochemical evolution of the continental crust. Rev. Geophys.
- 2035 33, 241–265.
- Thiemens, M. M., Sprung, P., Fonseca, R. O. C., Leitzke, F. P., Munker, C., 2019. Early Moon formation
- inferred from hafnium-tungsten systematics. Nature Geosci. 12, 696–700.
- Thomas, C. W., Liu, Q., Agee, C. B., Ssimow, P. D., Lange, R. A., 2012. Multi-technique equation of state
- for Fe₂SiO₄ melt and the density of Fe-bearing silicate melts from 0 to 161 ga. J. Geophys. Res. 117,
- 2040 B10206, doi:10.1029/2012JB009403.
- Tonks, W. B., Melosh, H. J., 1990. The physics of crystal settling and suspension in a turbulent magma
- ocean. In: Origin of the Earth. University of Arizona, pp. 151–174.
- Trail, D., Boehnke, P., Savage, P. S., Liu, M.-C., Miller, M. L., Bindeman, I., 2018. Origin and significance
- of Si and O isotope heterogeneities in Phanerozoic, Archean, and Hadean zircon. Proc. Nat. Acad. Sci.
- 2045 USA 115, 10287–10292.
- Trail, D., Watson, E. B., Tailby, N. D., 2011. The oxidation state of Hadean magmas and implications for
- early Earth's atmosphere. Nature 480, 79–82.

- Turcotte, D. L., Schubert, G., 1982. Geodynamics: Applications of Continuum Physics to Geological Problems. John Wiley, New York.
- Turner, S., Rushmer, T., Reagan, M., Moyen, J.-F., 2014. Heading down early on? start of subduction on Earth. Geology 42, 139–142.
- Turner, S., Wilde, S., Wörner, G., Schaefer, B., Lai, Y.-J., 2020. An andesitic source for

 Jack Hills zircon supports onset of plate tectonics in the Hadean. Nature Comm. 11, 1241,

 https://doi.org/10.1038/s41467-020-14857-1.
- van Hunen, J., Moyen, J.-F., 2012. Archean subduction: fact or fiction? Annu. Rev. Earth Planet. Sci. 40, 195–219.
- van Hunen, J., van den Berg, A. P., 2008. Plate tectonics on the early Earth: Limitations imposed by strength and buoyancy of subducted lithosphere. Lithos 103, 217–235.
- van Keken, P. E., Hacker, B. R., Syracuse, E. M., Abers, G. A., 2011. Subduction factory: 4.

 depth-dependent flux of H₂O from subducting slabs worldwide. J. Geophys. Res. 116, B01401,

 doi:10.1029/2010JB007922.
- Van Kranendonk, M. J., 2010. Two types of Archean continental crust: Plume and plate tectonics on early
 Earth. Am. J. Sci 310, 1187–1209.
- Van Kranendonk, M. J., Collins, W. J., Hickman, A., Pawley, M. J., 2004. Critical tests of vertical vs.
 horizontal tectonic models for the Archaean East Pilbara Granite-Greenstone Terrane, Pilbara Craton,
 Western Australia. Precambrian Res. 131, 173–211.
- Van Kranendonk, M. J., Smithies, R. H., Hickman, A. H., Champion, D., 2007. Review: secular tectonic evolution of Archean continental crust: interplay between horizontal and vertical processes in the formation of the Pilbara Craton, Australia. Terra Nova 19, 1–38.
- Vervoort, J. D., Blichert-Toft, J., 1999. Evolution of the depleted mantle: Hf isotope evidence from juvenile rocks through time. Geochim. Cosmochim. Acta 63, 533–556.

- Vervoort, J. D., Patchett, P. J., Blichert-Toft, J., Albarede, F., 1999. Relationships between Lu-Hf and Sm-Nd isotopic systems in the global sedimentary system. Earth Planet. Sci. Lett. 168, 79–99.
- Vervoort, J. D., Patchett, P. J., Gehrels, G. E., Nutman, A. P., 1996. Constraints on early Earth differentiation from hafnum and neodymium isotopes. Nature 379, 624–627.
- von Bargen, N., Waff, H. S., 1986. Permeabilities, interfacial areas and curvatures of partially molten systems: Results of numerical computations of equilibrium microstructures. J. Geophys. Res. 91, 9261–9278
- Wallace, P. J., 1998. Water and partial melting in mantle plumes: Inferences from the dissolved H₂O concentrations of Hawaiian basaltic magmas. Geophys. Res. Lett. 25, 3639–3642.
- Watson, E. B., Harrison, T. M., 2005. Zircon thermometer reveals minimum melting conditions on earliest Earth. Science 308, 841–844.
- Weiss, B. P., Maloof, A. C., Harrison, T. M., Swanson-Hysell, N. L., Fu, R. R., Kirschvink, J. L., Watson,
 E. B., Coe, R. S., Tikoo, S. M., Ramezani, J., 2016. Reply to Comment on "Pervasive remagnetization of detrital zircon host rocks in the Jack Hills, Western Australia and implications for records of the early dynamo". Earth Planet. Sci. Lett. 450, 409–412.
- Wilde, S. A., Valley, J. W., Peck, W. H., Graham, C. M., 2001. Evidence from detrital zircons for the existence of continental crust and oceans on the Earth 4.4 Gyr ago. Nature 409, 175–178.
- Zahnle, K., Arndt, N., Cockell, C., Halliday, A., Nisbet, E., Selsis, F., Sleep, N. H., 2007. Emergence of a habitable planet. Space Sci. Rev. 129, 35–78.
- Zahnle, K. J., Kasting, J. F., Pollack, J. B., 1988. Evolution of a steam atmosphere during Earth's accretion.

 Icarus 74, 62–97.
- Zerr, A., Boehler, R., 1993. Melting of (Mg,Fe)SiO₃-perovskite to 625 kilobars: Indication of a high melting temperature in the lower mantle. Science 262, 553–555.
- Zerr, A., Boehler, R., 1994. Constraints on the melting temperature of the lower mantle from high-pressure experiments on MgO and magnesiowüstitle. Nature 371, 506–508.

- Zhang, L., Fei, Y., 2008. Melting behavior of (Mg,Fe)O solid solutions at high pressure. Geophys. Res. Lett. 35, L13302, doi:10.1029/2008GL034585.
- Ziegler, L. B., Stegman, D. R., 2013. Implications of a long-lived basal magma ocean in generating Earth's
 ancient magnetic field. Geochem. Geophys. Geosys. 14, doi:10.1002/2013GC005001.

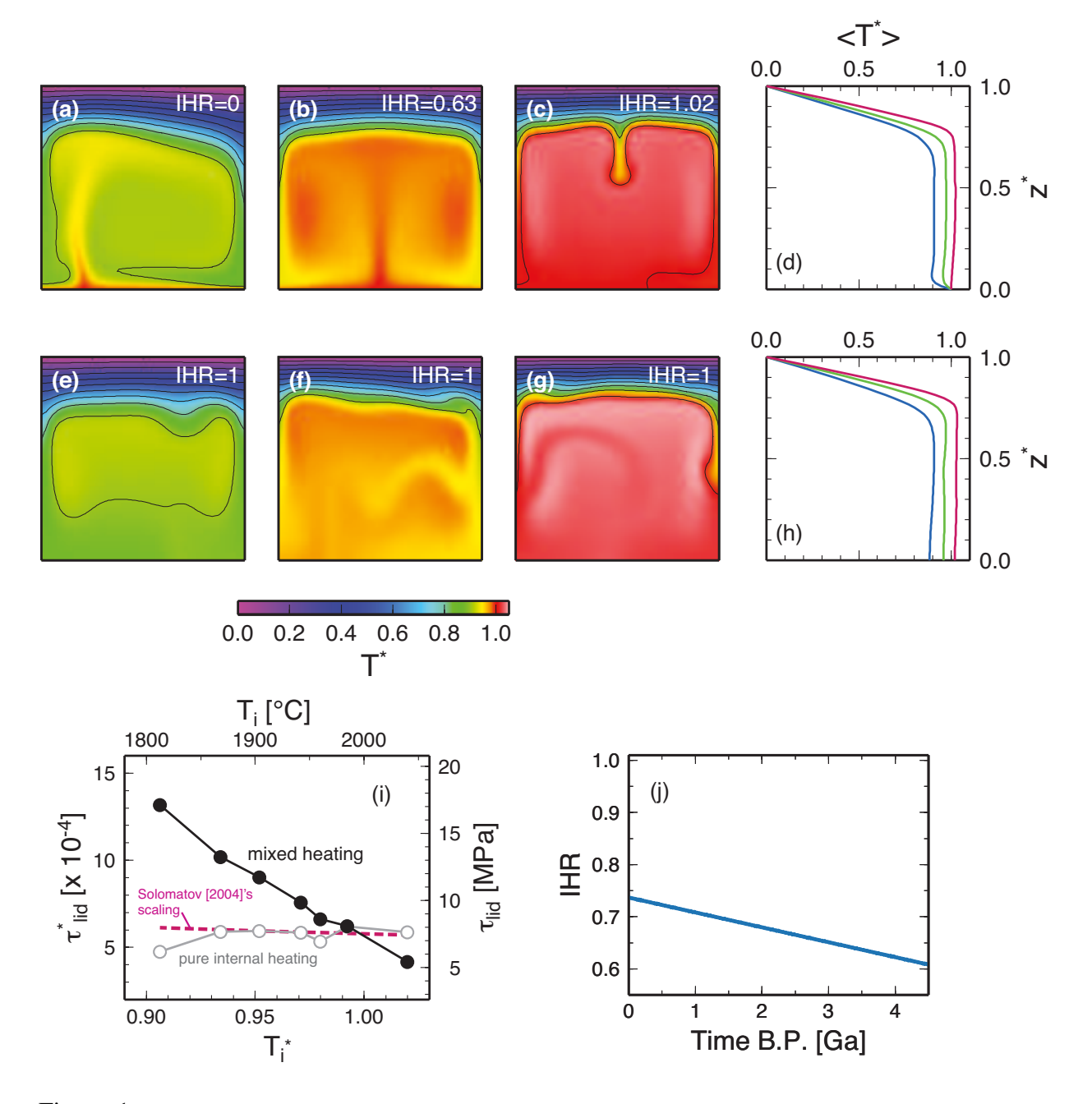


Figure 1: Influence of varying internal heat production on the magnitude of convective stress. (a)-(c) Reproduction of stagnant lid simulation in O'Neill et al. (2007). With the bottom temperature fixed to some constant value, increasing internal heat production moves the convection system from purely basally heated (a) to almost purely internally heated (c). This can also be seen in terms of the internal heating ratio (IHR), which varies from 0 to 1.02. (d) Horizontally averaged thermal profiles of (a) (blue), (b) (green), and (c) (red). (e)-(g) Purely internally-heated simulation, corresponding to (a)-(c), to isolate the effect of internal heating. (h) Same as (d) but for (e) through (g). (i) Convective stress as a function of internal temperature, which is in turn a function of internal heating. Solid circles correspond to mixed heating (as shown in (a)-(c)), whereas open circles to pure internal heating (as shown in (e)-(g)). Also shown as dashed is the stress scaling of Solomatov (2004). (j) A typical secular evolution of internal heating ratio over Earth history. The example shown corresponds to the thermal evolution shown in Figure 12a. Modified after Korenaga (2017b).

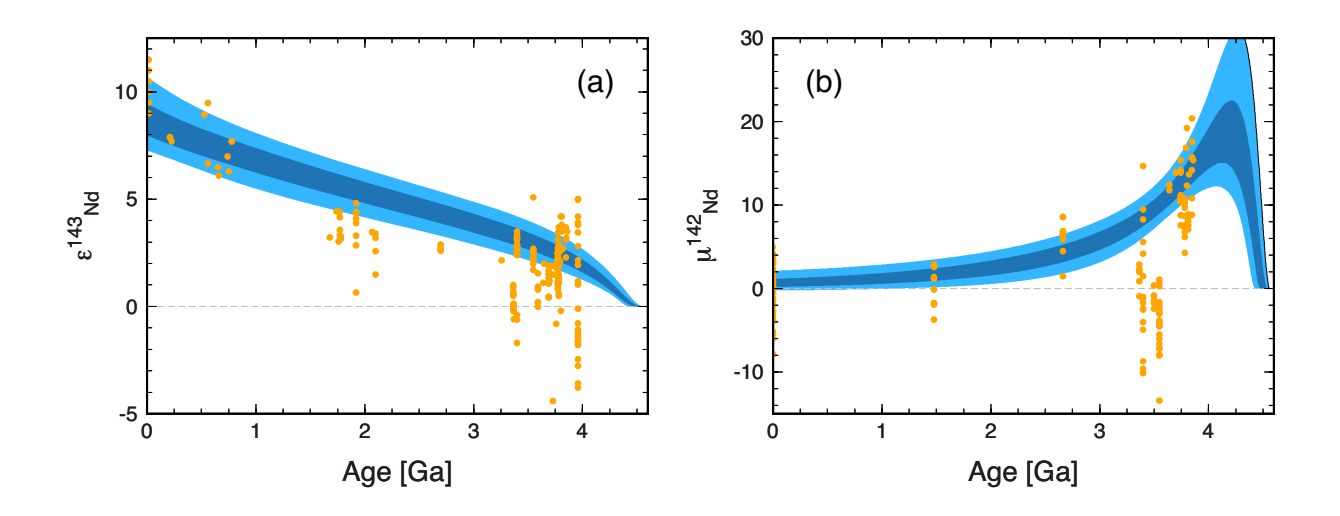


Figure 2: (a) 143 Nd and (b) 142 Nd evolution of the depleted mantle based on published data (Baadsgaard et al. 1986; Moorbath et al. 1997; Vervoort and Blichert-Toft 1999; Caro et al. 2006; Bennett et al. 2007; Murphy et al. 2010; Rizo et al. 2012; Jackson and Carlson 2012; Debaille et al. 2013; Roth et al. 2014; Puchtel et al. 2016; Caro et al. 2017; Morino et al. 2017). $\varepsilon_{\rm Nd}^{143}(t)$ is defined as $[(^{143}{\rm Nd}/^{144}{\rm Nd})_t/(^{143}{\rm Nd}/^{144}{\rm Nd})_t/(^{142}{\rm Nd}/^{144}{\rm Nd}/^{144}{\rm Nd})_t/(^{142}{\rm Nd}/^{144}{\rm Nd}/^{144}{\rm Nd}/^{144}{\rm Nd}/^{144}{\rm Nd}/^{144}{\rm Nd}/^{144}{\rm Nd}/^{144}{\rm Nd}/^{144}{$

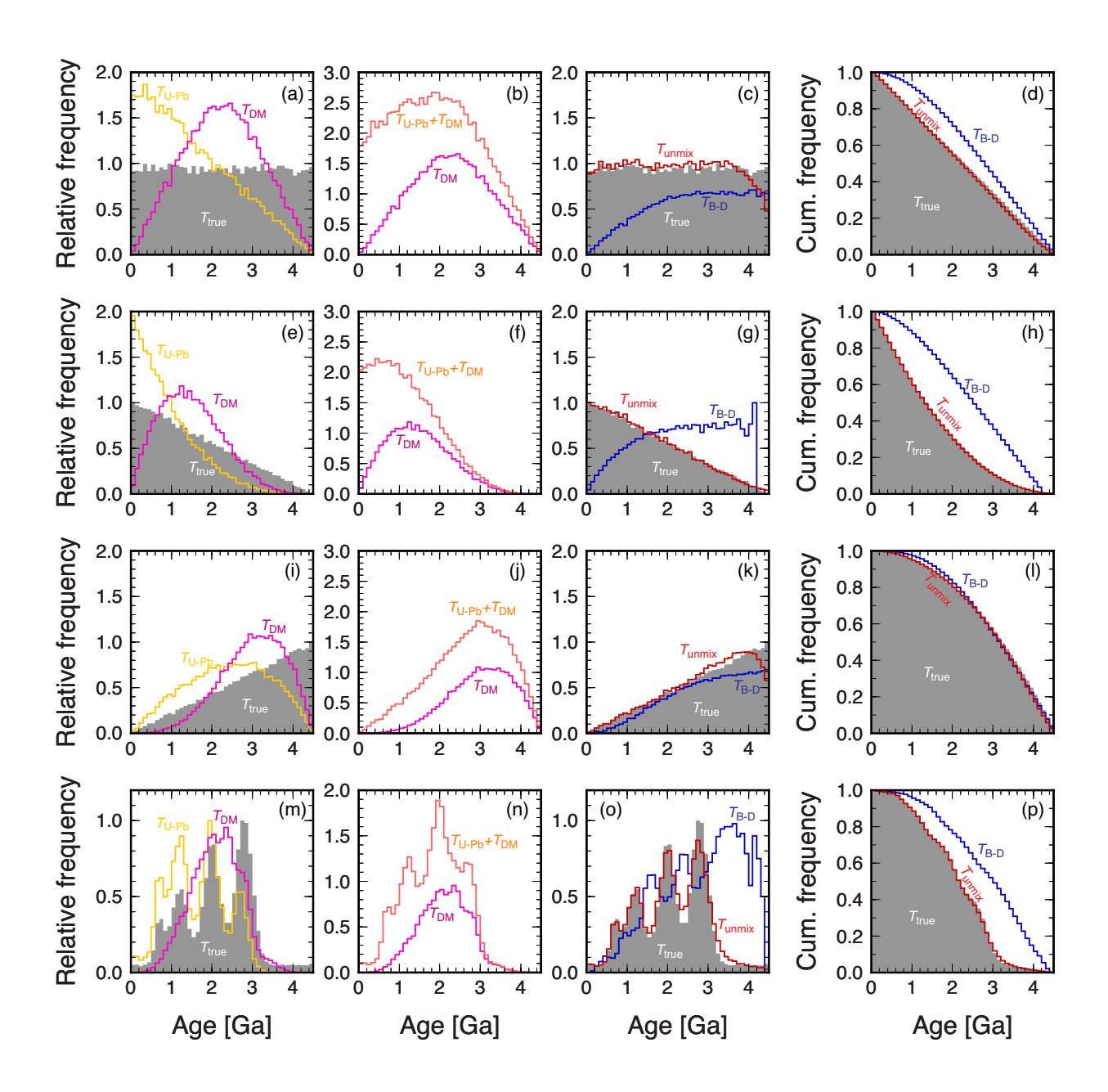


Figure 3: Results of applying the method of Belousova et al. (2010) to four different sets of synthetic data: (1st row) constant crust production through time, (2nd row) more production in recent times, (3rd row) less production in recent times, and (4th row) multiple peaks in crustal production. The 1st column shows the true distribution (gray) and the corresponding distributions of U-Pb crystallization age (yellow) and the depleted mantle model age (magenta). The 2nd column compares the model age distribution with the summation of the crystallization and model age distributions (orange). The 3rd column compares the result of dividing the model age distribution by the summation (blue), which, according to Belousova et al. (2010), would represent new crust generation rate, with the true distribution of crust production (gray). The 4th column is a cumulative version of the 3rd column. The age distribution obtained by the method of Belousova et al. (2010) (and popularized by Dhuime et al. (2012)) is labeled by $T_{\rm B-D}$. Also shown in the 3rd and 4th columns are the results of applying the unmixing method of Korenaga (2018b) (red; labeled by $T_{\rm unmix}$). See Korenaga (2018b) for how to make those synthetic data.

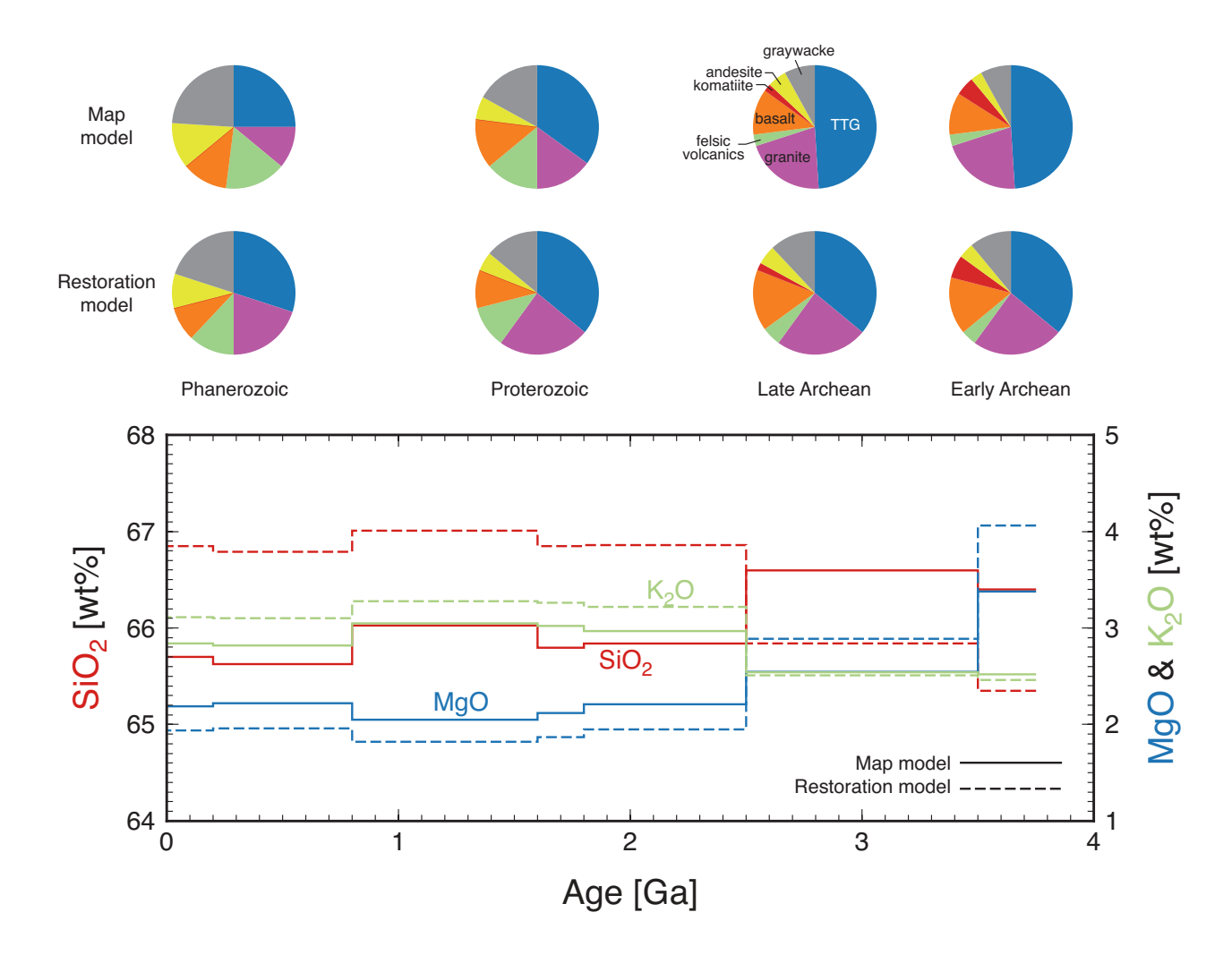


Figure 4: Secular evolution of upper continental crust composition according to the estimates of Condie (1993). Relative proportions of rock types (TTG, granite, felsic volcanics, basalt, komatiite, andesite, and graywacke) as well as SiO₂ (red), MgO (blue), and K₂O (green) contents are shown, for his map (solid) and restoration (dashed) models. Difference between these two models reflects corrections for erosion.

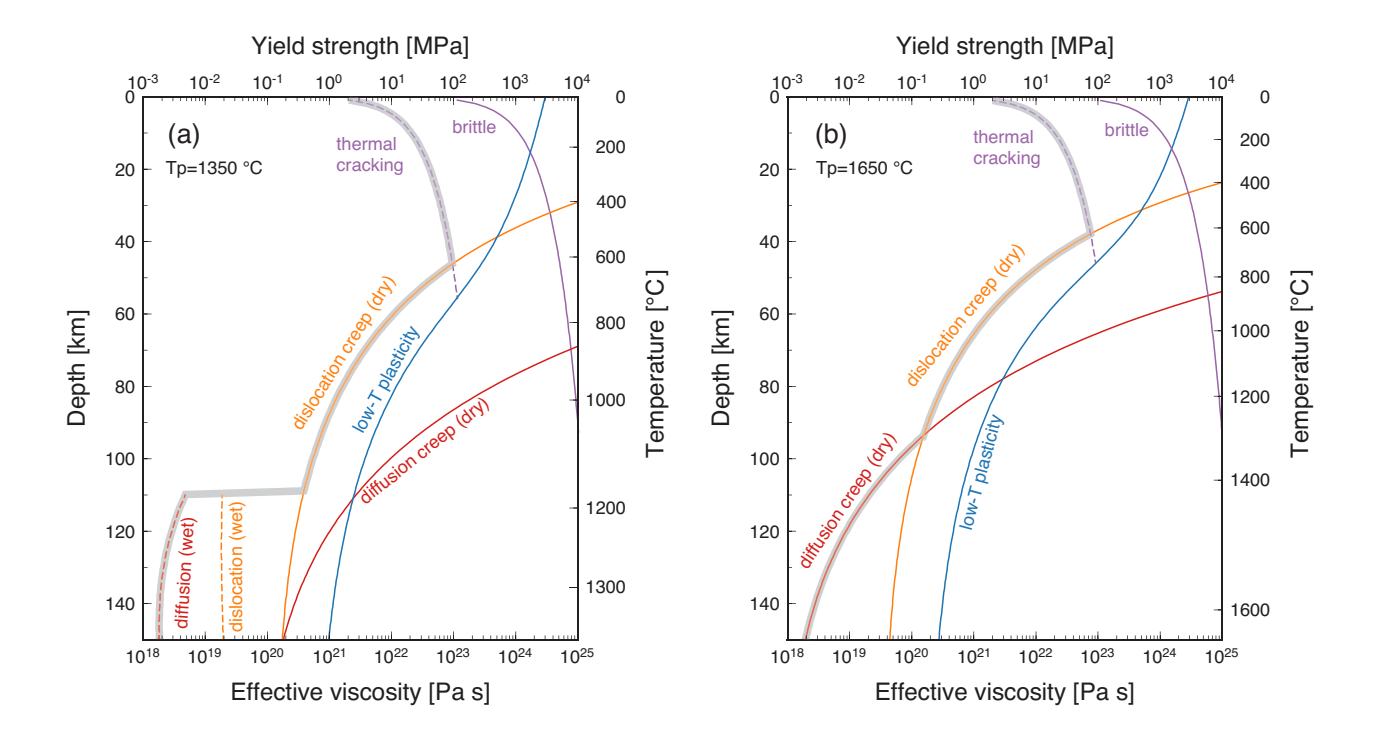


Figure 5: Hypothetical yield strength profiles (thick gray curves) for the shallow suboceanic mantle (a) at present with a potential temperature of 1350 °C and (b) at the Archean with a potential temperature of 1650 °C, both evaluated under a seafloor age of 100 Ma. The Archean asthenosphere is assumed to be dry. The thermal structure is based on half-space cooling and is shown on the right axis. Yield strength is calculated assuming a geological strain rate of 10⁻¹⁵ s⁻¹, so a yield strength of 1 GPa corresponding to an effective viscosity of 10²⁴ Pa s. For simplicity, the effect of crustal layer is ignored, and the rheology of olivine aggregates is used at all depths. Deformation mechanisms considered here include: (1) dry diffusion creep (red) with the grain size exponent of 2.2, the activation energy of 376 kJ mol⁻¹, the activation volume of 7 cm³ mol⁻¹, and the preexponential factor of 8.3×10^7 , (2) dry dislocation creep (orange) with the stress exponent of 3.6, the activation energy of 400 kJ mol⁻¹, the activation volume of 9 cm³ mol⁻¹, and the preexponential factor of 110, (3) wet diffusion creep (red dashed) with the grain size exponent of 1.7, the water content exponent of 1.2, the activation energy of 307 kJ mol⁻¹, the activation volume of 24 cm³ mol⁻¹. and the preexponential factor of 4.4×10^4 , (4) wet dislocation creep (orange dashed) with the stress exponent of 4.4, the water content exponent of 2, the activation energy of 171 kJ mol⁻¹, the activation volume of $24 \text{ cm}^3 \text{ mol}^{-1}$, and the preexponential factor of 1.4×10^{-4} . (5) low-temperature plasticity (blue) based on the reanalysis of the experimental data of Mei et al. (2010) by Jain et al. (2017), with the exponents of p = 1and q = 2, (6) brittle strength (purple) with the friction coefficient of 0.8 under optimal thrust faulting, (7) reduced brittle strength with thermal cracking (purple dashed), assuming the effective friction coefficient of 0.03 (Korenaga 2011). The flow-low parameters for diffusion and dislocation creep are sampled from the statistical models of Jain et al. (2019): model OL-DB₂ for dry conditions, and model OL-WB₁ for wet conditions. Thermal cracking is effective only up to ~ 700 °C (Korenaga 2007). Grain size is set at 1 cm, and the water content of the present-day asthenosphere is assumed to be 800 ppm H/Si (Hirth and Kohlstedt 1996).

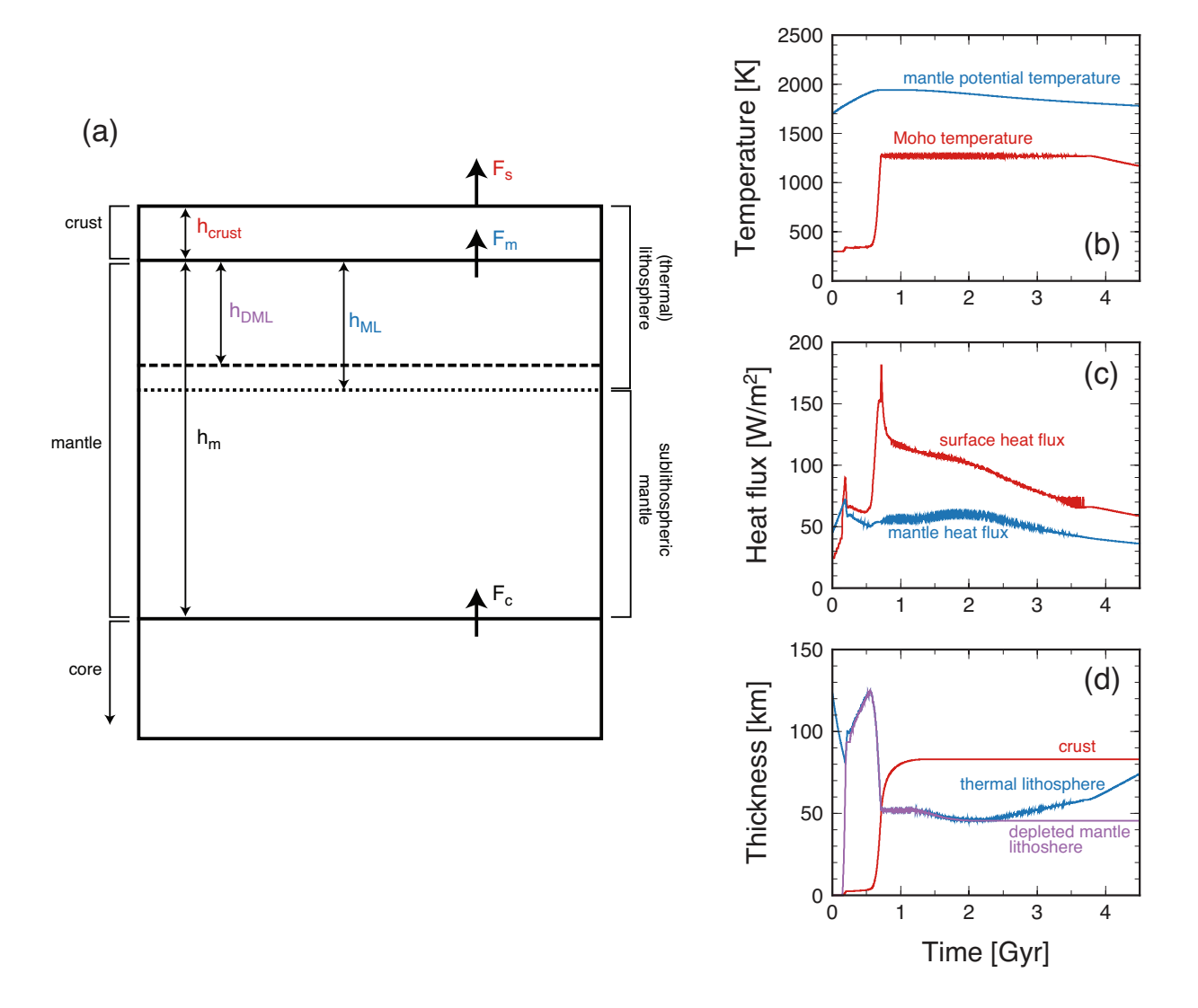


Figure 6: Evolution of an Earth-size planet in the mode of stagnant lid convection with magmatism (O'Rourke and Korenaga 2012). (a) Schematic description of the model structure. Depleted mantle lithosphere (DML) refers to the mantle that has been processed by melting and stays in the thermal boundary layer. The thickness of DML cannot exceed that of the mantle part of thermal lithosphere (ML). The section of the mantle below ML is the sublithospheric mantle. (b) Mantle potential temperature (blue) and Moho temperature (red). (c) Mantle heat flux (F_m ; blue) and surface heat flux (F_s ; red). Because crustal melting makes surface heat flux highly discontinuous, a Gaussian filter with a standard deviation of 4 Myr is applied for plotting purposes. (d) Thicknesses of mantle lithosphere (h_{ML} ; blue), DML (h_{DML} ; purple), and crust(h_{crust} ; red).

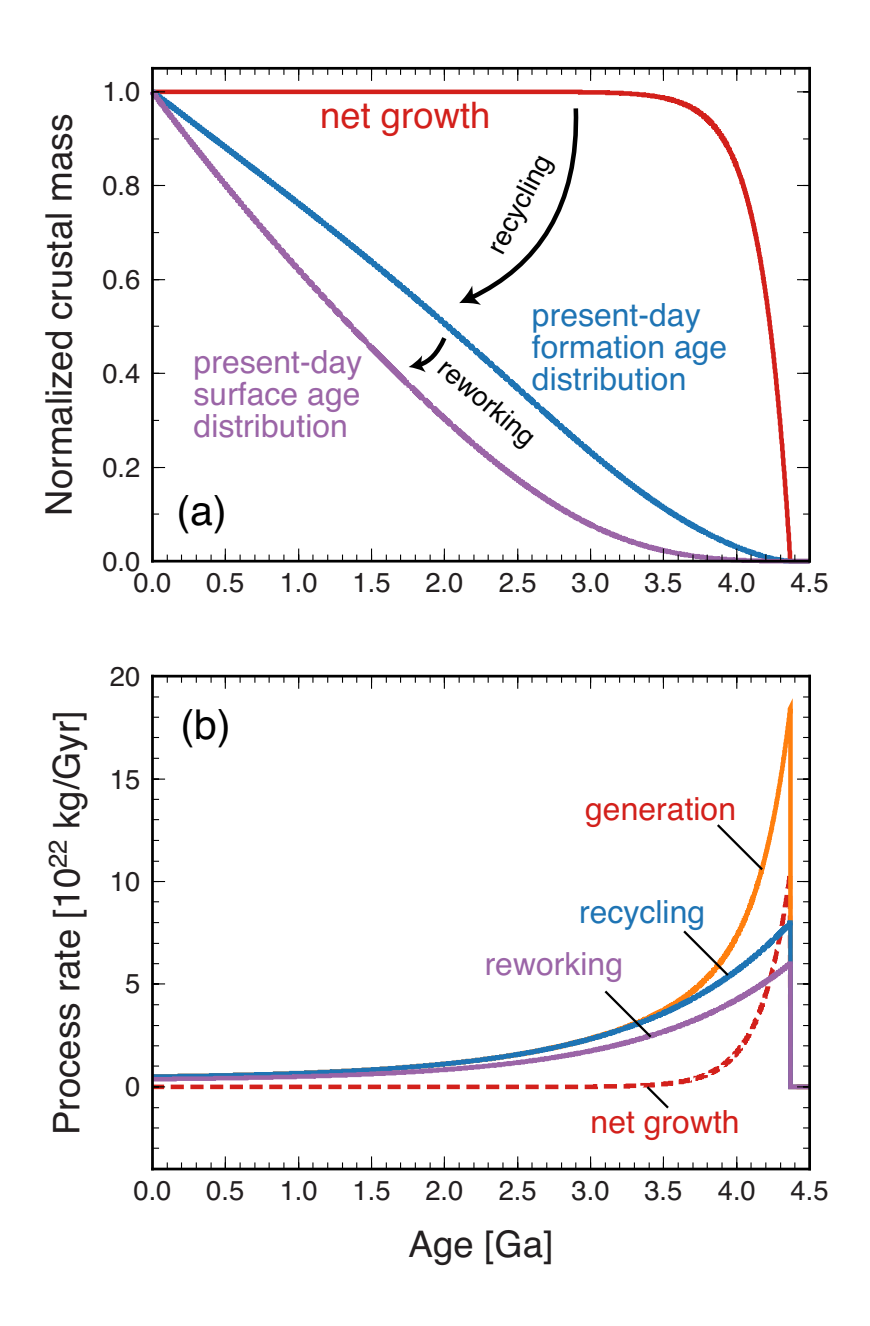


Figure 7: (a) Net growth of continental crust (red), the present-day cumulative distribution of crust formation ages (blue), and the present-day cumulative distribution of surface ages (purple). The difference between net growth and formation age distribution reflects the time-integrated effect of crustal recycling, and that between formation age and surface age distributions reflects the time-integrated effect of crustal reworking. (b) Crustal generation rate (orange), crustal recycling rate (blue), crustal reworking rate (purple), and net growth rate (red dashed), all corresponding to the example shown in (a).

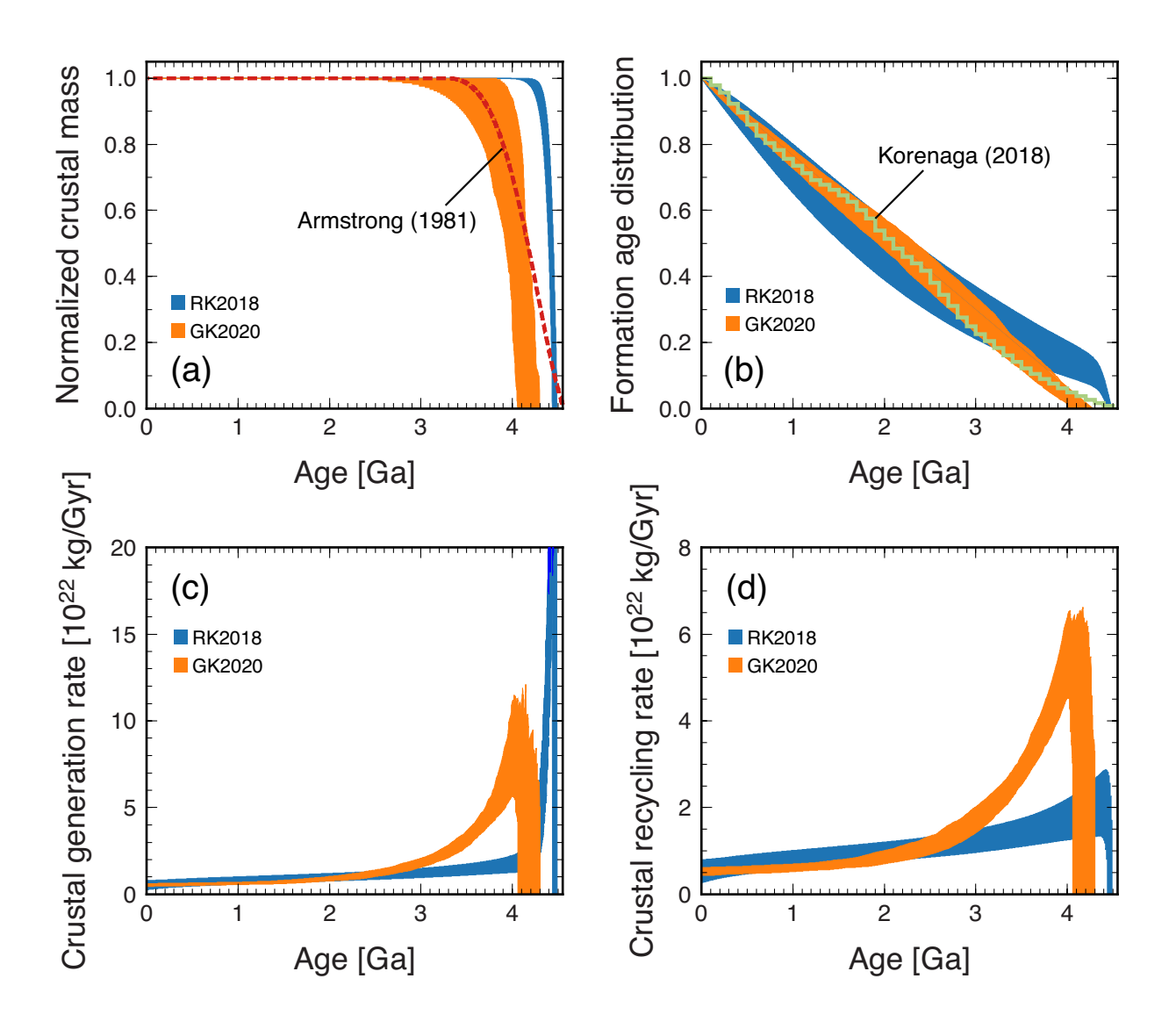


Figure 8: (a) Net growth models of Rosas and Korenaga (2018) (blue) and Guo and Korenaga (2020) (orange). Only middle 50 % of their solutions are shown here for clarity. The model of Armstrong (1981b) (red dashed) is also shown for comparison. (b) Predicted formation age distributions according to the models of Rosas and Korenaga (2018) (blue) and Guo and Korenaga (2020) (orange), and the formation age distribution estimated from detrital zircon ages (green) (Korenaga 2018b). The zircon-based distribution was used as a constraint in the inverse modeling of Guo and Korenaga (2020). (c) Crustal generation rate and (d) crustal recycling rate according to the models of Rosas and Korenaga (2018) (blue) and Guo and Korenaga (2020) (orange).

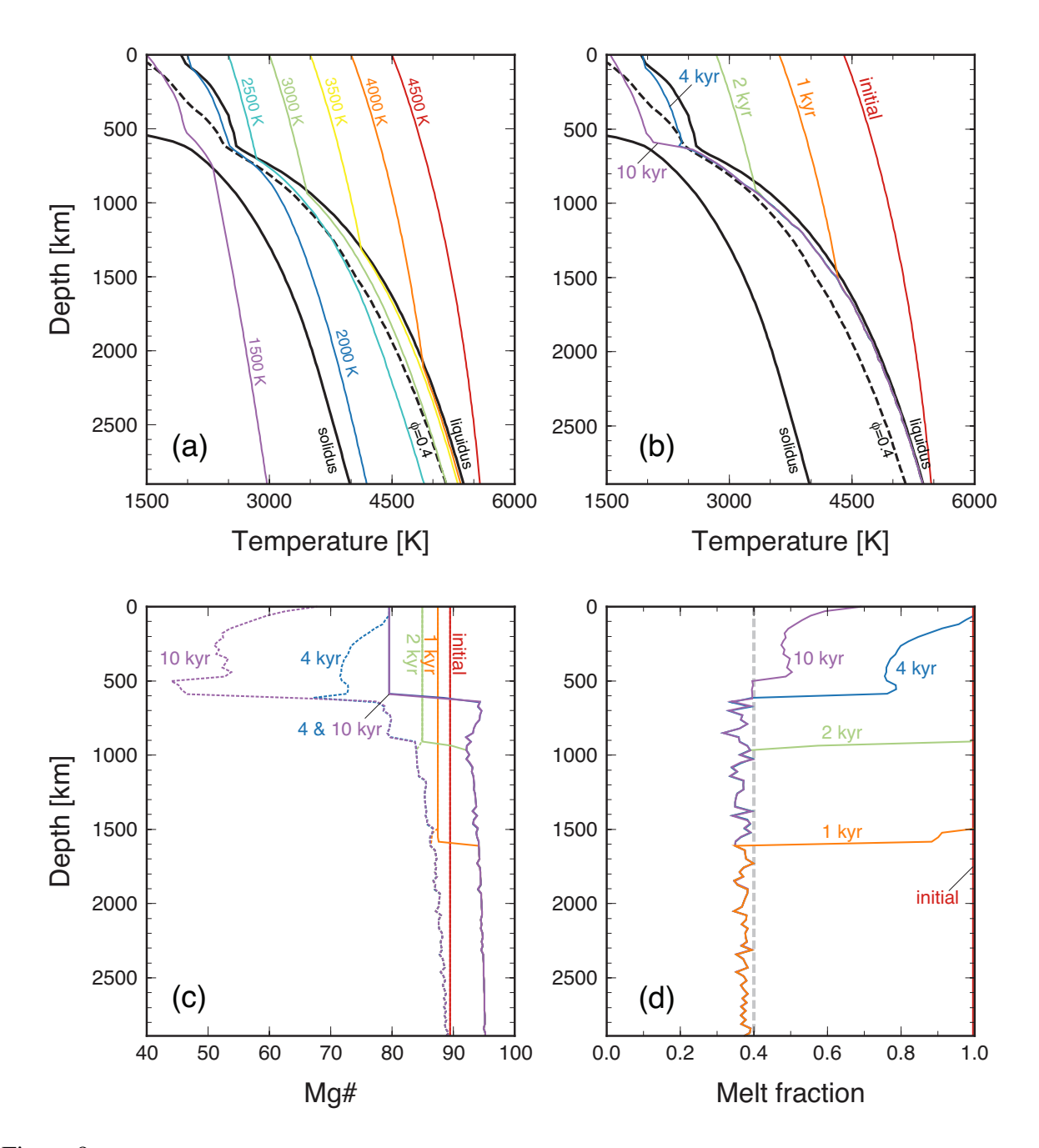


Figure 9: (a) Phase diagram for a pyrolitic mixture of MgO-FeO-SiO₂ (MgO: 42.2 wt%, FeO: 8.7 wt%, and SiO₂: 49.1 wt%) based on the thermodynamic database of Miyazaki and Korenaga (2019a). Dashed line denotes melt fraction of 0.4. Colored lines represent mantle adiabats with different potential temperatures. Note that, unlike in the petrological literature, potential temperature in the context of magma ocean research includes the effect of melting. (b) Thermal evolution of a solidifying magma ocean with the effect of crystal accumulation: initial (red), 1 kyr (orange), 2 kyr (green), 4 kyr (blue), and 10 kyr (purple). (c) Chemical evolution in terms of Mg# corresponding to (b). Solid lines denote local system composition, whereas dashed lines denote melt composition. (d) The evolution of melt fraction corresponding to (b). Melt fraction of 0.4 shown by dashed line marks the rheological transition below which a melt-solid mixture behaves as a solid. The lower mantle temperature stays above the line of melt fraction of 0.4 in (b), but there is no contradiction between (b) and (d); this is simply because the phase diagram shown in (a) and (b) is based on the initial composition. After Miyazaki and Korenaga (2019b).

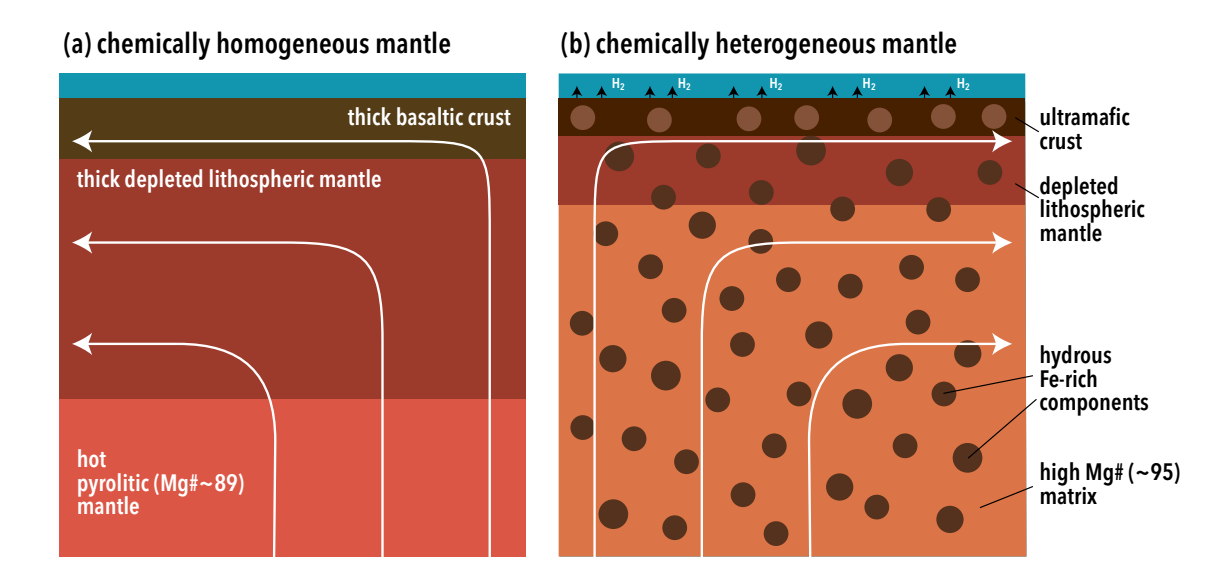


Figure 10: (a) Plate tectonics with a hot pyrolitic mantle results in the formation of thick basaltic crust and thick depleted lithospheric mantle. (b) Plate tectonics with a chemically heterogeneous mantle expected from small-scale Rayleigh-Taylor instabilities in a solidifying magma ocean. The melting of the high Mg# matrix produces an ultramafic crust, which would promote carbonate formation and serpentinization. The melting of iron-rich blobs produces an iron-rich crust, which reduces the chemical buoyancy of the oceanic lithosphere.

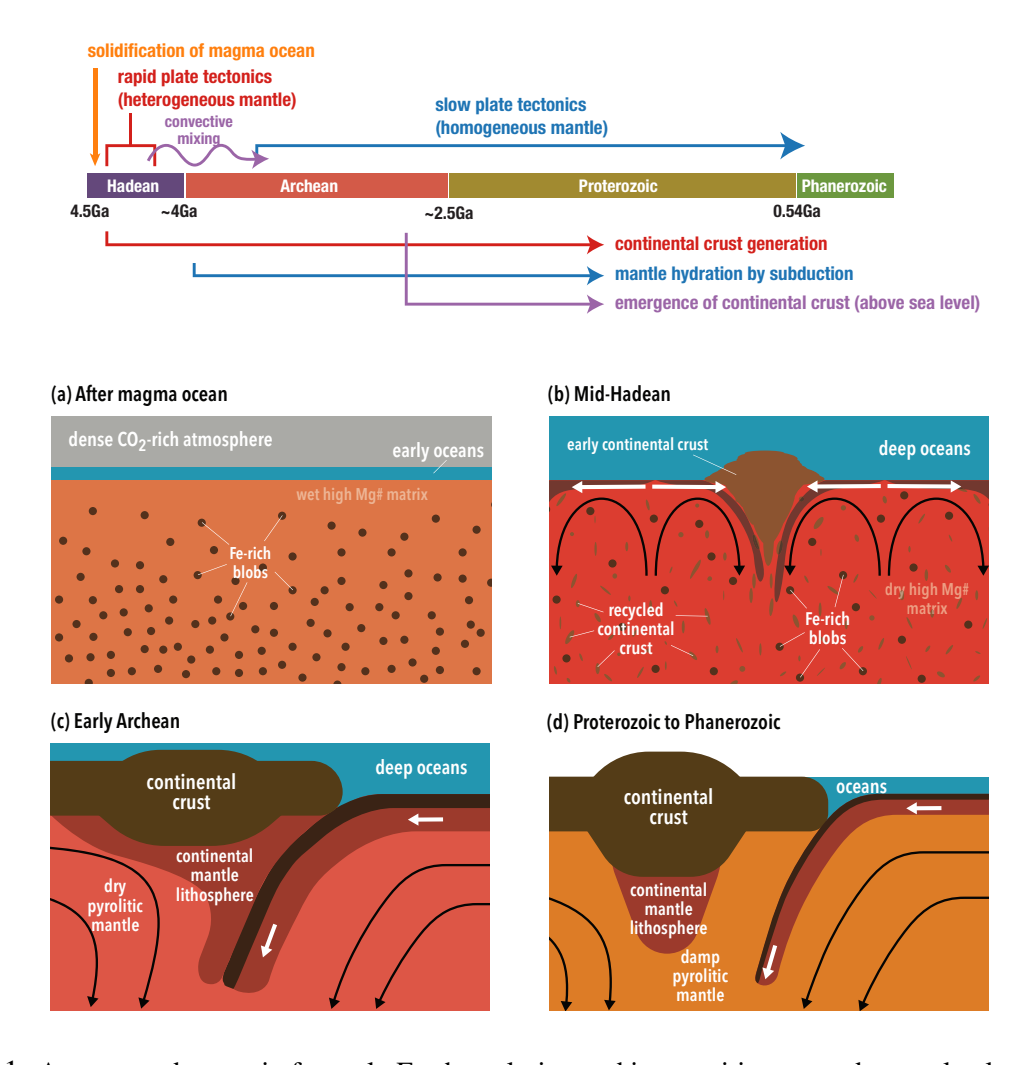


Figure 11: A suggested scenario for early Earth evolution and its transition to modern-style plate tectonics. (a) Right after the solidification of a magma ocean, the mantle is chemically heterogeneous, with a high Mg# matrix and small-scale iron-rich blobs. Inheriting from gas-melt equilibria established during the magma ocean stage, both matrix and blobs contain a substantial amount of water, whereas most of carbon exists as CO₂ in the atmosphere. The water budget in the atmosphere and oceans is thus limited. (b) During the early to mid-Hadean, the high Mg# matrix, combined with high temperature and high water content, allows rapid plate tectonics, which facilitates the sequestration of atmospheric carbon and the degassing of mantle water. A diverse range of melt composition is expected by interaction between the melting of the high Mg# matrix and that of iron-rich blobs, and the rapid subduction of such a chemically heterogeneous crust could help to build early continental crust. Though not depicted here, plume activities are also expected to be intense, which can further modify the melting behavior of this chemically complex mantle. (c) During the late Hadean to the early Archean, convecting mixing eventually restores a pyrolite mantle, the melting of which creates thick basaltic crust and thick depleted mantle lithosphere. Oceanic lithosphere thus becomes a thermal and chemical boundary layer. Thick oceanic lithosphere subducts with a large radius of curvature, leaving little room for the wedge mantle. The convecting mantle is as dry as the continental mantle lithosphere, and owing to this lack of intrinsic viscosity difference between them, the continental lithosphere (including both crust and mantle lithosphere) is subject to intense deformation by convective currents. (d) Continuous operation of plate tectonics gradually hydrates the mantle again, and modern-style plate tectonics manifests from the late Archean. The dry continental mantle lithosphere is now relatively stronger than the damp convecting mantle, protecting the continental crust from below. This corresponds to the stabilization of cratons. The volume of oceans gradually decreases concurrently, allowing the emergence of dry landmasses.

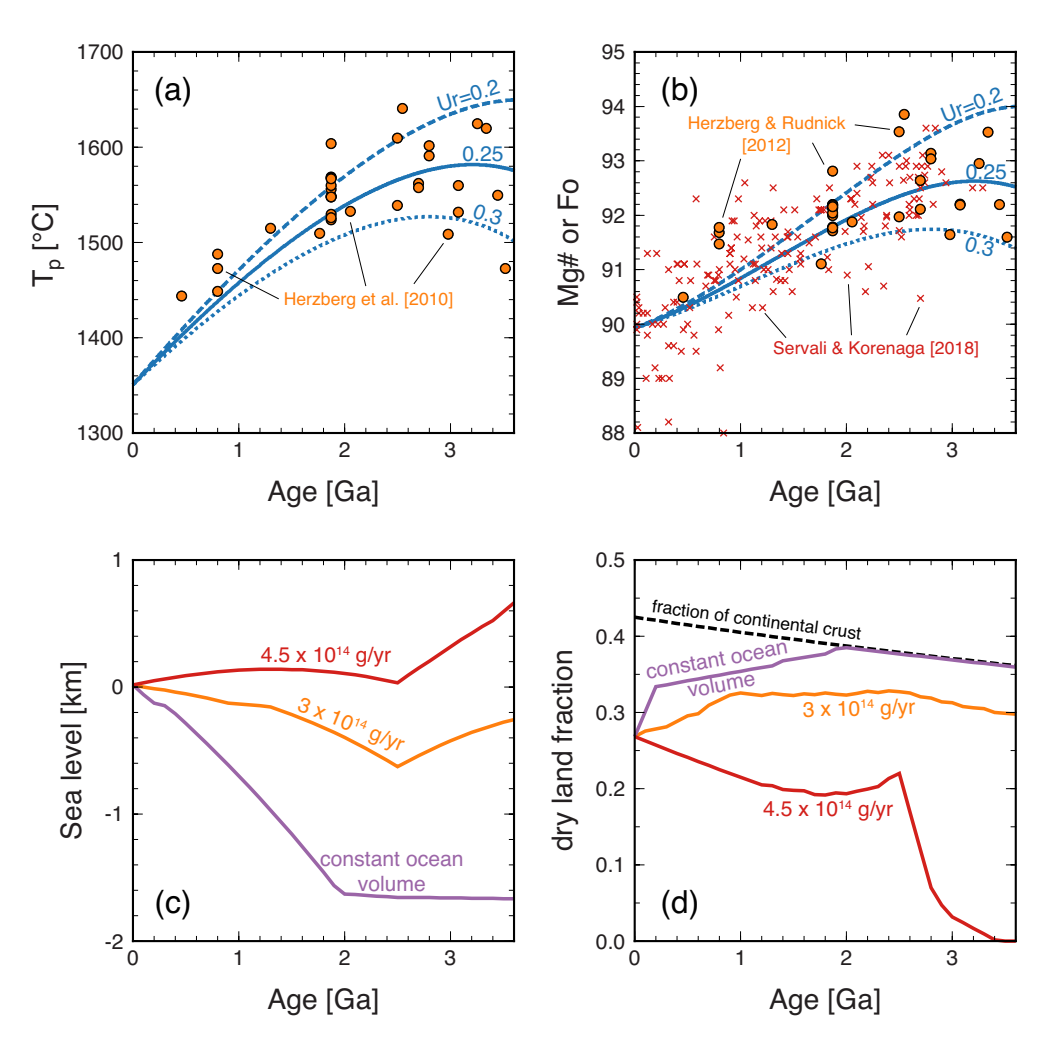


Figure 12: Mid-Archean to Phanerozoic evolution of Earth's interior and surface environment. (a) The thermal history of the upper mantle for the last 3.5 Gyr, according to petrological estimates (orange circles; Herzberg et al. (2010)), and parameterized convection modeling with different assumptions on the amount of radiogenic heating (blue curves). After Servali and Korenaga (2018). (b) The secular evolution of the composition of continental mantle lithosphere in terms of Mg# or the forsterite content of olivine. Orange circles represent prediction based on Precambrian non-arc basalts (Herzberg and Rudnick 2012), and red crosses denote cratonic xenolith data (Servali and Korenaga 2018). Blue curves denote predictions based on the parameterized convection modeling. Modified after Servali and Korenaga (2018). (c) Different scenarios for sea level change based on the continental freeboard modeling of Korenaga et al. (2017). The mass of continental crust is constant during this period (cf. Figure 8). The results shown here follow mostly the reference case adopted by Korenaga et al. (2017): half-space cooling for seafloor subsidence, 5 km thicker continental crust at 2.5 Ga, more buoyant continental mantle lithosphere in the Archean, and reduced continental topography in the past, but the constant density of continental crust through time is assumed to reflect the discussion of §3.3. Three different net water fluxes are tested: 0 (purple), 3×10^{14} g yr⁻¹ (orange), and 4.5×10^{14} g yr⁻¹ (red). In the last two cases the volume of oceans at 2.5 Ga is higher than the present volume by ~ 50 % and ~ 70 %, respectively. A nearly constant sea level during the Precambrian as indicated by epicontinental sedimentary records (Korenaga et al. 2017) suggests that long-term net water flux is approximately $3.5-4 \times 10^{14}$ g yr⁻¹. (d) Fraction of dry landmasses on surface, corresponding to the three cases in (c). Because the thickness of continental crust is assumed to be slightly thicker in the past (Galer and Mezger 1998), the surface area of continental crust decreases with age even with the constant crustal mass assumed here.